Fisheries

SOUTH AUSTRALIAN RESEARCH & DEVELOPMENT INSTITUTE
PIRSA

Stock assessment of Australian Sardine (*Sardinops sagax*) off South Australia 2019

Ward, T.M., Smart, J., Grammer, G., Ivey, A., and McGarvey, R.

SARDI Publication No. F2007/000765-7
SARDI Research Report Series No. 1048

SARDI Aquatics Sciences
PO Box 120 Henley Beach SA 5022

February 2020

Report to PIRSA Fisheries and Aquaculture

SOUTH AUSTRALIA

Government of South Australia
Primary Industries and Regions SA

SARDI
SOUTH AUSTRALIAN RESEARCH AND DEVELOPMENT INSTITUTE

Stock assessment of Australian Sardine (*Sardinops sagax*) off South Australia 2019

Report to PIRSA Fisheries and Aquaculture

Ward, T.M., Smart, J., Grammer, G., Ivey, A. and McGarvey, R.

SARDI Publication No. F2007/000765-7
SARDI Research Report Series No. 1048

February 2020

This publication may be cited as:
Ward, T.M., Smart, J., Grammer, G., Ivey, A. and McGarvey, R. (2020). Stock assessment of Australian Sardine (*Sardinops sagax*) off South Australia 2019. Report to PIRSA Fisheries and Aquaculture. South Australian Research and Development Institute (Aquatic Sciences), Adelaide. SARDI Publication No. F2007/000765-7. SARDI Research Report Series No. 1048. 108pp.

South Australian Research and Development Institute
SARDI Aquatic Sciences
2 Hamra Avenue
West Beach SA 5024

Telephone: (08) 8207 5400
Facsimile: (08) 8207 5415
http://www.pir.sa.gov.au/research

DISCLAIMER
The authors warrant that they have taken all reasonable care in producing this report. The report has been through the SARDI internal review process, and has been formally approved for release by the Research Director, Aquatic Sciences. Although all reasonable efforts have been made to ensure quality, SARDI does not warrant that the information in this report is free from errors or omissions. SARDI and its employees do not warrant or make any representation regarding the use, or results of the use, of the information contained herein as regards to its correctness, accuracy, reliability and currency or otherwise. SARDI and its employees expressly disclaim all liability or responsibility to any person using the information or advice. Use of the information and data contained in this report is at the user's sole risk. If users rely on the information they are responsible for ensuring by independent verification its accuracy, currency or completeness. The SARDI Report Series is an Administrative Report Series which has not been reviewed outside the department and is not considered peer-reviewed literature. Material presented in these Administrative Reports may later be published in formal peer-reviewed scientific literature.

SARDI Publication No. F2007/000656-7
SARDI Research Report Series No. 1048

Author(s):	Ward, T.M., Smart, J., Grammer, G., Ivey, A. and McGarvey, R.
Reviewer(s):	Linnane, A., and Bailleul, F.
Approved by:	Dr. S. Mayfield Science Leader - Fisheries
Signed:	
Date:	27 February 2020
Distribution:	PIRSA Fisheries and Aquaculture, SAASC Library, Parliamentary Library, State Library and National Library
Circulation:	Public Domain

TABLE OF CONTENTS

LIST OF FIGURES

LIST OF TABLES

ACKNOWLEDGEMENTS

This report was undertaken under a Service Level Agreement with PIRSA Fisheries and Aquaculture. SARDI Aquatic Sciences contributed in-kind support to the salaries of Associate Professor Tim Ward, Dr Gretchen Grammer and Dr Jonathan Smart. Recent catch samples were provided by Seatech Marine. Sardine fishers provided catch and effort data in Daily Logbooks. The Fisheries Information Services at SARDI Aquatic Sciences provided summaries of catch and effort data. The report was reviewed by Drs Adrian Linnane and Fred Bailluel (SARDI) and approved for release by Dr Stephen Mayfield, Science Leader, Fisheries (SARDI Aquatic Sciences).

EXECUTIVE SUMMARY

This report assesses the status of the southern stock of Australian Sardine (*Sardinops sagax)*. It informs management of the South Australian Sardine Fishery (SASF), which is Australia's largest fishery by weight. The SASF was established in 1991. It is a purse-seine fishery with limited entry. The primary management tool is the Total Allowable Commercial Catch (TACC). The key performance indicator is the estimate of spawning biomass obtained using the Daily Egg Production Method (DEPM).

Sustainability is assessed against reference points specified in the tiered harvest strategy (PIRSA 2014). The TACC is set by applying exploitation rates of 10 to 25%, based on decision rules relating to the size of the spawning biomass and level of research and monitoring (i.e. frequency of application of the DEPM and population modelling). The limit reference point is 75,000 t. The target and upper target reference points are 150,000 t and 190,000 t, respectively.

Spatial management was introduced into the SASF in 2010. In 2014-18, the SASF was divided into the Gulfs and Outside Zones. There is a cap on the annual catch from the Gulfs Zone, determined by the mean fork length (FL) of Sardine taken in the zone during the previous year.

In this report, we re-analyse data obtained using the DEPM since 1995 and provide a revised time-series of estimates of spawning biomass. We also use a new age-structured model (SardEst) to integrate fishery-independent and fishery-dependent information.

Findings of the re-analysis of the DEPM data suggested that adult reproductive parameters (sex ratio, spawning fraction, and relative fecundity, i.e. eggs per gram of female weight) were stable among years, and do not need to be estimated annually. Inter-annual variability in mean daily egg production (P_0) was also low in comparison to statistical uncertainty. The confidence intervals of estimates of spawning biomass were reduced by >50% when adult parameters and P_0 were re-estimated using data obtained over the last 20 years. Under this refined approach to applying the DEPM, estimates of spawning biomass are driven primarily by the estimate of spawning area.

In February-April 1995, the spawning biomass of Sardine off South Australia was estimated to be approximately 298,000 t. Mass mortality events in late 1995 and 1998, that mainly effected adults, reduced the spawning biomass to less than 100,000 t. The stock recovered relatively quickly and remained between 140,000 t and 200,000 t from 1999 to 2005. Since 2006, the adult stock has been

above 200,000 t. In 2019, the estimate of spawning biomass (95% CI) for Sardine off South Australia obtained using the DEPM was 233,684 (181,214–286,153) t.

The total annual catch of the SASF remained below 8,000 t up to 2001. Catches increased rapidly after 2002 to reach 42,475 t in 2005. From 2006 to 2016, the annual catch ranged from ~26,000 t to ~38,000 t. Since 2017, the annual catch has been above 40,000 t. In 2018, the total catch was 42,474 t. The catch from the Gulfs Zone has been capped at 30,000 t since 2015. The catch from the Outside Zone increased from 1,460 t in 2010 to 12,141 t in 2018.

Sardine taken from the Gulfs Zone are usually younger and smaller than those taken from the Outside Zone. The modal age of fish from the Gulfs Zone has typically been 3+ years, but was reduced to 2+ years from 1996 to 1999, following the mass mortality events, and during 2006-2008, after 38,734 t were taken from the zone in 2005. The modal age also fell to 2+ years in 2010-11, but returned to 3+ years from 2013 onwards, following the introduction of the size-based decision rules.

SardEst was fitted to annual estimates of spawning biomass and age-composition. Annual catches were used to condition estimates of fishing mortality. The model was not spatially structured (i.e. did not incorporate two zones). SardEst generally fitted well to estimates of spawning biomass and age-composition. The unfished equilibrium total biomass (i.e. including juveniles) was estimated to be 588,000 t (± 115,000 t). In 1999, the total biomass was estimated to be 447,000 t (± 93,000 t), equating to depletion level of 76%. The model estimate of spawning biomass for 2019 was ~239,000 t (± 93,000 t), suggesting an exploitation rate of 18%.

The estimate of spawning biomass obtained using the DEPM (~234,000 t) and from the integrated population model (239,000 t) were both above the target reference point of 150,000 t and the upper reference point of 190,000 t identified in the management plan. Consistent with other recent assessments of the SASF (e.g. Ward et al. 2017; Stewardson et al. 2018), the southern stock of Sardine is classified as **Sustainable.**

Statistic	2019	2018	2017	2016
TACC	42,750 t	42,750 t	42,750 t	38,000 t
Spawning Biomass (DEPM)	233,600 t	275,600 t	289,700 t	220,400 t
Spawning Biomass (Model)	238,550 t	260,180 t	262,590 t	251,200 t
Status	**Sustainable**	**Sustainable**	**Sustainable**	**Sustainable**

Keywords: Daily Egg Production Method, spawning biomass, pelagic fishes, spawning fraction, egg production.

1. INTRODUCTION

1.1 Overview

Stock assessment reports on the South Australian Sardine Fishery (SASF) have been published annually or biennially since 1999 (Ward and McLeay 1999). Since 2005, the reports have used age-structure models to integrate fishery-dependent and fishery-independent data (Ward et al. 2005). The aims of this report are to: summarise relevant scientific information on Sardine (*Sardinops sagax)* and describe the history and management of the SASF (Chapter 1); summarise catch and effort data (Chapter 2); present age structure and reproductive information (Chapter 3); re-analyse historical fishery-independent estimates of spawning biomass (Chapter 4); introduce a new integrated stock assessment model (Chapter 5); and assess the status of the stock, evaluate management options and identify future research needs (Chapter 6).

1.2 Fisheries, abundance fluctuations and stock structure

Sardine, *Sardinops sagax* (Jenyns 1842), occurs off the west coasts of North and South America, off southern Africa, around Japan and off the southern coasts Australia and New Zealand (Parrish et al. 1989; Grant and Leslie 1996; Grant et al. 1998). The Standard Fish Names List for Australia specifies that the common name for *Sardinops sagax* is Australian Sardine. In this report we use the term Sardine to refer to *S. sagax* in Australia and elsewhere.

Sardine has historically supported important commercial fisheries throughout its global range; biomasses and catches have fluctuated dramatically over multi-decadal scales (e.g. Schwartzlose et al. 1999). For example, the biomass off California fishery peaked at just over four million tons in the 1930s and declined to <3,000 tons in the 1970s (Schwartzlose et al. 1999). Similarly, the Japanese catch peaked at 5.43 million tons in 1988 but declined to 0.3 million tons in 1996 (Schwartzlose et al. 1999). Currently, the biomass and catches of Sardine off the west coasts of North America (Hill et al. 2017) and southern Africa (https://sapfia.org.za/tac/) are low.

Fluctuations in the abundance and catches of Sardine in the Benguela, Californian and Humboldt Current systems off the west coasts of southern Africa and North and South America, respectively, have occurred synchronously (Schwartzlose et al. 1999; Tourre et al. 2007). During periods of low Sardine abundance, the local species of Anchovy (*Engraulis* spp.) has replaced Sardine as the dominant species small pelagic fish (Schwartzlose et al. 1999). 'Global synchrony' in the fluctuations in the relative abundance of Sardine and Anchovy appear to have been driven by multi-decadal changes in global ocean conditions (Schwartzlose et al 1999; Tourre et al. 2007, Checkly et al. 2017).

The multi-decadal fluctuations in the relative abundance of Sardine and Anchovy that have been recorded elsewhere have not been observed off southern Australia (Schwartzlose et al. 1999; Ward et al. 2001b). Sardine is the dominant clupeoid in this region, occurring throughout coastal and shelf waters. In contrast, Anchovy (*Engraulis australis*) is confined mainly to inshore waters (Schwartzlose et al. 1999; Ward et al. 2001a, Dimmlich et al. 2004, 2009; Dimmlich and Ward 2006). The abundance of Sardine off southern Australia was reduced by mass mortality events that occurred in 1995 and 1998/99, which each killed more fish over a larger area than any other recorded fish-kill (Jones et al 1997; Ward et al. 2001a, b). After the two Sardine mortality events, which each killed more than 50% of the adult population, the distribution of Anchovy expanded into shelf waters usually dominated by Sardine (Ward et al. 2001a, b). This finding suggests that the fluctuations in relative abundance of Sardine and Anchovy observed globally may also be possible in Australian waters (Ward et al. 2001a, b).

The rapid spread of the 1995 and 1998/99 mortality events across southern Australia demonstrated the connectivity of Sardine across this entire geographical range (Whittington et al. 2008). Despite this connectivity, Sardine off southern Australia is considered to be a meta-population (Whittington et al. 2008) comprised of four biological stocks (Izzo et al. 2017). The south-western stock occurs off Western Australia; the southern stock off South Australia; the south-eastern stock off Victoria, Tasmania and southern NSW; and the eastern stock off northern New South Wales and southern Queensland. There is some evidence to suggest that the south-western and eastern stocks each include two separate sub-components (Gaughan et al. 2002; Izzo et al. 2017; Sexton et al. 2019).

Commercial fishing for Sardine has been conducted off southern Australia since the 1800s (Kailola et al. 1993), but combined national catches did not exceed 1,000 t until the 1970s. Catches off eastern Australia remained below 500 t up until 2003/04, before reaching a peak of almost 5,000 in 2008/09 and then declining to <1,000 per annum from 2011/12 onwards (Ward et al. 2019). Several fisheries for Sardine developed off south-western Australia during the late 1970s. The total annual catch for Western Australia peaked at ~8,000 t in 1990 (Kailola et al. 1993) and has not exceeded 3,500 t since the mid-2000s, when the stock had recovered from the mass mortality events of the 1990s (Ward et al. 2019). The South Australian Sardine Fishery was established in 1991 (Ward and Staunton-Smith 2002). It grew rapidly and the total annual catch has exceeded 40,000 t since 2017 (Ward et al. 2019). Catch and effort data for the SASF are presented in Chapter 1 of this report.

1.3 Biology, stock assessment, ecological importance and fisheries management

Sardines have been studied intensively in Australia and elsewhere; they are short-lived (< 10 years), fast-growing and highly fecund (e.g. see Ganias et al. 2012). Growth increments in sagittal otoliths

(ear bones) have been widely used to estimate age (Butler et al. 1996, Fletcher and Blight 1996; Rogers et al. 2003). Despite difficulties associated with interpreting and counting opaque and translucent zones (Butler et al. 1996, Fletcher and Blight 1996, Rogers and Ward 2007), it is clear that Sardine grow faster and reach larger sizes in the productive boundary currents off Africa and North America than they do in the less productive waters off southern Australia (e.g. Fletcher and Blight 1996; Ward et al. 2006). Size, age and growth information for Sardine off South Australia are presented in Chapters 2 and 3 of this report.

Sardine are serial spawners with asynchronous oocyte development and indeterminate fecundity (e.g. Ganias et al 2012). Females release numerous batches of pelagic eggs throughout a spawning season that typically extends for several months (Lasker 1985). Approximately 10-12% of females spawn each night during the peak spawning season (Ganias et al. 2012). The number of eggs in a batch, i.e. batch fecundity, is correlated with female size (Lasker 1985). In Australia, Sardine usually spawn in shelf waters (Blackburn 1950, Fletcher and Tregonning 1992, Fletcher et al. 1994). The timing of spawning varies between locations; off South Australia the peak spawning season occurs during January to April (Ward et al. 2001a, 2001b, Ward and Staunton-Smith 2002). Information on the reproductive biology of Sardine off South Australia are provided in Chapters 3 and 4 of this report.

Sardine are planktivores (Espinoza et al. 2009). They have two feeding modes: filter-feeding on micro-zooplankton and phytoplankton and particulate-feeding on macro-zooplankton. Sardine switch between these two modes depending on relative prey density (van der Lingen 1994, 2002; Louw et al. 1998). Off South Australia, Sardine appear to feed mainly on crustaceans, fish eggs and larvae and gelatinous zooplankton (Daly 2007).

Sardines are an important food source for many predatory fishes, squid, seabirds and marine mammals (e.g. Pikitch et al. 2012). However, the reliance of predators on Sardine and other small pelagic fishes varies among ecosystems and species (e.g. Smith et al. 2011; Hilborne et al. 2017). The trophic role of Sardines is particularly important in the “wasp-wasted” ecosystems, such as those found in the productive California, Humboldt and Benguela Current systems where one or two species usually dominate the pelagic fish biomass (e.g. Cury et al. 2000). In contrast, several studies have shown that Australia’s less productive pelagic ecosystems support a wide range small to medium sized planktivores and that few predators are highly dependent on a single prey species (Bulman et al. 2011; Smith et al. 2015). Off South Australia, marine predators feed opportunistically on a wide range of prey species and none have been shown to be predominately dependent on Sardine as a food (Goldsworthy et al. 2013).

Harvest strategies that include agreed operational targets and decision rules have been successfully incorporated into the management systems of several commercial small pelagic fisheries, including the South African Pelagic Fishery and Pacific Sardine Fishery (De Oliveira et al. 1998, Hill et al. 2005). Most fisheries have established precautionary targets, limits and decision rules to account for uncertainty in stock assessments, high levels of recruitment and their ecological importance. Cury et al. (2011) suggest a maximum rate of approximately one-third of the maximum observed prey abundance could be applied as a principal in low trophic level fisheries. Smith et al. (2011) showed that broader ecosystem impacts from fishing low trophic level species could be reduced by halving exploitation rates from typical maximum sustainable yield levels (i.e. ~60%). Smith et al. (2015) suggested that target and limit reference points for spawning biomass of small pelagic species in Australian waters, including Sardine, of 50% (B_{50}) and 20% (B_{20}) of the unfished level, respectively, are "safe from an ecosystem perspective and provide reasonable levels of yield". Smith et al. (2015) also suggest that exploitation rates below 33% are likely to maintain the median spawning biomass of Sardine above B_{50} and the chance of falling below B_{20} at less than 10%.

1.4 The South Australian Sardine Fishery

The SASF is managed by the *Fisheries Management (Marine Scalefish Fisheries) Regulations 2006* and *Fisheries Management Act 2007*. Management goals for the SASF are consistent with the objectives of the *Fisheries Management Act 2007* and are outlined in the current Management Plan (PIRSA 2014). Management measures include entry limitations, gear restrictions and individual transferable quotas. Purse seine nets must not exceed 1,000 m in length or 200 m depth. There are 14 license holders with several companies operating multiple licenses. The costs of the policy, compliance and research programs that are needed to manage the SASF are recovered through license fees collected by PIRSA Fisheries and Aquaculture.

The Total Allowable Commercial Catch (TACC) was set at 1,000 t in 1992 (calendar year), and increased to 3,500 t during 1993–1997 (Figure 1–1). In 1998, the TACC was set at 12,500 t, but was reduced to 3,500 t after the mass mortality event in late 1998 and to 3,800 t in both 1999 and 2000. The stock recovered rapidly, and the TACC increased to 51,100 t in 2005. From 2007 to 2017, the TACC increased from 30,000 t to 42,750 t. The TACC for 2019 was 42,750 t. From 2010, onwards, there has been a cap on the catch taken from Spencer Gulf (Figure 1–1, Figure 1–2). The SASF is now divided into two zones: Gulfs Zone and Outside Zone (Figure 1–2). The TACC for 2017-19 of 42,750 t, included up to 30,000 t from the Gulfs Zone and 12,750 t from the Outside Zone (Figure 1–1).

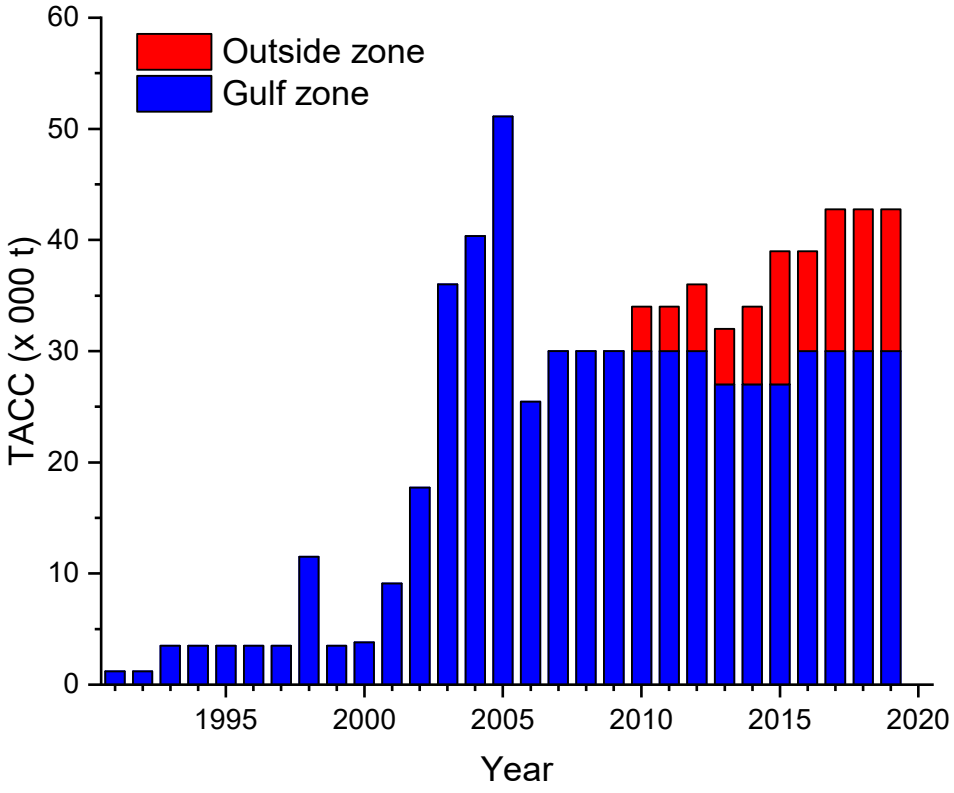

Figure 1-1. Total Allowable Commercial Catch (TACC) for the South Australian Sardine Fishery (SASF) between 1991 and 2019 for Gulfs Zone and Outside Zone (see Figure 1–2).

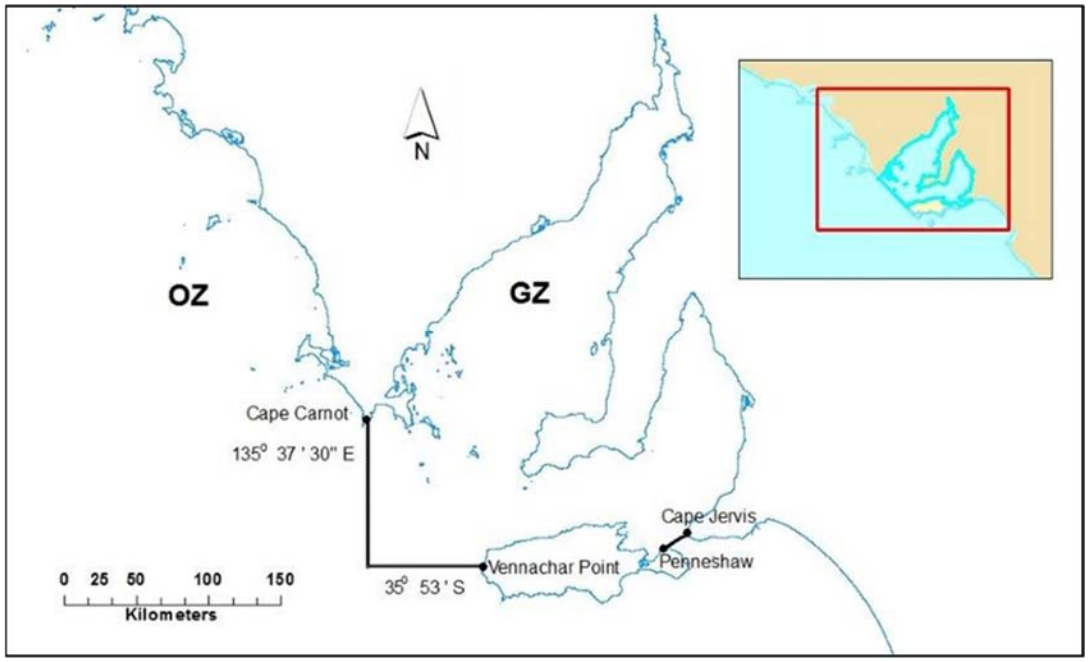

Figure 1-2. The two spatial management zones defined in the harvest strategy for the SASF. Abbreviations: OZ, Outside Zone; GZ, Gulfs Zone (source PIRSA 2014).

Since 1998, the key biological performance indicator for the SASF has been the estimate of spawning biomass obtained using the DEPM. From 1997 to 2006, the TACC for the following calendar year was set as a proportion of the spawning biomass (i.e. 10.0–17.5%, depending on the size of the spawning biomass). From 2007 to 2009, the indicative TACC was set at 30,000 t (PIRSA 2007), while the estimate of spawning biomass obtained using the DEPM remained between 150,000 and 300,000 t. In 2014, a tiered Harvest Strategy (Figure 1–3) was established that sets the TACC based on the size of the spawning biomass and level of monitoring and assessment (Table 1–1). At Tier 3, DEPM and fishery assessments are done in alternate years and the maximum TACC is 38,000 t. At Tier 1, DEPM and fishery assessments are both undertaken annually and the maximum TACC is 47,500 t. At Tier 2, either DEPMs or assessments are done annually (with the other done biennially) and the maximum TACC is 42,750 t. Lower TACCs are set at each Tier if the spawning biomass is below 190,000 t. The SASF was managed at Tier 1 in 2015 and 2016 and at Tier 2 from 2017 to 2019.

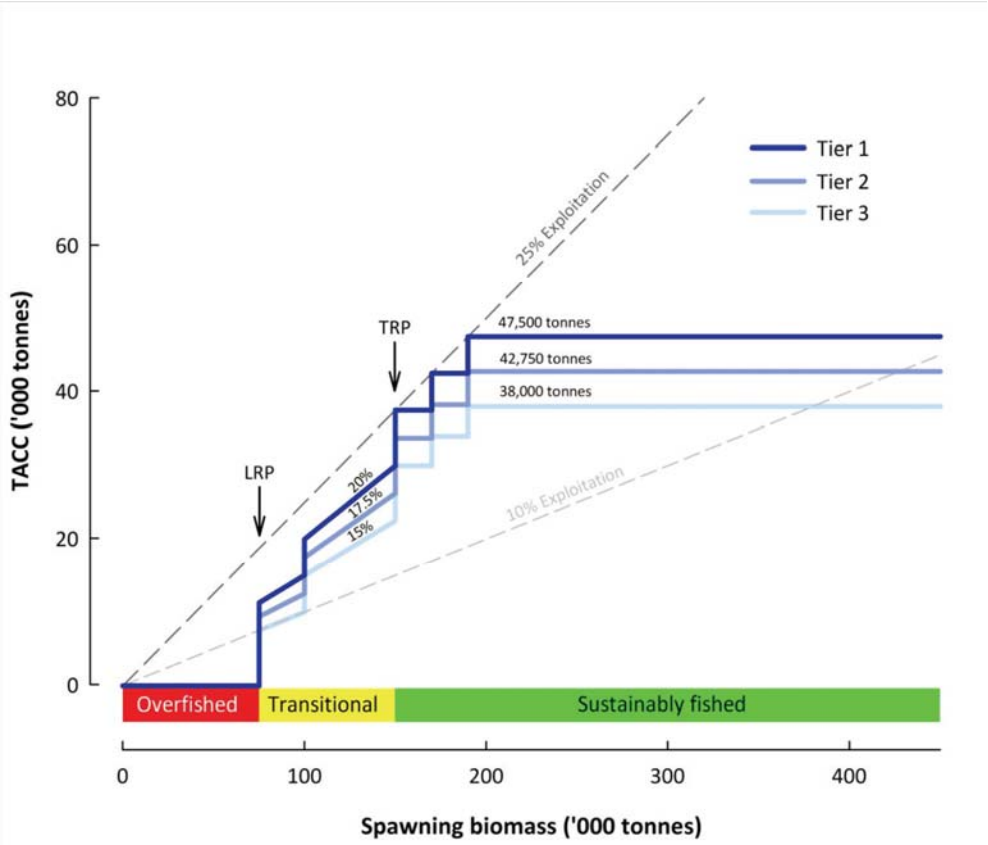

Figure 1-3. The relationship between spawning biomass, stock status and level of exploitation (or TACC) of the Sardine harvest strategy for each tier (LRP = limit reference point; TRP = target reference point).

Table 1-1. Decision making rules for the tiered Harvest Strategy.

Spawning Biomass			Tier 1		Tier 2		Tier 3	
			TACC (t)	Maximum Exploitation	TACC (t)	Maximum Exploitation	TACC (t)	Maximum Exploitation
190000 t <	SpB		47,500 t	25%	42,750 t	22.5%	38,000 t	20%
170000 t <	SpB	≤ 190000 t	42,500 t	25%	38,250 t	22.5%	34,000 t	20%
150000 t <	SpB	≤ 170000 t	37,500 t	25%	33,750 t	22.5%	30,000 t	20%
100000 t <	SpB	≤ 150000 t	20% of SpB	20%	17.5% of SpB	17.5%	15% of SpB	15%
75,000 t <	SpB	≤ 100000 t	15% of SpB	15%	12.5% of SpB	12.5%	10% of SpB	10%
	SpB	≤ 75000 t	Closed	0%	Closed	0%	Closed	0%

Spatial management was established in the SASF in 2010 and formalised in 2014 (Figure 1–2). The catch that can be taken from the Gulfs Zone is determined from the mean size (Fork Length, FL) of Sardine taken in catches from that zone in the previous year (Table 1–2; Figure 1–2). If the mean size is above 142 mm FL, up to 30,000 t can be taken from the Gulfs Zone whereas if it is below 135 mm FL, the maximum catch is 24,000 t. If the mean size is between 135 and 142 mm, the maximum catch from the Gulfs Zone is 27,000 t.

Table 1-2. Catch allocation decision table for the harvest strategy for the SASF to guide the maximum TACC allowed from the Gulfs Zone (GZ) (PIRSA 2014).

Mean size of Sardines (MSS, mm Fork Length) in GZ	Maximum catch limits for GZ
142 mm < MSS	30,000 t
135 mm < MSS ≤ 142 mm	27,000 t
MSS ≤ 135 mm	24,000 t

1.5 Stock Status Classification

A national stock status classification system has been developed to assess key Australian fish stocks (Table 1-3; Stewardson et al. 2018). The classification system combines information on current stock size and the level of fishing pressure to assess 'stock status' (Stewardson et al. 2018). Each stock is classified as: 'sustainable', 'depleting', 'recovering', 'depleted', 'undefined' or 'negligible' as outlined in Table 1–3.

As described previously, for the purposes of fisheries management the Australian Sardine population is considered to be comprised of four separate stocks (Whittington et al. 2008, Izzo et al. 2017). The SASF targets the Southern Australian stock, which occurs off South Australia and western Victoria (Izzo et al. 2012). The Southern Australian stock was assessed as being sustainable in the most recent Status of Key Australian Fish Stocks (Stewardson et al. 2018).

Table 1-3. Stock status terminology (Stewardson et al. 2018).

	Stock status	Description	Potential implications for management of the stock
	Sustainable	Stock for which biomass (or biomass proxy) is at a level sufficient to ensure that, on average, future levels of recruitment are adequate (*i.e.* recruitment is not impaired) and for which fishing mortality (or proxy) is adequately controlled to avoid the stock becoming recruitment impaired	Appropriate management is in place
	Depleting	Biomass (or proxy) is not yet depleted and recruitment is not yet impaired, but fishing mortality (or proxy) is too high (overfishing is occurring) and moving the stock in the direction of becoming recruitment impaired	Management is needed to reduce fishing pressure and ensure that the biomass does not become depleted
	Recovering	Biomass (or proxy) is depleted and recruitment is impaired, but management measures are in place to promote stock recovery, and recovery is occurring	Appropriate management is in place, and there is evidence that the biomass is recovering
	Depleted	Biomass (or proxy) has been reduced through catch and/or non-fishing effects, such that recruitment is impaired. Current management is not adequate to recover the stock, or adequate management measures have been put in place but have not yet resulted in measurable improvements	Management is needed to recover this stock; if adequate management measures are already in place, more time may be required for them to take effect
	Undefined	Not enough information exists to determine stock status	Data required to assess stock status are needed
	Negligible	Catches are so low as to be considered negligible and inadequate information exists to determine stock status	Assessment will not be conducted unless catches and information increase

2. FISHERY INFORMATION

2.1 Introduction

This chapter presents catch, effort, size composition data and catch-per-unit-effort (CPUE) for the SASF from 1 January 1991 to 31 December 2018. This information is used to describe the main spatial and temporal patterns in the fishery and provides key inputs to the stock assessment model (Chapter 5).

2.2 Methods

2.2.1 Data Collection

Catch and effort data were collated from commercial fishing logbooks. Prior to 2001, catch and effort were reported according to the pre-existing South Australian Marine Fishing Areas (MFAs). Following the implementation of SASF logbooks in 1998, catch and effort were reported by latitude and longitude. Estimated catches presented by month and year are aggregated from daily catches recorded in logbooks. CPUE estimates are based on these aggregated catches and corresponding effort data. Actual total annual catches were estimated from the Catch Disposal Records (CDRs) collated from landings by PIRSA Fisheries and Aquaculture.

2.2.2 Commercial catch sampling

Between 1995 and 2018, samples of the commercial catch were collected from vessels under a range of sampling protocols, recently, independent observers present on about 10% of fishing trips have taken a sample of approximately 50 fish from each observed shot. Size frequencies were constructed from caudal fork lengths (FLs) aggregated into 10 mm length classes for all samples. Age determination methods are described in Chapter 3.

Sex ratio (R)

The proportion of females in commercial catch samples was calculated using the equation:

$$R = \frac{nF}{(nF + nM)}$$

where *nF* was the number of females and *nM* was the number of males in the samples. Sex was not recorded for commercial samples obtained in 2007.

2.3 Results

2.3.1 Effort, catch and CPUE

Annual patterns

The SASF expanded quickly after its inception in 1991, with total effort and catches recorded in logbooks increasing from 5 boat-nights and 7 t in 1991 to 736 boat-nights and 3,241 t in 1994 (Figure 2–1). Total effort and catch were reduced in 1995 following the first mass mortality event (Ward et al. 2001b), but increased rapidly to reach 530 boat-nights and 5,973 t in 1998. In 1999, after the second mass mortality event in late 1998 (Ward et al. 2001b), effort and catch declined to 345 boat-nights and 3,081 t, respectively.

Since the second mortality event, the fishery has expanded rapidly, with total effort reaching 1,274 net-sets across 1,233 boat-nights in 2005, with an estimated total catch of 39,831 t (Figure 2–1). Between 2007 and 2016, total effort was relatively stable at approximately 760–1100 net-sets over 630–900 boat-nights with an estimated catch of 27,500–36,100 t. In 2017 and 2018, estimated catches (logbooks) were 40,632 t and 39,979 t, respectively.

Total annual catches recorded in CDRs exceeded catches estimated in logbooks in most years. Actual catches increased from 2,597 t in 1995 to 42,475 t in 2005, and fell to 25,137 t in 2006 (Figure 2–1). Since 2007, catches in CDRs have ranged from 29,854 t in 2009 to 42,511 t in 2017. The total catch in 2018 was 42,474 t.

Mean $CPUE_{(boat\text{-}night)}$ increased from 1.3 t.boat-night^{-1} in 1991 to 11.3 t.boat-night^{-1} in 1998. It reached its highest level of 56.9 t.boat-night^{-1} in 2018. Mean $CPUE_{(net\text{-}set)}$ increased from 7.4 t.net-set^{-1} in 2000 to approximately 32.6 t.net-set^{-1} in 2004. $CPUE_{(net\text{-}set)}$ increased to 40.1 t.net-set^{-1} in 2013 and remained stable until 2017 when it dropped to 37.5 t.net-set^{-1} in 2017, before rising to a high of 44.4 t.net-set^{-1} in 2018 (Figure 2– 1).

Intra-annual patterns

The intra-annual pattern in fishing effort has been reasonably consistent over the last 20 years (Figure 2–2). Relatively little fishing was conducted during August to October. Effort and catches typically increased in November/December. Catches continued to increase during January-February and usually peaked in March–June. The peak fishing season reflects the generally calm weather between April and June and the high demand tuna feed during this period. The months in which significant catches have been taken from the Outside and Gulfs Zone have varied among years.

Spatial patterns

From 1991 up until the second mortality event in 1998 most Sardines were taken from Spencer Gulf (Figure 2–3). From 1999 onwards, a small proportion of the catch has usually been taken from the Outside Zone, mainly off Coffin Bay (Figure 2–3, 2–4). In 2002 and 2003, the fishery expanded northwards in Spencer Gulf (Figure 2–4). From 2003 to 2012, significant catches were also taken from Investigator Strait in most years. Since 2010, when additional quota was allocated outside Spencer Gulf, an increasing proportion of the total catch has been taken from the eastern Great Australian Bight. More than 6,500 t have been taken from the Outside Zone since 2014 (Figure 2–3). In 2017, the TACC from the outside Zone was increased to 12,750 t. In 2017 and 2018 significant catches were taken south of Kangaroo Island.

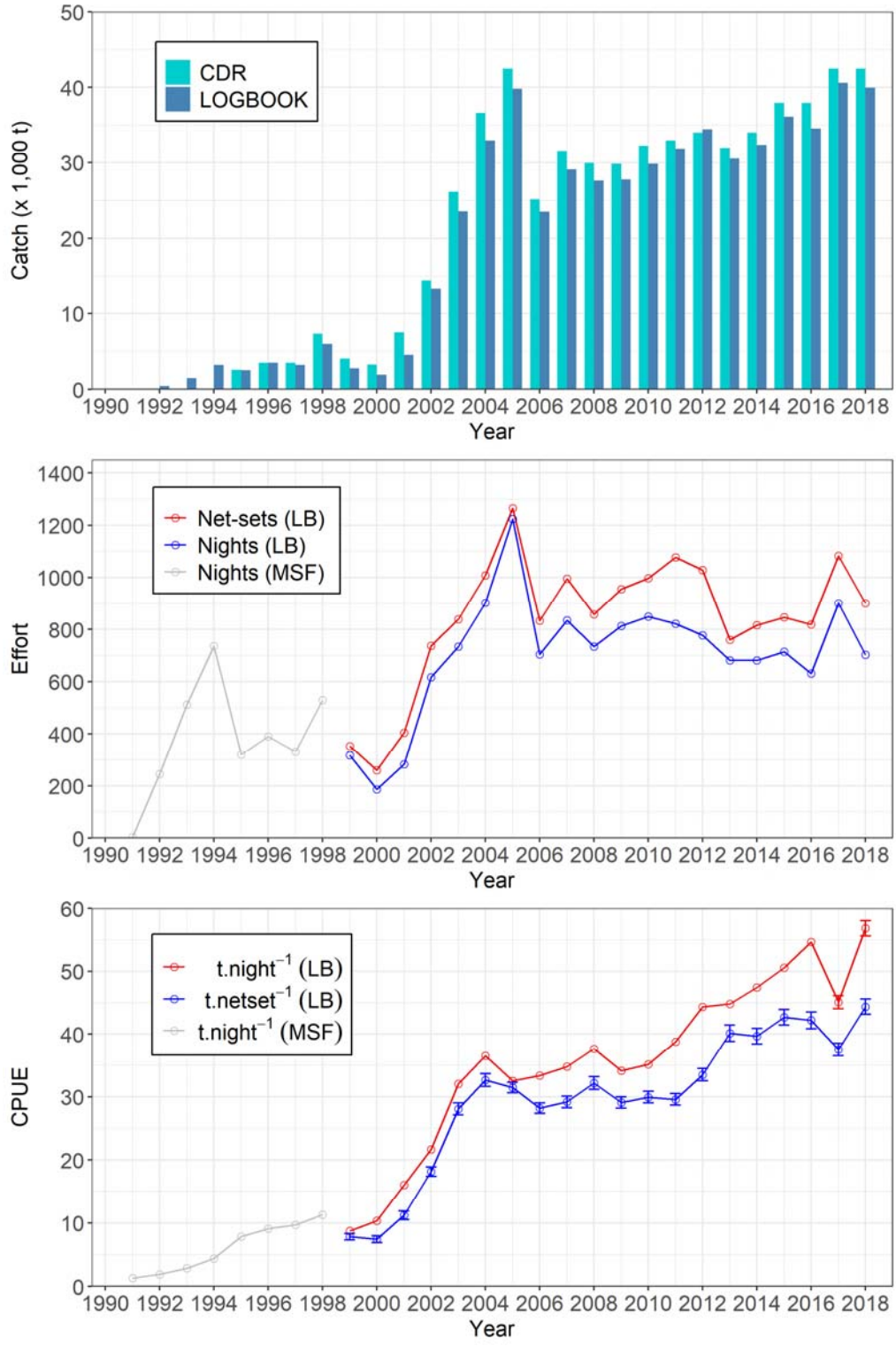

Figure 2-1. Total catches (estimated from logbooks, CDR), fishing effort (nights, net-sets) and mean annual CPUE (t.night^{-1}, t.net-set^{-1}, ± SE). Data prior to 1999 is derived from Marine Scalefish Fishery (MSF) records, specific SASF logbooks (LB) were introduced in 1999.

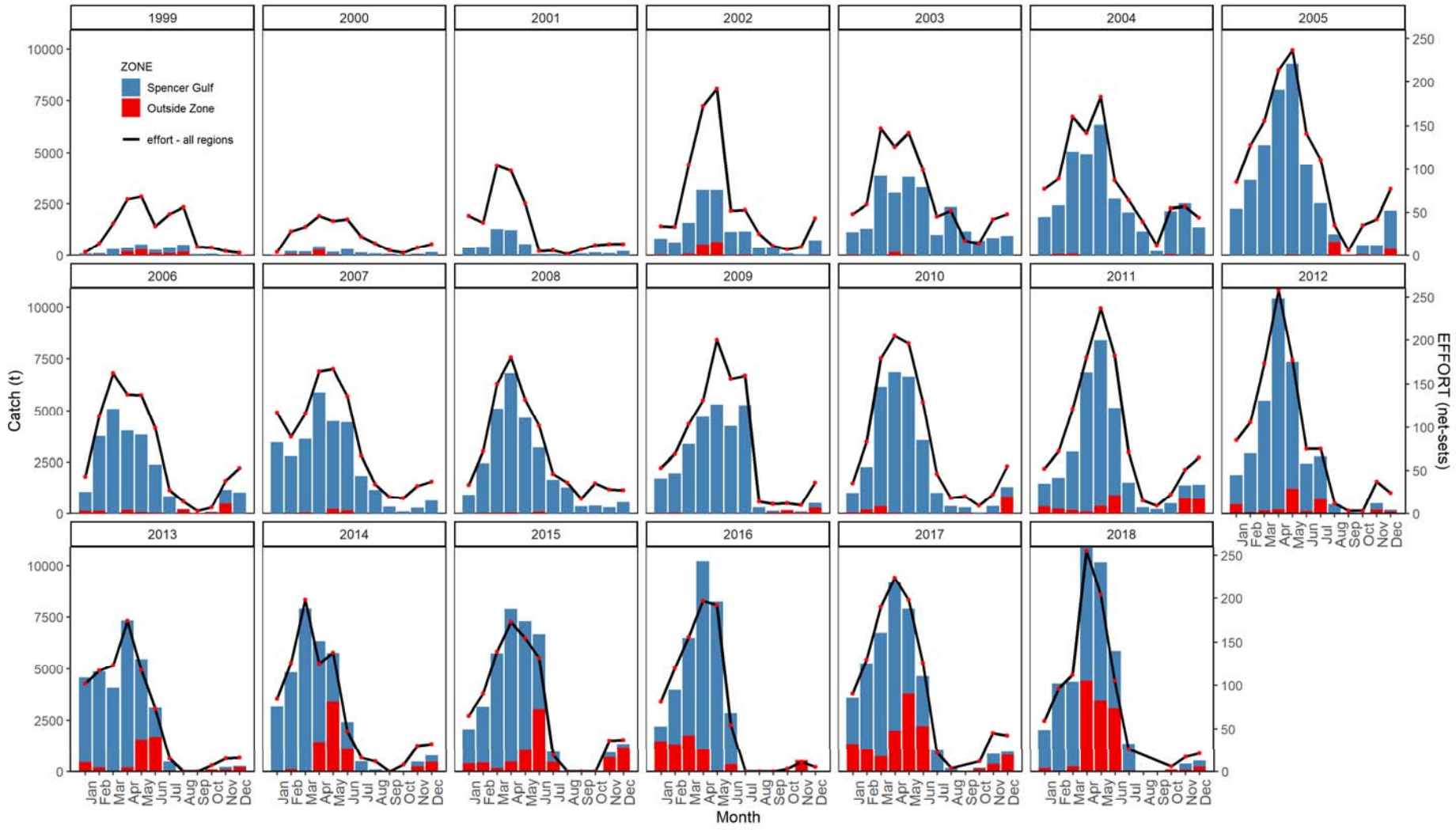

Figure 2-2. Intra-annual patterns in Sardine catch (tonnes, bars) by region and effort (net-sets, red points with black lines, all regions) in SASF between 1999 and 2018

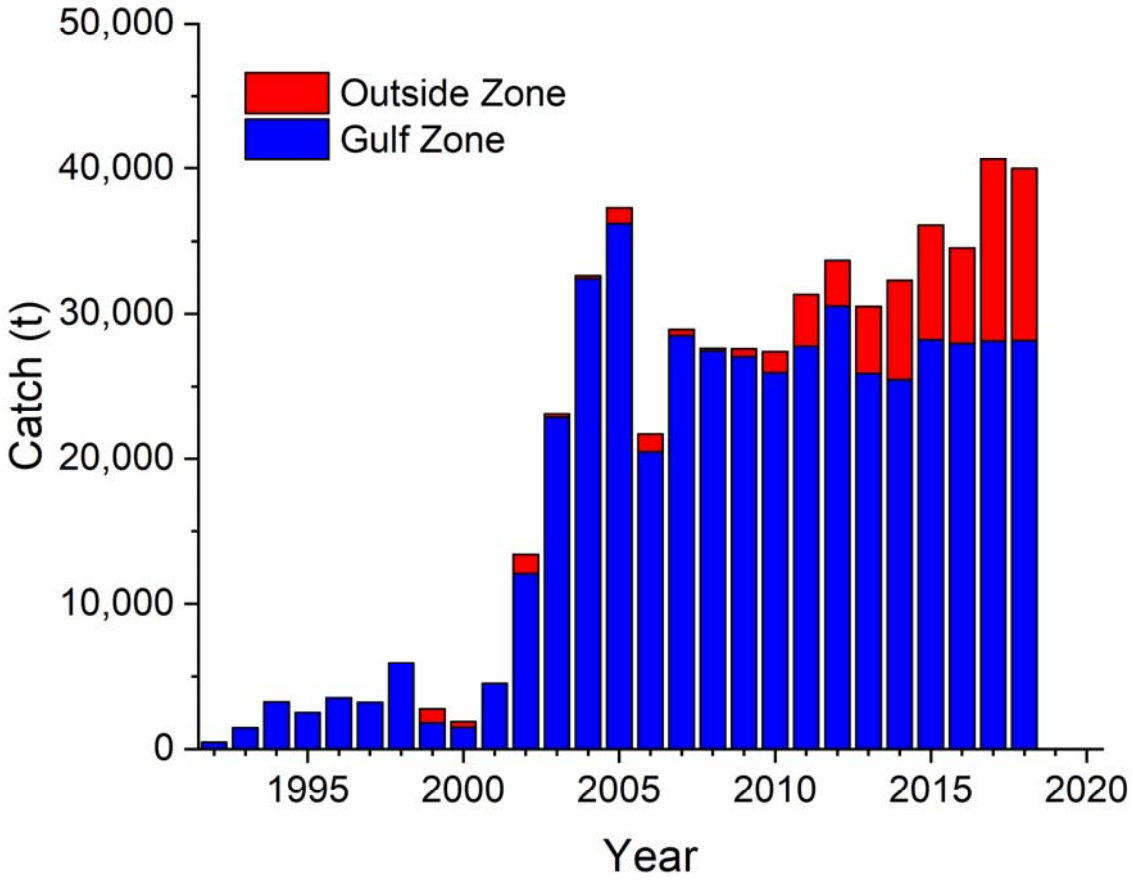

Figure 2-3. Annual Sardine catch (tonnes) by zone between 1992 and 2018.

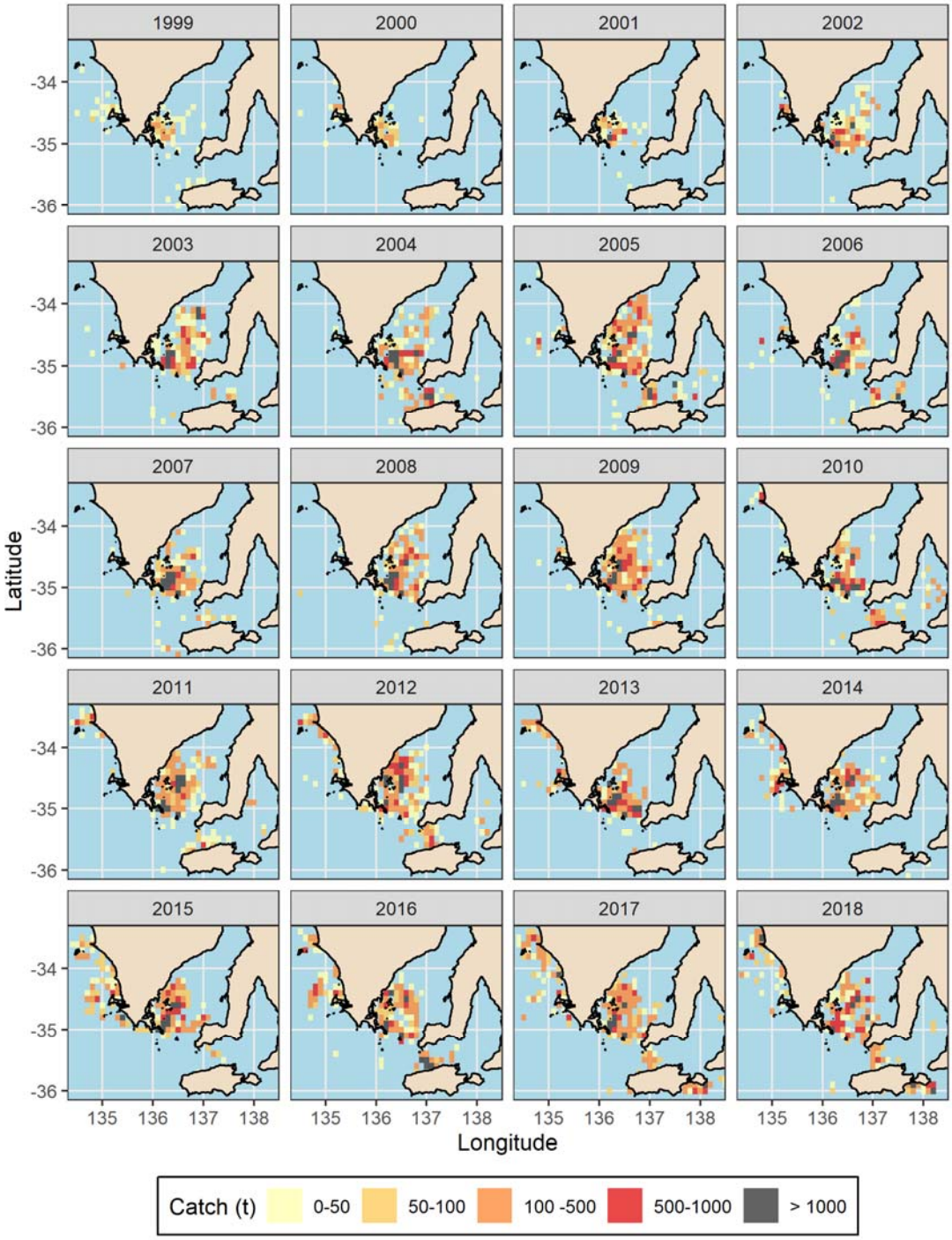

Figure 2-4. Spatial trends in Sardine catches (tonnes) between 1999 and 2018

2.3.2 Catch composition

Size frequency

In 1995, the modal size for Sardine caught in the Gulfs Zone was 140 mm FL with fish mostly ranging from 130 to 170 mm FL (Figure 2–5). The modal size of Sardine in the Gulfs Zone declined to 130 mm FL in 1996 and was 120 mm FL in 1998. Between 1999 and 2002, Sardine from the Gulfs Zone were mostly >140 mm FL with modes between 150 and 170 mm FL. In 2003 and 2004, catch samples were bimodal as significant quantities of juveniles (80–120 mm FL) were caught in addition to adults (150–180 mm FL). Prior to 2003, few catch samples from the Gulfs Zone included Sardine ≤100 mm FL. Between 2005 and 2010, size distributions from the Gulfs Zone remained stable with a mode at 140–150 mm FL and fish ranging from 120 to 190 mm FL. The modal size declined to 130 mm FL in 2011 and 2012. In 2013–2016, the mode increased to 140 mm FL and in 2017 and 2018 the modal size was 150 mm FL (Figure 2-5).

Larger size ranges have been caught in the Outside Zone throughout the history of the fishery. In the Outside Zone Sardine of 150–180 mm FL dominated catches between 1995 and 1998 (Figure 2–6). In 1999, after the second mortality event the modal length fell to 130 mm FL, but increased to 140 mm FL in 2000. In 2004, the modal size was 140 mm FL and this increased to 170–190 mm FL in 2005–06. Few fish were taken in the Outside Zone in 2007–09 (none sampled in 2009). Between 2010 and 2013, the modal size for fish from the Outside Zone remained at 160 mm FL. In 2014 catches were bimodal, with modes at 130 and 170 mm FL. The modal size was 160 mm FL in 2015 and 2016. In 2017 and 2018 sizes were evenly spread over a wide size range from 90 to 190 mm FL.

Mean size

The mean size of Sardine from Spencer Gulf ranged from 133 to 149 mm FL between 1995 and 1998 and rose to 166 mm FL in 2002 (Figure 2–7). Between 2003 and 2009, mean fish length in Spencer Gulf was relatively stable between 148 and 159 mm FL and declined to 128 mm FL in 2012. The mean length in Spencer Gulf between 2013 and 2018 was stable and ranged from 139 to 149 mm FL.

The mean size of Sardine from the Outside Zone was generally higher than Spencer Gulf (Figure 2–7), particularly in 2005 and 2006. Between 2010 and 2016, the mean size remained stable and ranged between 155–163 mm FL, but then dropped to 144 mm FL in 2017. In 2018 the mean size of Sardine from the Outside Zone was 150 mm FL.

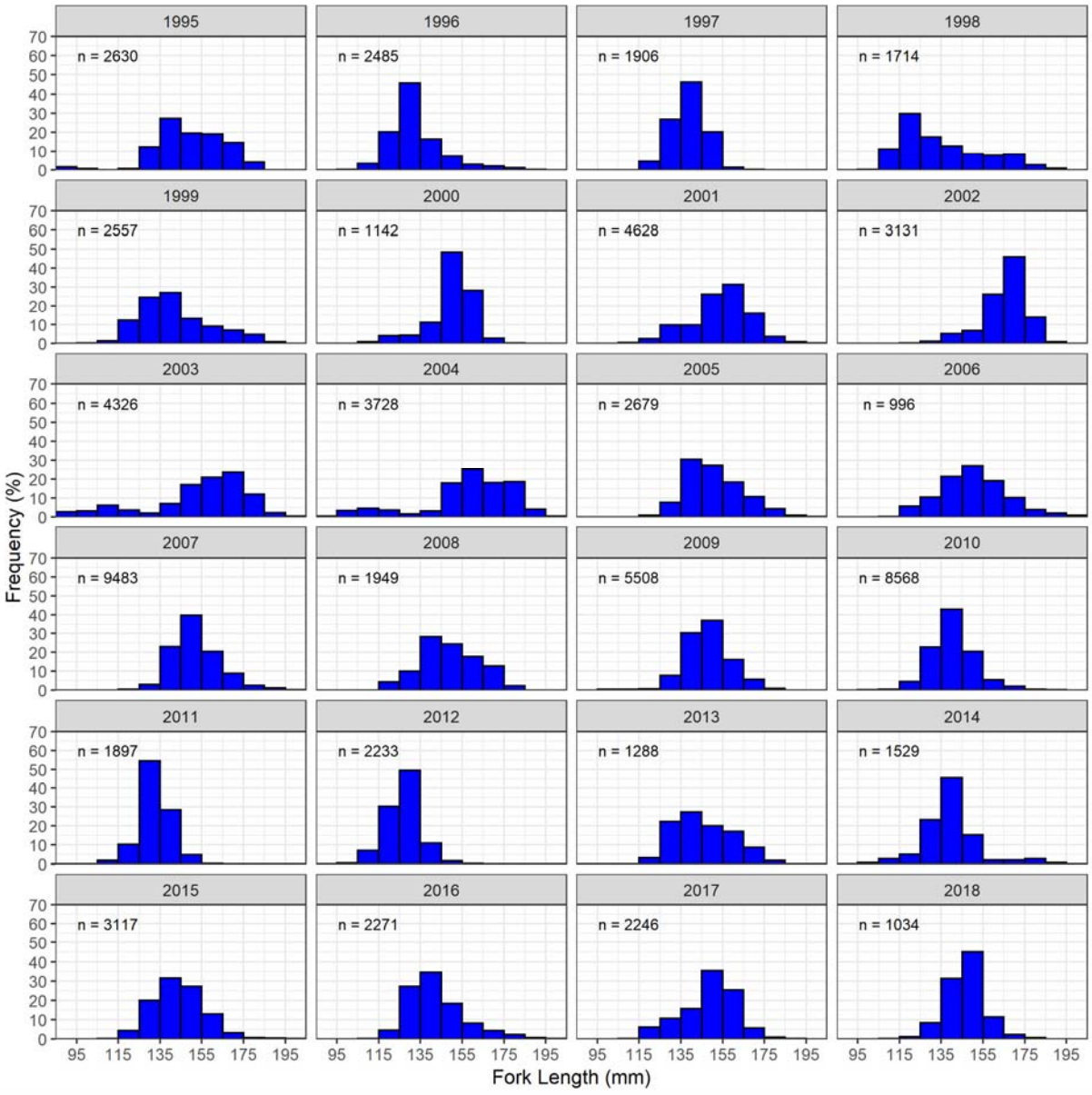

Figure 2–5. Length frequency distributions of Sardine from commercial catch samples for the Gulfs Zone between 1995 and 2018.

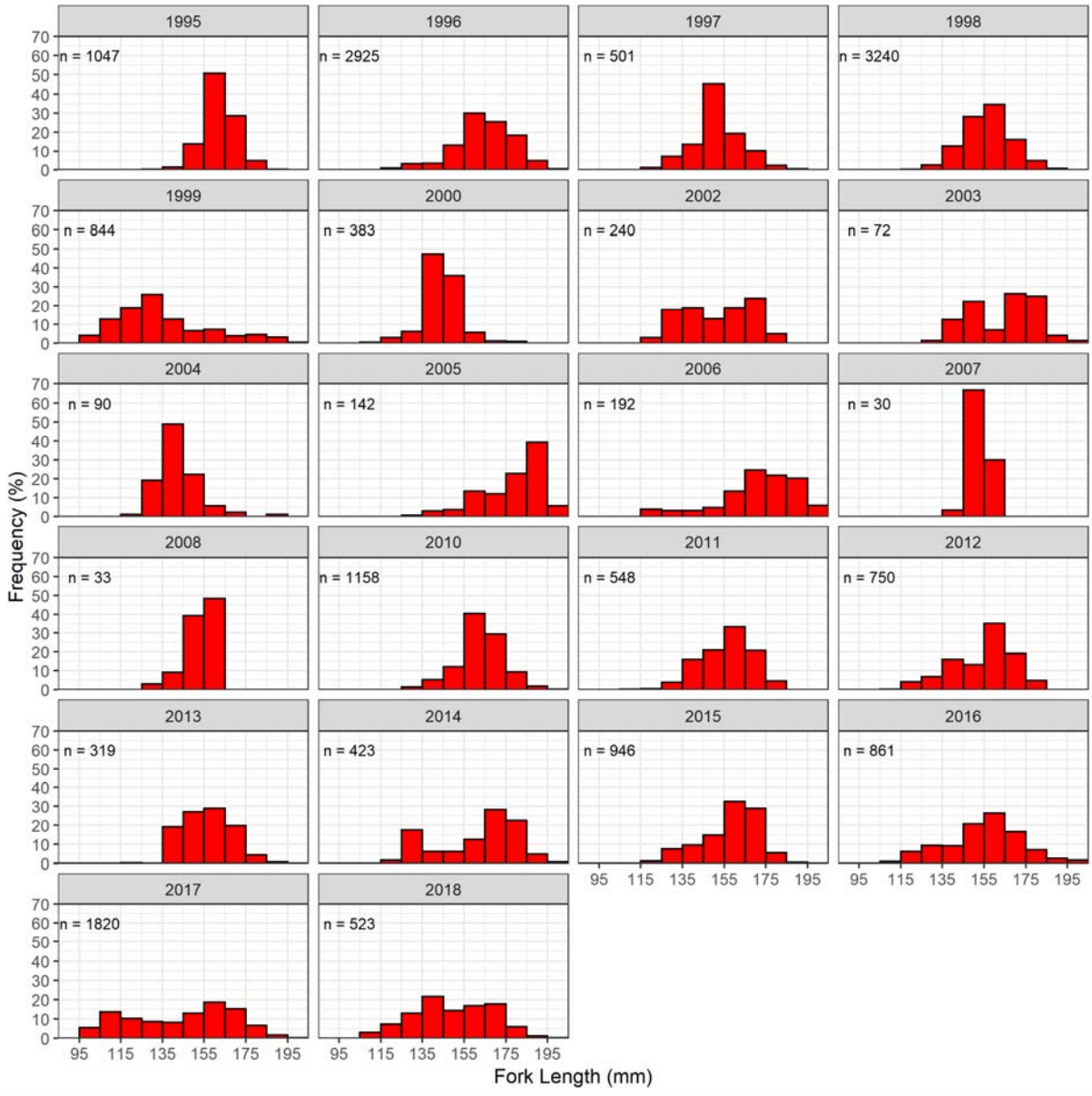

Figure 2–6. Length frequency distributions of Sardine from commercial catch samples for the Outside Zone between 1995 and 2018.

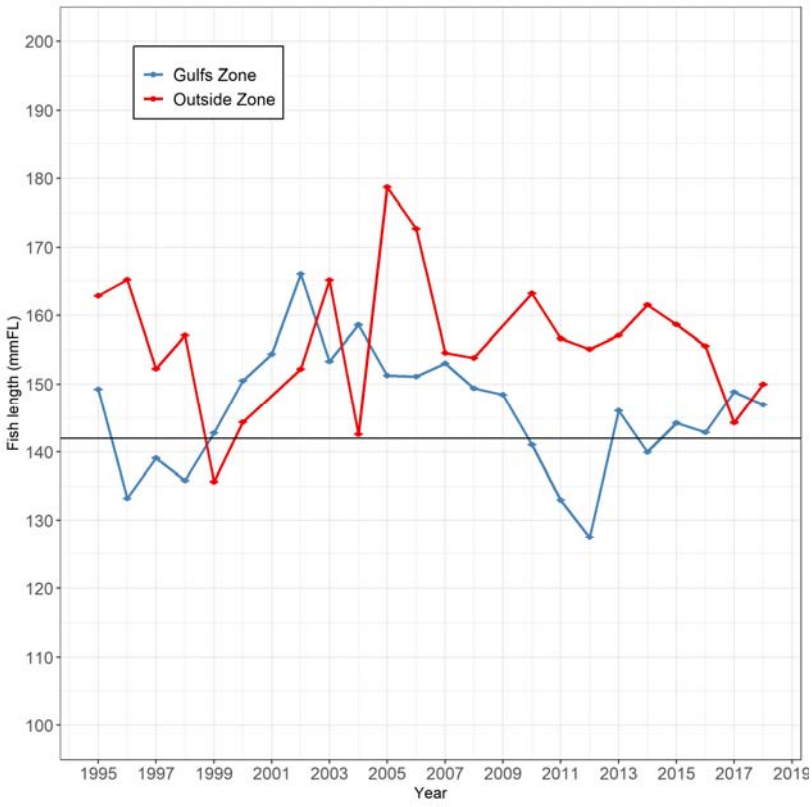

Figure 2–7. Average fork length (mm FL) by year for commercial samples from the three regions of the SASF, error bars are standard error. Horizontal line indicates the reference point for maximum catch limit for the Gulfs Zone of 142 mm FL (Table 1–2).

Sex ratio

The mean sex ratio (by number) in commercial catches has varied over the history of the fishery. Exact ratio tests indicated significant differences between the sexes caught in several years (Table 2–1) which always resulted in a higher proportion of females (Figure 2–8). The highest proportion of females occurred in 1995 and 2005 at 63%, while the lowest proportion of females was 47% which occurred in 2000 and 2013 (Figure 2–8).

Table 2–1. Mean annual sex ratios for commercial catch samples from all regions between 1995 and 2018. Data were unavailable for 2007.

Year	Females	Males	nf/(nm+nf)
1995	1248	728	0.63
1996	1501	1049	0.59
1997	317	251	0.56
1998	1088	928	0.54
1999	1117	779	0.59
2000	358	398	0.47
2001	1461	929	0.61
2002	1662	1412	0.54
2003	2020	1715	0.54
2004	1827	1477	0.55
2005	1601	959	0.63
2006	608	585	0.51
2008	1168	797	0.59
2009	3088	2317	0.57
2010	4078	4152	0.50
2011	923	929	0.50
2012	1003	1063	0.49
2013	682	760	0.47
2014	828	843	0.50
2015	1445	1540	0.48
2016	1793	1515	0.54
2017	1751	1319	0.57
2018	1047	878	0.54

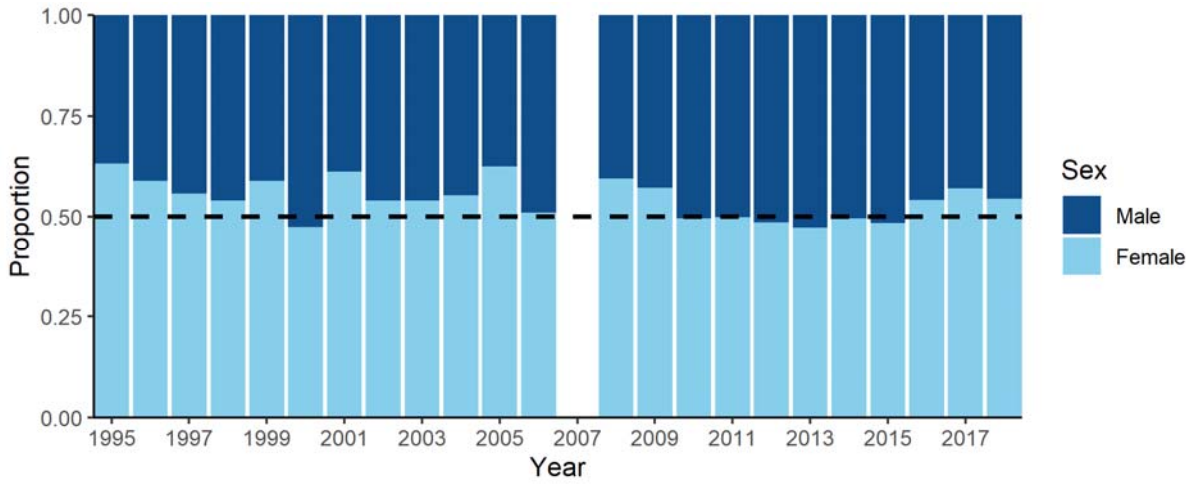

Figure 2–8. Sex ratio of commercial catch samples from all regions between 1995 and 2018. Data are unavailable for 2007. Dashed line represents a 1:1 sex ratio.

2.4 Discussion

One of the most notable features of the SASF has been its rapid growth. The TACC for 2017-19 of 42,750 t was 40 times the TACC in 1992 (1,000 t) and more than ten times the TACC in 2000 (3,500 t). This rapid growth has occurred despite the impacts of two mass mortality events, each of which killed more fish than any other single-species mortality event recorded (Jones et al. 1997, Ward et al. 2001b).

Another notable feature of the SASF is the stability in catches over recent years. This stability has been achieved by establishing a precautionary harvest strategy that addresses the imprecision in estimates of spawning biomass obtained using the DEPM. Under the current harvest strategy for the SASF, the maximum TACC of 47,500 t can only be set when DEPM surveys and integrated stock assessments are done annually and the spawning biomass is greater than the upper target reference point of 190,000 t. The maximum TACC at Tier 2, where the fishery is currently positioned, in 42,750 t, with DEPM surveys done annually and integrated stock assessments done every second year.

The concentration of fishing effort in a relatively small proportion of the total area over which the managed population is distributed is also a notable feature of the SASF. Since 2010, a range of management arrangements have been implemented to limit the catch from Spencer Gulf, reduce the capture of small fish from the gulf and increase the catch from the Outside Zone. This approach culminated in the establishment of explicit rules for limiting the total catch that can be taken from the Gulfs Zone, based on the mean size of fish taken from that Zone in the previous year. This approach has been successful in increasing the mean size of fish taken from the Gulfs Zone. The spatial management arrangements have also resulted in a shift in effort and catch. The percentage of the catch taken in the Outside Zone increased substantially between 2010 and 2018. The maximum catch recorded in CDRs from the Outside Zone was 12,141 t in 2018, which represented 29.5% of the total catch that year.

Changes in management arrangements and fishing patterns over the history of the SASF have influenced the size composition of fish taken in catches. In particular, size-based decision rules implemented in 2010 have resulted in fishers selectively targeting large fish in the Gulfs Zone. Recent catches from the Outside Zone have also contained larger fish than samples from the Gulfs Zone. Size composition data from the commercial catch are unlikely to be representative of the population; size selectivity is likely to have changed over time.

The increase in CPUE over the history of the SASF reflects increased catch capacity of the fleet. The reduction in CPUE in 2017 was interpreted by fishers to reflect a change in schooling behaviour during that year. The results of the DEPM survey for 2017 did not suggest that the population had declined in 2017. These results reaffirm the unsuitability of CPUE for monitoring the abundance of pelagic fishes taken in a purse-seine fishery. CPUE is not used as an index of abundance in the population modelling undertaken in Chapter 5.

3. AGE COMPOSITION AND REPRODUCTIVE BIOLOGY

3.1 Introduction

Age determination studies of Sardine have involved counting growth increments in scales (Blackburn 1950) and sagittal otoliths (ear bones) (Butler et al. 1996, Fletcher and Blight 1996), and modelling the formation of marginal increments in otoliths (Kerstan 2000). Daily deposition of growth increments in the otoliths of larvae and juveniles has been validated in laboratory trials (Hayashi et al. 1989). Age validation studies involving the capture and maintenance of Sardine and other clupeoids have proven to be problematic owing to logistical difficulties (Fletcher 1995) and sensitivity to handling (Rogers et al. 2003). Other methodological approaches have been used to show that translucent zones form annually in the sagittae of 1+ year old Sardine off South Africa (Waldron 1998), ≤2+ year olds off North America (Barnes et al. 1992) and ≥4+ year olds off Western Australia (Fletcher and Blight 1996). Despite this theoretical basis for using increment-based age-determination methods, the application of these standard approaches has proven to be problematic in Western Australia, South Australia and California due to difficulties associated with interpreting and counting opaque and translucent zones (Butler et al. 1996, Fletcher and Blight 1996, Rogers and Ward 2007).

Studies of growth dynamics of Sardine in the Benguela and California Current systems suggest that growth rates of larvae (up to 0.85 mm.day^{-1}) and juveniles (0.48–0.63 mm.day^{-1}) are high (Butler et al. 1996, Quinonez-Velazquez et al. 2000). In South Africa, Sardine were found to reach larger asymptotic sizes ($L\infty$ = 221 mm) and have lower growth constants (k = 1.09 year^{-1}) than those off southern California ($L\infty$ = 205 mm, k = 1.19 year^{-1}, Thomas 1984, Butler et al. 1996). Parameter estimates for Sardine in Western Australia (Fletcher and Blight 1996) suggest that growth in this area is slower and that fish reach smaller asymptotic sizes than those in the more productive eastern boundary current systems.

A detailed study by Rogers and Ward (2007) showed that the growth rates of Sardine are higher in South Australian waters than off other parts of the Australian coastline, but lower than those in more productive boundary current ecosystems (Ward et al. 2006). A notable finding of the study was that fish in commercial catches were younger (and smaller) than those obtained in fishery-independent samples. This finding has implications for the use of age structured models (based on fishery samples) for stock assessment of the SASF (see Chapter 5).

This chapter describes the methods used to determine age compositions from the commercial catch of Sardine in South Australian waters. Catch-at-age information presented in this chapter is key input to the population model presented in Chapter 5.

3.2 Methods

3.2.1 Age-determination

Otolith preparation and interpretation

Sagittal otoliths were collected from sub-samples (n = 10–20) of the commercial catch samples and fishery-independent samples (Chapter 2). Otoliths were soaked overnight in 10% sodium hypochlorite solution to remove excess tissue, rinsed in distilled water and dried in IWAKI™ plastic microplates. Translucent zone counts were made for one whole otolith from each fish under reflected light, immersed in water against a flat black background (Butler et al. 1996).

Readability indices (RI)

Sardine otoliths were classified as 1 = excellent, 2 = good, 3 = average, 4 = poor and 5 = unreadable based on standard criteria relating to their interpretability (see Rogers and Ward 2007).

Decimal age estimates from annuli counts

To estimate decimal age for adults with a translucent zone count of one or more an arbitrary birth-date of March 1 was assigned, which represents the time of peak spawning. The midpoint of translucent zone formation was assumed to be mid-winter (Rogers and Ward 2007). Decimal age (A) was calculated as:

$$A = \begin{cases} (\alpha - \beta_p)/365 + TZC + 0.334 & \alpha \le \beta_s \\ (\alpha - \beta_s)/365 + TZC + 0.334 & \alpha > \beta_s, \end{cases}$$

where α is the date of capture, β_s is the assumed translucent zone formation date from the same year as α, β_p is the assumed translucent zone formation date from the previous year, TZC is the translucent zone count and 0.334 (4 decimal months) adjusts for the difference between the assigned birth-date and the approximate timing of the first translucent zone.

Age estimations from otolith weight

The relationship between age and otolith weight was determined using a linear model fitted to decimal age and otolith weight data from those otoliths with readability scores of 1 and 2. Aged otoliths from commercial catch samples between 1995 and 2018 and fishery-independent samples between 1998 and 2018 were pooled for the analysis. The resulting model was used to derive an age estimate for all otoliths based on otolith weight. Due to the change in the spatial patterns of fishing over time it is not possible to separate annual effects from regional effects on the relationship (i.e. region and season were confounded), so data from all regions were used in the analysis

3.2.2 Size-at-maturity

Ovaries were staged macroscopically where stage 1 = immature, stage 2 = maturing, stage 3 = mature, stage 4 = hydrated (spawning) and stage 5 = spent (recently spawned). Testes were staged where stage 1 = immature, stage 2 = mature and stage 3 = mature (running ripe). Only fish sampled during the spawning season (1 December to 31 March) were included as outside of this period stages 2 and 5 are difficult to macroscopically differentiate.

The length at which 50% of the population was mature (L_{50}) was estimated using Binomial GLM's with a logit link function (logistic regression). The model was fitted to separately for males and females using binary maturity assignments where immature = 0 (stage 1) and 1 = mature (stages ≥ 2). The proportion of the mature population at length '*L'* calculated as:

$$P(L) = P_{max}\left(1 + e^{-\ln(19)\left(\frac{L-L_{50}}{L_{95}-L_{50}}\right)}\right)^{-1}$$

where *P(L)* is the proportion of the population mature at fork length '*L'* and P_{max} is the maximum proportion of mature individuals. Size-at-maturity models were fit to each sampling year to determine if L_{50} has changed over the history of the fishery. Some years were omitted as insufficient data were collected within the spawning season to accurately fit the model.

A size-at-maturity ogive was produced using the data pooled across all years and fishery dependent and independent sampling. These data were also restricted to within the spawning season and Gulfs Zone.

3.2.3 Growth

Length-at-age was estimated using the standard von Bertalanffy growth function (VBGF) fitted to individuals that were aged with a readability score of 1 or 2. Discrete ages were converted to decimal ages using the methods outlined previously. Preliminary analyses indicated that growth was not sex dependent and therefore the sexes were pooled. This allowed the inclusion of juvenile fish that were aged using daily ring counts and had been too young to accurately determine sex (Rogers and Ward 2007). The VBGF was represented by the equation:

$$L_t = L_\infty - (L_\infty - L_0)e^{-kt}$$

Where L_t was the length at time 't', L_∞ was the asymptotic length, k was the growth completion parameter (yr^{-1}) and L_0 was the length-at-age-zero. Length-at-age 95% confidence intervals were computed using 1000 bootstrap iterations.

3.2.4 Gonosomatic index (GSI)

Mean monthly gonosomatic indices (GSI) were calculated from both fishery independent and commercial samples using the equation:

$$GSI = \left[\frac{Gwt}{Fwt_{gonadfree}} \right].100$$

where *Gwt* is gonad weight and *Fwt* is gonad-free fish weight for fish with gonads of macroscopic stages ≥ 2. The mean estimate of GSI of all fish above size-at-maturity was used for both males and females to determine spawning season. It is important to note that it is sometimes difficult to macroscopically distinguish between Stage 2 and Stage 5 gonads in frozen samples.

3.3 Results

3.3.1 Age-determination

Between 1995 and 2016, a total of 20,541 otoliths from commercial and fishery-independent samples were read (Table 3–1). Otolith reads were not conducted for otoliths collected in 2017 and 2018. Less than 0.1% were assigned a Readability Index (RI) score of 1, while 6.0%, 50.0% and 27.6% were assigned scores of 2, 3 and 4, respectively. Approximately 16.4% were assigned an RI of 5 (Figure 3–1, Table 3–1 and 3–2).

Table 3-1. Summary of otolith Readability Index scores for otoliths collected between 1995 and 2016.

	Readability					
Year	**1**	**2**	**3**	**4**	**5**	**Total**
1995	0	87	411	159	2	659
1996	1	145	367	109	10	632
1997	0	154	275	54	3	486
1998	18	200	800	262	11	1,291
1999	0	50	546	389	18	1,003
2000	2	82	490	65	2	641
2001	0	59	1,431	689	113	2,292
2002	0	53	1,527	895	133	2,608
2003	0	39	1,057	229	18	1,343
2004	10	121	690	465	265	1,551
2005	1	13	301	235	368	918
2006	0	9	180	135	469	793
2008	0	9	144	183	303	639
2009	0	27	314	370	784	1,495
2010	4	64	469	577	74	1,188
2011	1	7	111	138	91	348
2012	0	0	9	14	13	36
2013	0	15	222	146	143	526
2014	0	9	253	150	110	522
2015	0	6	297	184	310	797
2016	0	33	389	224	127	773
2017	0	0	0	0	0	0
2018	0	0	0	0	0	0
All Years	**37**	**1182**	**10283**	**5672**	**3367**	**20,539**

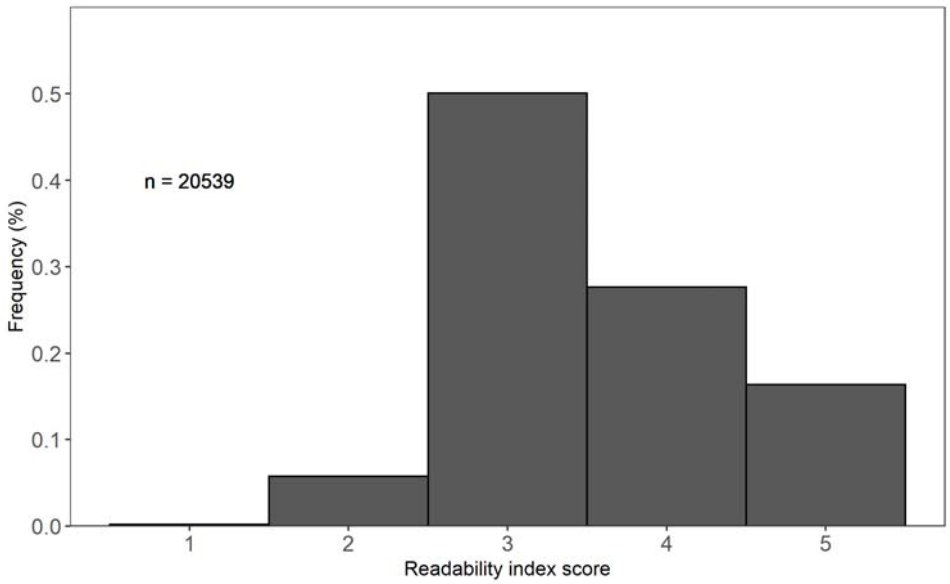

Figure 3-1. Readability Index scores assigned to otoliths from all samples between 1995 and 2016.

Otolith weight relationship

The modelled relationship between decimal age and otolith weight provided a reasonable fit to the data (R^2 = 0.77; Figure 3–2). However, while the 95% confidence intervals were narrow, the variation around the linear relationship was large. Therefore, while age can be inferred from otolith weight, the lack of precision resulting from this method means that these age estimates must be used with caution.

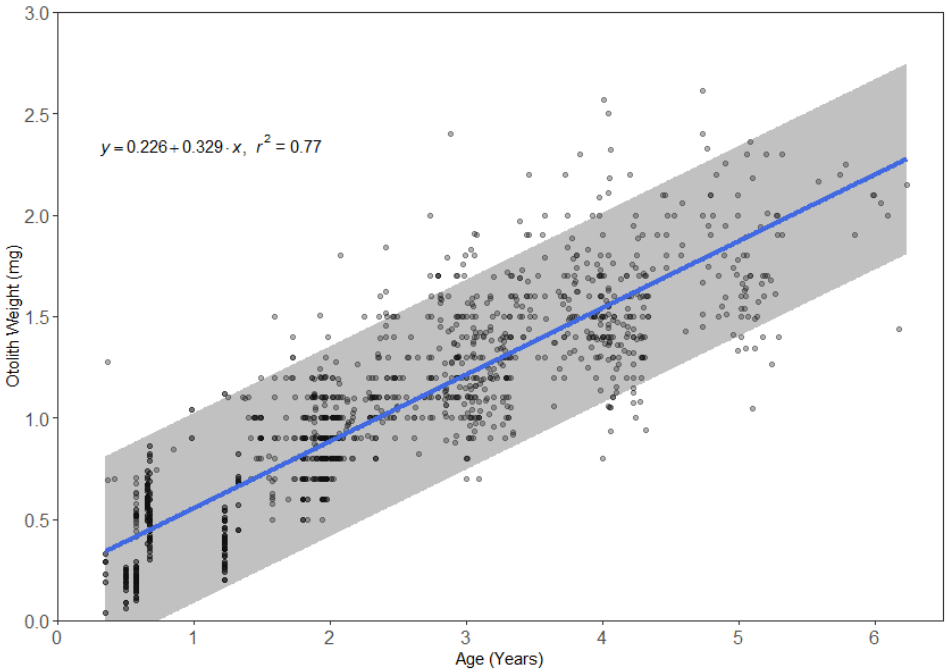

Figure 3-2. Regression of decimal age and otolith weight for Sardine otoliths of readability 1 and 2 from commercial and fishery-independent samples collected between 1995 and 2016. The light grey area represents 95% confidence intervals.

3.3.2 Age composition

Age composition data from commercial catches were available from 1995 to 2018, with the exception of 2007 when no otoliths were collected. Ages ranged from 0+ to 8+ years. In 1995, fish aged 2+, 3+, and 4+ years dominated catches from the Gulfs Zone, but in 1996–1998, catches were mostly dominated by age 1+ and 2+ fish, with a noticeable reduction in older fish in 1997 (Figure 3–3). These trends reflect the 1995 mass mortality event which mainly affected adult fish. In 1999, 2+ year olds (fish that were juveniles in 1998 and largely unaffected by the 1998 mass mortality event) dominated the catch. Fish that were spawned during 1997 and 1998 continued to dominate catches from the Gulfs Zone as 2+ and 3+ year olds in 2000. From 2001 to 2009, 3+ year olds dominated the catch from the Gulfs Zone in all years, except 2006 and 2008, when 2+ year olds were most abundant in catch samples (Figure 3–3). From 2010 to 2012, 2+ year olds dominated catches from the Gulfs Zone whereas from 2013 to 2018, 3+ year old fish were most abundant.

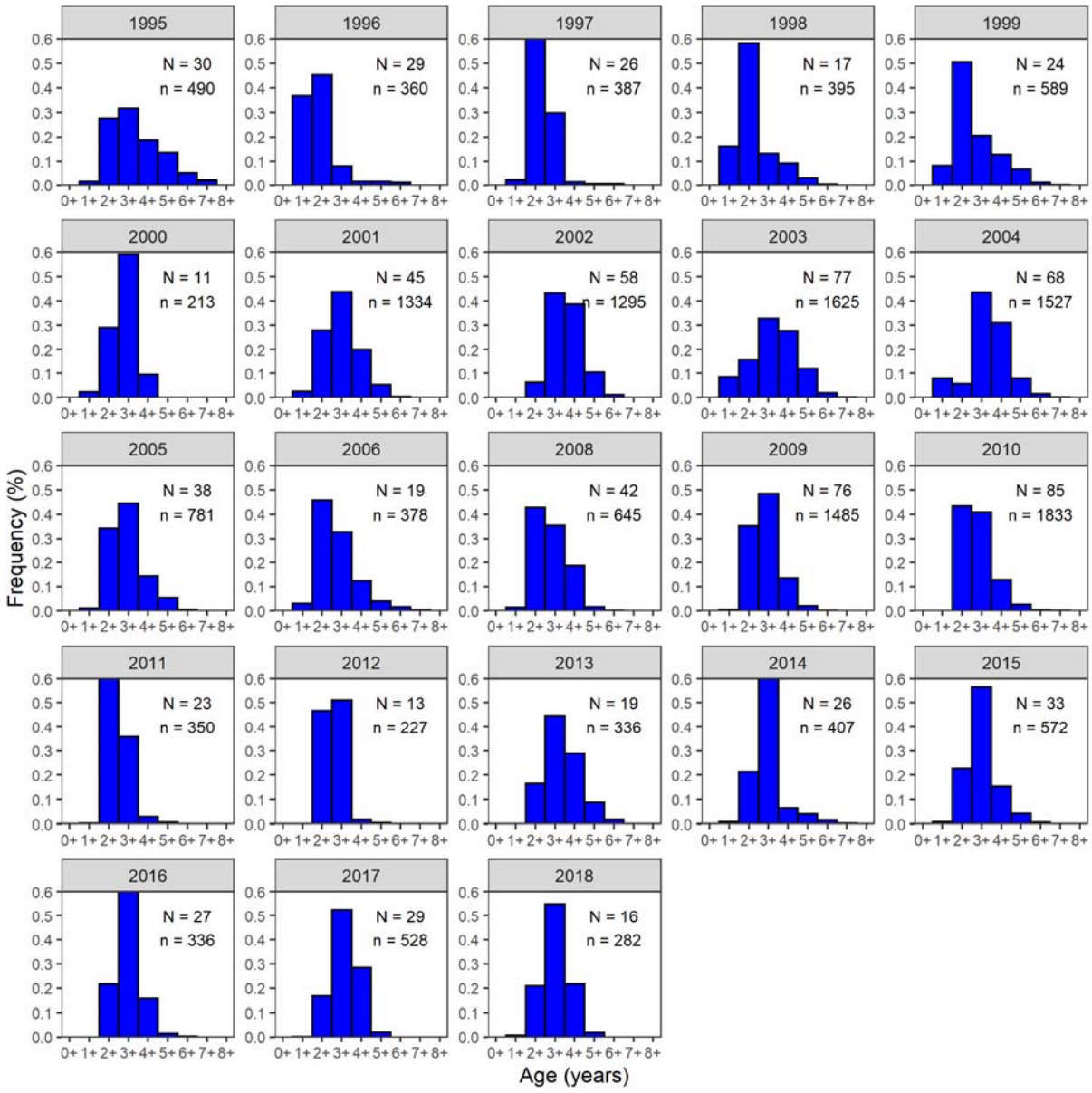

Figure 3-3. Age distributions for commercial catch samples of Sardine from the Gulfs Zone between 1995 and 2018. Note that no data were available for 2007. Ages are derived from an otolith-weight-age relationship calculated for all years from readability 1 and 2 otoliths and applied to all weighed otoliths for each year.

Catches from the Outside Zone have generally been comprised of older fish than those from the Gulfs Zone (Figure 3–4). In most years, fish aged 3+, 4+ and 5+ years dominated catches from the Outside Zone. However, fish aged 2+ years dominated catches in 1999, immediately after the 1998 mortality event, as well as in 2000 and in 2004. In 2018, 2+ year olds were the most abundant age class although all year classes up to 6+ were well represented.

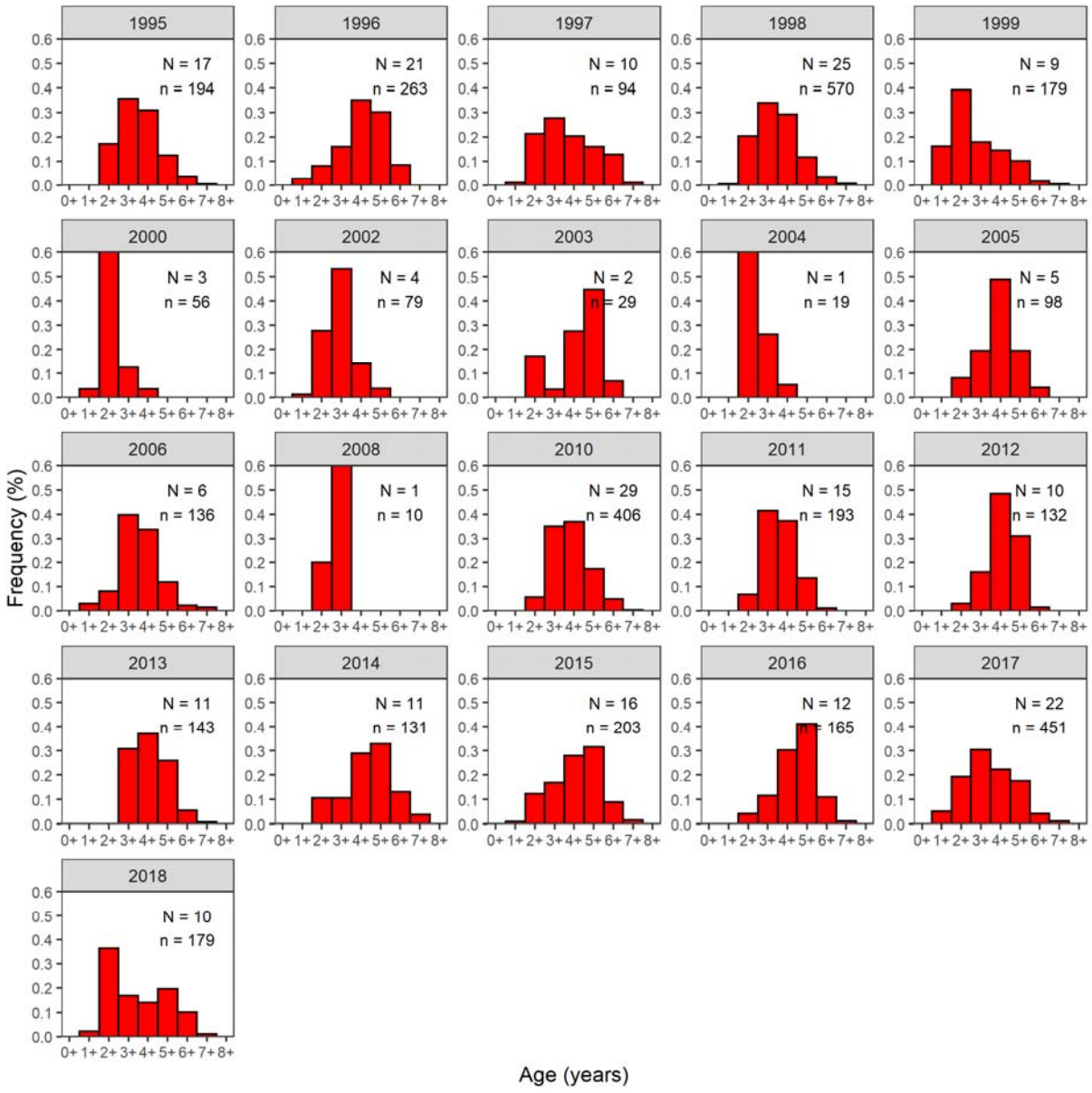

Figure 3-4. Age distributions for commercial catch samples of Sardine from the Outside Zone between 1995 and 2018. Note that no data were available for 2007. Ages are derived from an otolith-weight-age relationship calculated for all years from readability 1 and 2 otoliths and applied to all weighed otoliths for each year.

3.3.3 Growth

Fixing t_0 is a common approach for species whose life history includes a larval phase. The best fitting VBGF curve provided parameter estimates of: L_∞ = 177.8, mmFL, k = 0.71 year^{-1}, L_0 = 3.45 mmFL (Figure 3–5).

3.3.4 Size-at-maturity

Size-at-maturity (SAM, L_{50}) estimated for Sardine from the commercial catch samples from Gulfs Zone between 1995 and 2016 varied slightly among seasons (Figure 3–6). SAM could not be estimated in 1998, 2007, 2012, 2013 and 2014 due to a lack of commercial samples collected during the spawning season. The inter-annual variation that occurred was due to differing sample sizes between years. All males below 116 mm FL and females below 118 mm FL had immature gonads. The estimate of L_{50} using data from all years combined was 139.3 mm FL and 143.5 mm FL for males and females, respectively (Figure 3–7).

3.3.5 Gonosomatic index (GSI)

There was a large amount of seasonal variability in GSI. However, sample size was variable, with sufficient samples obtained only from the Gulfs Zone in most years. GSI peaked between November and March (Figure 3–8). Very high values occurred in February which resulted from fishery-independent surveys in this period targeting spawning fish. Higher mean GSI values were observed for males than females, which may be caused by male gonads not decreasing in size as much as females after each spawning event. Higher mean GSI values were also observed from larger fish.

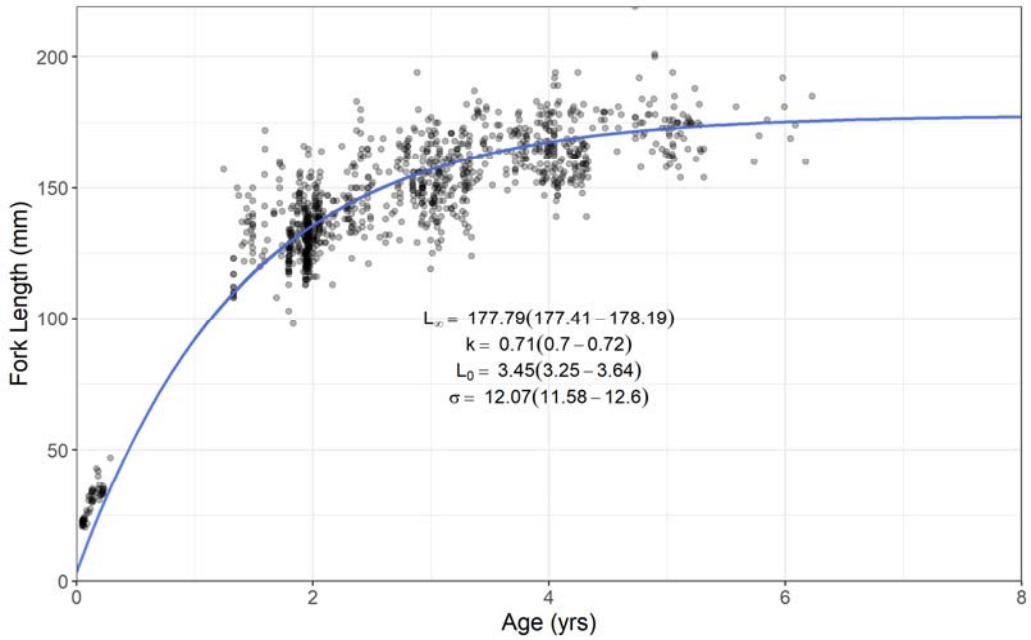

Figure 3-5. von Bertalanffy growth model fitted to length-at-age data (grey points) of individuals with readability scores of 1 or 2 collected between 1995 and 2016. The grey shaded area represents 95% confidence intervals.

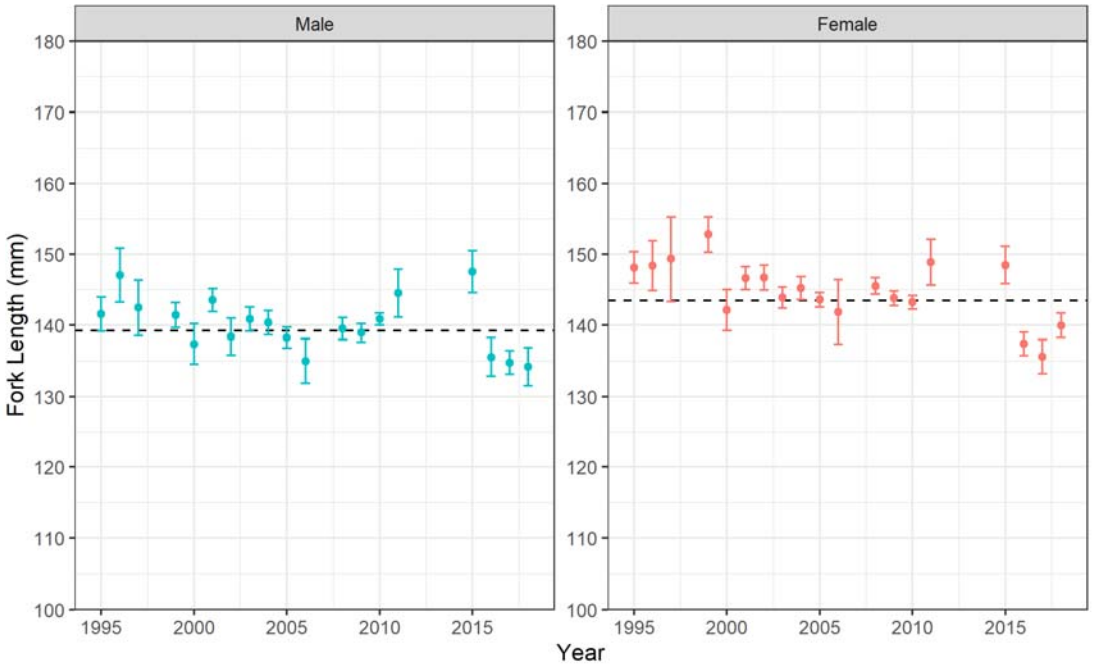

Figure 3-6. Size-at-maturity (L_{50}) for male and female Sardine collected in Gulfs Zone by year, between 1995 and 2018. Some years were omitted due to low sample size. Error bars are 95% confidence intervals. Dashed lines represent the mean L_{50} across all years calculated in Figure 3–6.

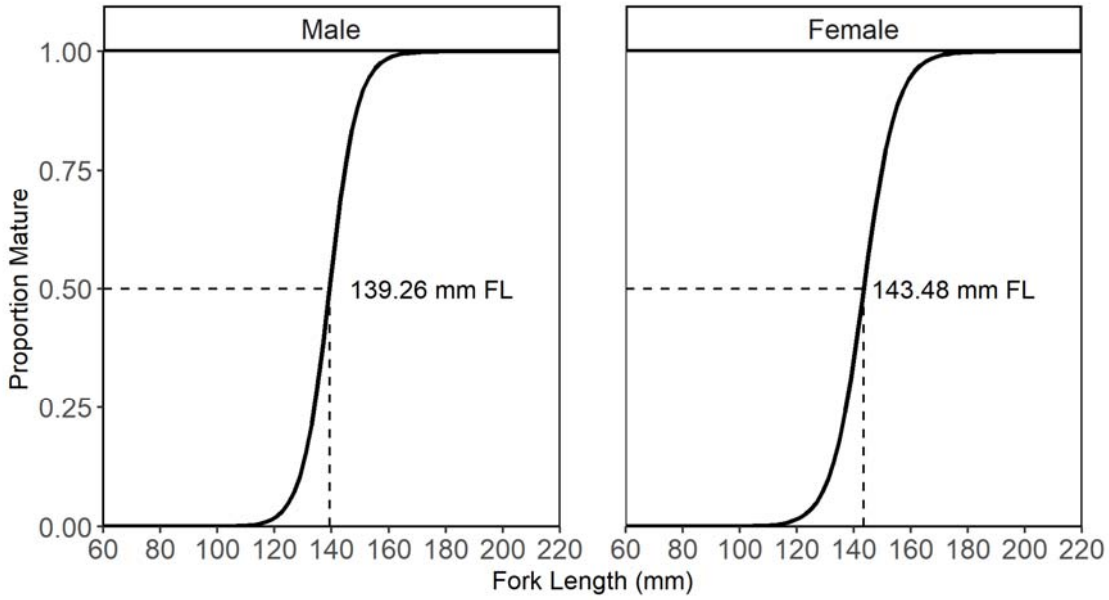

Figure 3-7. Size-at-maturity (L_{50}) for male and female Sardine collected from the Gulfs Zone for all years combined.

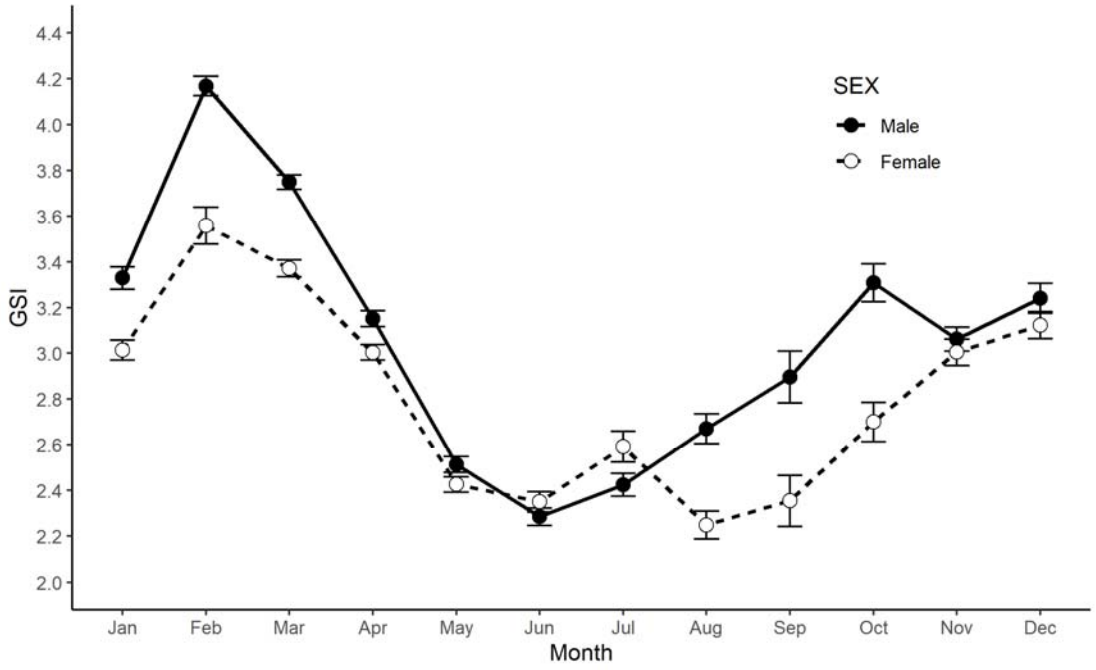

Figure 3-8. Mean monthly gonosomatic index of male and female Sardine from the Gulfs Zone commercial samples from 1995 to 2018 combined. Error bars are standard error. Fish below the size-at-maturity have been excluded.

3.4 Discussion

The relatively high level of uncertainty associated with estimating the age of Sardine from annual growth increments in otoliths has been noted elsewhere (Fletcher 1994, Rogers and Ward 2007). This issue can be partly overcome by using an age-otolith weight relationship developed from otoliths with high readabilities to estimate the age of Sardine with otoliths that are more difficult to read. This approach requires a relatively large number of otoliths to be read each year to provide adequate numbers of otoliths with high readability. This approach should be applied with caution as the relationship between otolith weight and fish age is relatively imprecise. The use of alternative approaches to assigning ages warrants consideration.

The growth rates of individuals vary with age (Rogers and Ward 2007), with moderate to high growth rates occurring prior to sexual maturity, with slower growth rates as adults. Several studies have found that fish length display limited modal progression through samples, whereas cohorts could be tracked using otolith weight (Fletcher 1994, Rogers et al. 2004). This variability in growth rates limits the use of age-length keys for estimating the age of Sardine.

As discussed in the previous chapter (with respect to fish size), changes in management arrangements and fishing practices over the history of the fishery have driven changes in the age composition of catches. As a result, catch samples are unlikely to be representative of the population and size/age selectivity is likely to have changed over time. The effects of these limitations of the age structure data need to be considered when interpreting the outputs of the population model (Chapter 5).

Despite these sampling limitations, a coherent picture of the spatial distribution by size and age is emerging for the southern stock of Sardine. Sardine taken from the Gulfs Zone are usually younger and smaller than those taken from the Outside Zone. Sardine taken from the most northerly fishing grounds in the Gulfs Zone are also smaller and younger than those taken further south (Figure 2-4; SARDI unpublished data). These findings are consistent with observations for many species of small and medium-sized pelagic fishes (e.g. Australian anchovy, Jack Mackerel), where larger, older fish tend to be found in deeper waters, further offshore than smaller, younger fish (Dimmlich and Ward 2016; Sexton et al 2018).

A coherent picture is also emerging in the temporal patterns in the size and age of Sardine taken from the Gulfs Zone. In 1995, before the two mass mortality events, Sardine taken from Spencer Gulf had a modal age of 3+ years. From 1996 to 1999, the modal age was reduced to 2+ years

but re-stabilised at 3+ years from 2000 to 2005. However, the modal age of Sardine taken from Spencer Gulf fell 2+ years in 2006-2008, after 38,734 t were taken from the Gulfs Zone in 2005. The modal age increased to 3+ years in 2009, before falling to 2+ years in 2010 and 2011. The modal age returned to 3+ years from 2013 onwards, when rules capping the catch from the Gulfs Zone were introduced. The large size and age of fish taken from the Gulfs Zone from 2013-2018 demonstrates the success of the size-based decision rules in reducing the capture of under-sized Sardine and preventing growth overfishing in the SASF.

4. SPAWNING BIOMASS OF SARDINE OFF SOUTH AUSTRALIA BETWEEN 1995 AND 2019

4.1 Introduction

The Daily Egg Production Method (DEPM) was developed for stock assessment of the Northern Anchovy, *Engraulis mordax* (Parker 1980, Lasker 1985), and has been applied to approximately 20 species of small to medium-sized pelagic fishes (Stratoudakis et al. 2006, Dimmlich et al. 2009, Neira et al. 2009, Ward et al. 2009, 2016). The method is widely used in coastal fisheries because it is often the most practical option available for assessment of pelagic species (Ward et al. 1998).

The DEPM relies on the premise that spawning biomass can be calculated by dividing the mean number of pelagic eggs produced per day throughout the spawning area (i.e. total daily egg production) by the mean number of eggs produced per unit mass of adult fish (i.e. mean daily fecundity; Parker 1980; Lasker 1985). Total daily egg production is the product of mean daily egg production (P_0) and total spawning area (A). Mean daily fecundity is the product of mean sex ratio (by weight, R), mean spawning fraction (proportion of mature females spawning each day/night, S) and mean relative fecundity (number of oocytes per gram of female weight, F/W). Spawning biomass (SB) is calculated according to the equation:

$$SB = P_0 * A/(R * S * F/W) \qquad \text{Equation 1}$$

The DEPM can be applied to fishes that spawn multiple batches of pelagic eggs over an extended spawning season (Parker 1980, Lasker 1985). Data used to estimate total daily egg production are obtained from fishery-independent ichthyoplankton surveys. Adult samples used to estimate mean daily fecundity are obtained from research surveys or samples obtained from commercial vessels using a variety of methods (Stratoudakis et al. 2006; Ward et al. 2011). The main assumptions of the DEPM are that: 1) surveys are conducted during the main (preferably peak) spawning season; 2) the entire spawning area is sampled; 3) eggs are sampled without loss and identified without error; 4) levels of egg production and mortality are consistent across the spawning area; and 5) representative samples of spawning adults are collected during the survey period (Parker 1980, Alheit 1993, Hunter and Lo 1997, Stratoudakis et al. 2006).

Although the DEPM is used widely, a range of logistical and statistical challenges have been encountered and estimates of spawning biomass are known to be imprecise (e.g. Stratoudakis et al. 2006; Bernal et al. 2012, Dickey-Collas et al. 2012; Ward et al. 2018). There are considerable

uncertainties associated with the estimation of several parameters, especially P_0 (Fletcher et al. 1996, McGarvey and Kinloch 2001, Gaughan et al. 2004). Ward et al. (2011, 2018) showed that the log-linear model of Piquelle and Stauffer (1985) provides more precise estimates of P_0 than other models and recommended its use for Sardine (*Sardinops sagax*) off South Australia. However, recent studies have shown that inter-annual variations in estimates of P_0 for Sardine off South Australia are low in comparison to statistical uncertainty (e.g. Ward et al. 2018, SARDI unpublished a, b). These findings support previous studies (e.g. Mangel and Smith 1990; Gaughan et al. 2004) that have shown that spawning biomass of Sardine is not correlated with P_0, but is strongly correlated with A. Studies by both Mangel and Smith (1990) and Gaughan et al. (2004) showed that inter-annual variations in total daily egg production are driven primarily by variations in A. In contrast, inter-annual variations in P_0 are much less influential. The potential benefits (e.g. increased precision) of estimating P_0 using data obtained over multiple years rather than data obtained in an individual year warrants further investigation (SARDI unpublished b).

Inter-annual variability in mean daily fecundity may also be relatively low compared to the statistical uncertainty and sampling error associated with estimation of adult parameters (see SARDI unpublished b). For example, the sex ratio (by numbers) of a Sardine stock is likely to be stable among years at about 1:1, however adult samples obtained in some years are dominated by either males or females and are unlikely to be representative of the adult population. In addition, samples that are dominated by males/females tend to provide estimates of S that are quite different from the mean spawning fraction for Sardine worldwide of ~0.10–0.12 (Ganais et al. 2009), and may also not be representative of the level of spawning activity across the entire adult population. As Sardines school by size and fish size varies spatially (e.g. bigger fish offshore), it is also challenging to obtain reliable annual estimates of mean female weight (W). It is also often difficult to collect enough females with hydrated oocytes to estimate batch fecundity (F) reliably in any one year. The potential benefits (e.g. increased precision) of estimating mean daily fecundity using data obtained over multiple years rather than data obtained in an individual year needs to be evaluated (see SARDI unpublished b).

The DEPM has been used to estimate the spawning biomass of Sardine in waters off South Australia since 1995 (e.g. Ward et al. 1998, 2011, 2017, 2018). Data collected over this period provide a valuable opportunity to examine patterns of inter-annual variability and statistical uncertainty in key DEPM parameters. In this chapter, we evaluate the potential benefits (e.g. increased precision) of estimating some DEPM parameters from all of the available data rather than from data collected in each individual year. Revised estimates of spawning biomass are

calculated for the period from 1995 to 2019. Recommendations are provided about how to undertake future surveys to evaluate the status of Sardine off South Australia. Opportunities to further improve the way the DEPM is applied to Sardine off South Australia are identified.

4.2 Methods

4.2.1 Total Daily Egg Production

Ichthyoplankton surveys

Ichthyoplankton surveys have been conducted during the spawning season (January–April) of Sardine off South Australia since 1995. The surveys take about 28 days and have been done from the *RV Ngerin*. Surveys were undertaken every year between 1995 and 2019, with the exception of 2008, 2010, 2012 and 2015. The orientation of transects and the number of sites sampled have varied among surveys (Figure 4–1). During 1995 and 1996, when the primary goal was to identify areas where Sardine spawned, transects were orientated from north to south and relatively few sites were sampled. After 1997, transects were orientated from north-east to south-west to improve sampling efficiency. From 1998 onwards, there has been a general increase in the number of sites sampled during each survey. From 2006 onwards, the number of sites sampled in Spencer Gulf has been doubled.

An adaptive approach to egg sampling has been applied since 2014 to ensure that each survey covered as much of the spawning area as possible. Under this adaptive sampling protocol, additional samples have been taken at sites located outside the area covered by the historical pre-determined sampling sites (Figure 4–1). Decisions about whether (or not) to take additional samples were based on the presence/absence of eggs in samples taken using the Continuous Underway Fish Egg Sampler (CUFES) at sites located on the seaward end of transects. Sampling at additional sites continued until Sardine eggs were not present in the CUFES samples.

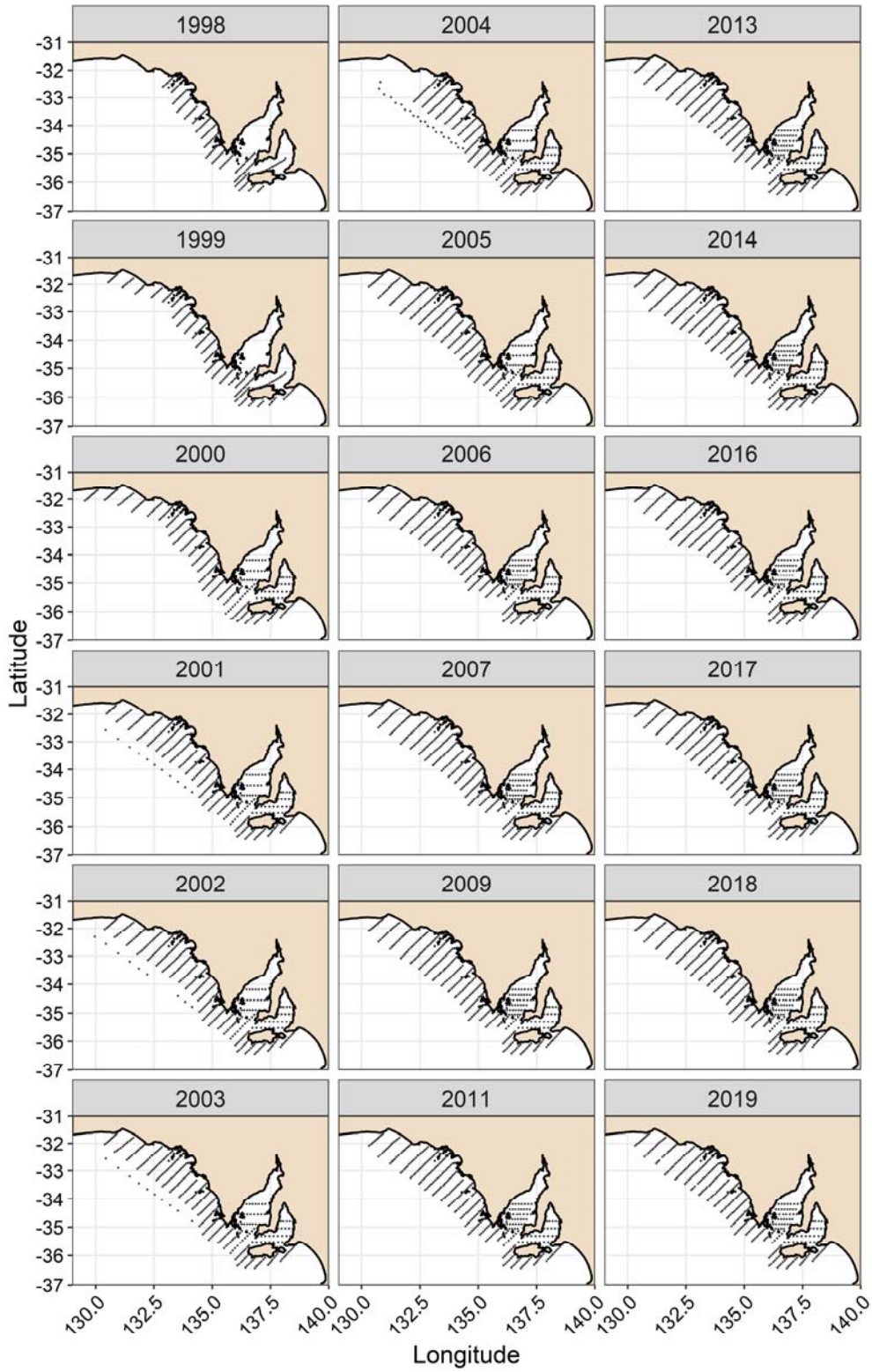

Figure 4-1. Location of sites sampled during ichthyoplankton surveys conducted off South Australia between 1995 and 2019.

Plankton sampling

Samples were collected at each site shown in Figure 4-1 using paired Californian Vertical Egg Tow (CalVET) plankton nets. The CalVET nets have an internal diameter of 0.3 m, 330 µm mesh and plastic cod-ends. During each tow the nets were deployed to within 10 m of the seabed at depths <80 m or to a depth of 70 m at depths >80 m. Nets were retrieved vertically at a speed of ~1 $m.s^{-1}$. A *Sea-Bird* Conductivity-Temperature-Depth (CTD) profiler attached to the CalVET nets was used to measure oceanographic parameters (e.g. temperature, salinity, fluorescence) at each site. General Oceanics™ flowmeters were used to estimate the distance travelled by each net. Samples from the two cod-ends were combined and stored in 5% buffered formaldehyde and seawater solution.

Egg identification and staging

Sardine eggs were identified using the published descriptions of Neira *et al*. (1998) and White and Fletcher (1998). Eggs were staged based on the descriptions by White and Fletcher (1998). The number of eggs of each stage in each sample were counted. Eggs in the first and last stages were excluded from the statistical analyses because they have been shown to be under- and over-represented in plankton samples, respectively (SARDI unpublished a), Stratoudakis et al. 2006, Bernal et al. 2012, Dicky-Collas et al. 2012).

Egg ageing and treatment of zero count egg samples

The development rate of Sardine eggs is dependent on ambient water temperature (Picquelle and Stauffer 1985, Pauly and Pullin 1988). Based on the temperature data from the CTD, egg samples were allocated to one of three temperature bins that covered the range of temperatures encountered during surveys (14–18°C, 18–22°C, and 22–26°C). The temperature bins were comparable to those used by Le Clus and Malan (1995) to describe the developmental rates of Sardine eggs. These published development rates were used to assign a mean age to each egg in each sample (Ward et al. 2018).

After each egg was assigned an age, the eggs in each sample were grouped into daily cohorts. This was done because a sample usually included eggs spawned on more than one night. The total number of eggs in each daily cohort was calculated by summing the number of eggs of each stage assigned to a spawning day (i.e. day 0, day 1, day 2). The age of a daily cohort was calculated from the average age of each stage within the daily cohort, weighted by the number of eggs in each stage.

Samples with eggs could contain several possible combinations of daily cohorts depending on water temperature, spawning time (peak around 2:00 am) and sampling time. Zero counts were allocated for daily cohorts where the cohort was expected to be present but was not found within the sample (Ward et al. 2018). Samples with no eggs were excluded from the analyses and not considered part of the spawning area.

Egg density

The number of eggs of each stage under one square metre of water (P_t) was estimated at each site according to the equation:

$$P_t = \frac{C\,D}{V},$$

Where, C is the number of eggs of each age in each sample, D is the depth (m) to which the net was deployed, and V is the volume of water filtered (m^3) (Smith and Richardson 1977). Plots of egg distribution and abundance were prepared using Surfer® (Ver. 8).

Spawning area

The spawning area (A) was estimated for each survey (Lasker 1985, Somarakis et al. 2004) using the Voronoi natural neighbour method (Watson 1981). The survey area was divided into a series of contiguous polygons approximately centred on each site using the 'deldir' package in the statistical program 'R (R Development Core Team 2019, Turner 2016; Figure 4–2). The area represented by each site (km^2) was calculated. A was defined as the total area of the polygons where live Sardine eggs were present in the plankton sample (see Fletcher et al. 1996).

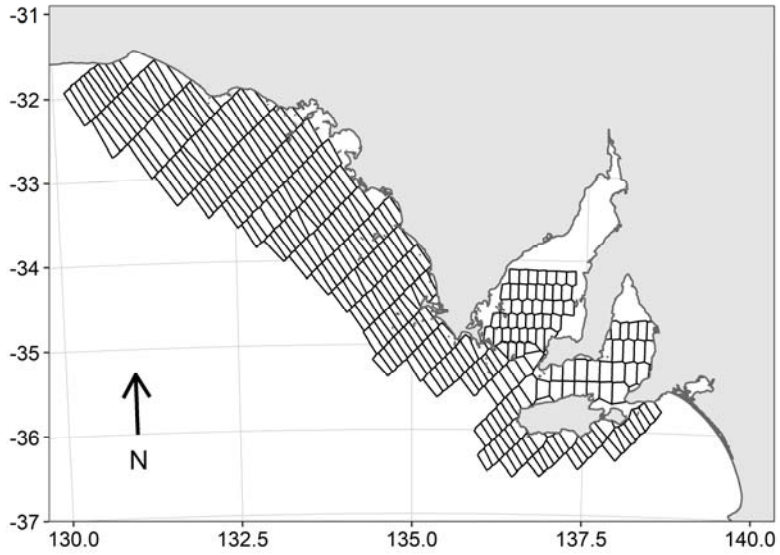

Figure 4-2. Polygons generated using the Voronoi natural neighbour method and used to estimate the spawning area of Sardine in 2019.

Mean Daily Egg Production (P_0)

Five different models were used to estimate mean daily egg production (P_0) and instantaneous egg mortality rate (z, day^{-1}). The underlying model was the exponential egg mortality model (Lasker 1985):

$$P_t = P_0 e^{-z\,t},$$

where P_t is the egg density at age t and z is the instantaneous rate of egg mortality. This base model was applied in several ways. Non-linear least squares regression was used to fit the equation above:

$$nls(P_t \sim P_0 e^{-z\,t}),$$

A linear version of the exponential egg mortality model was fitted to estimates of egg age and density for each daily cohort at each site (Picquelle and Stauffer 1985):

$$\ln P_b = \ln(P_i + 1) - Zt,$$

where P_i is the density of eggs of each daily cohort of age t at site i and z is the instantaneous rate of egg mortality. Estimates of P_b obtained using least squares regression of the log-linear

version of the exponential mortality model have a negative bias, therefore a bias correction factor was applied following the equation of Picquelle and Stauffer (1985):

$$P_0 = e^{\left(\ln P_b + {\sigma^2}/{2}\right)} - 1,$$

where σ^2 is the variance of the estimate of biased mean daily egg production (P_b). This equation is hereafter referred to as the 'log-linear model'.

Two general linear models (GLMs) and a general linear mixed model (GLMM), each using a different error structure, were also used to estimate P_0:

$$E[P_0] = g^{-1}(-zt + \varepsilon),$$

where E[P_0] is the expected value of P_0, g^{-1} is the inverse-link function, zt is the instantaneous rate of daily egg mortality at age t, and ε is the error term. The negative binomial and quasi error structures used are considered suitable for over-dispersed data, such as egg density by age (e.g. Ward et al. 2011, 2018). The instantaneous egg mortality rate (z) was estimated as a free parameter in each of the models.

Estimates of P_0 and z obtained by fitting the five models to egg data collected each year and to data obtained in all years from 1998 to 2019 (combined) are presented in Appendix A. In the results section of this report, only estimates of P_0 and z obtained by fitting the log-linear model to egg data collected during each year and all years from 1998 to 2019 (combined) are presented. Only estimates obtained from the log-linear model are presented in the results because Ward et al. (2011, 2018) showed that the log-linear model fits zero-inflated and over-dispersed egg data better than the other models, and consistently provides more plausible and precise estimates of P_0 and z.

4.2.2 Mean Daily Fecundity

Adult sampling

Mid-water trawling and sampling from commercial catches undertaken during 1995-97 did not provide samples suitable for estimating adult reproductive parameters of Sardine off South Australia. The lack of reliable estimates of these adult parameters reduced the reliability of estimates of spawning biomass obtained during this period (e.g. Ward et al. 2001a).

From 1998 to 2018, samples of mature Sardine were collected from sites located in the eastern Great Australian Bight, southern Spencer Gulf and Investigator Strait using a gill-net (Figure 4–3). In the late afternoon, a dual frequency echo sounder (60 and 180 KHz) was used to search areas where schools of adult Sardines were known to aggregate. A gillnet comprised of three panels, each with a different multi-filament nylon mesh size (*Double Diamond*: 210/4 ply meshes 25, 28 and 32 mm) was deployed from the port side of the *RV Ngerin* at protected locations where schools were encountered. Surface and sub-surface lights (150 W) were illuminated near the net after it was set. Net soak times varied from 15 minutes to 3 hours depending on the number of fish caught.

After the net was retrieved, fish were removed and dissected immediately. All Sardines collected were counted and sexed. Mature males and immature fish were frozen. Mature females were fixed in 10% buffered formaldehyde seawater solution. Calculations of female weight, sex ratio, batch fecundity and spawning fraction are based on samples collected annually between 1998 and 2018 and from all samples combined.

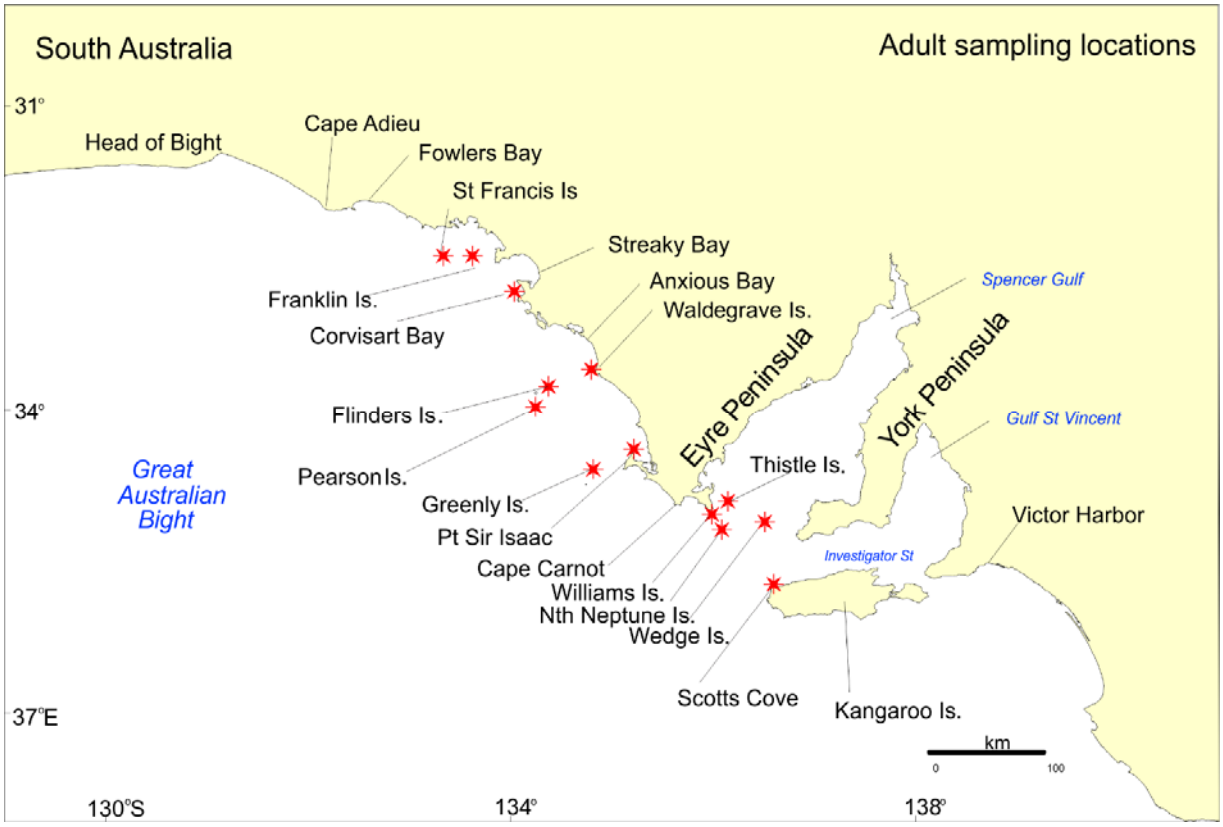

Figure 4-3. Sampling locations for adult Sardine off South Australia.

Adult parameters

Estimates of each adult parameter were calculated for individual years between 1998 and 2018 (where samples suitable were available). Overall estimates of each parameter were also calculated from the entire dataset collected over this period (SARDI unpublished b).

Mean female weight (W)

Mature females from each research sample were removed from formalin and weighed (± 0.01 g). *W* was calculated from the average of sample means weighted by sample size:

$$W = \overline{\left[\overline{W_i} * \frac{n_i}{N} \right]}$$

where, $\overline{W_i}$ is the mean female weight of each sample *i*; *n* is the number of fish in each sample and *N* is the total number of fish collected in all samples.

Sex ratio (R)

The mean sex ratio of mature individuals in the population was calculated from the average of sample means weighted by sample size:

$$R = \overline{\left[\overline{R_i} * \frac{n_i}{N} \right]}$$

where n_i is the number of fish in each sample, *N* is the total number of fish collected in all samples and $\bar{R}_i$ is the mean sex ratio of each sample calculated from the equation:

$$\bar{R}_i = \frac{nF}{(nF+nM)}$$

where *F* and *M* are the respective total weights of mature females and males in each sample, *i*.

Spawning fraction

Ovaries of mature females were examined histologically. The ovaries were sectioned and stained with haematoxylin and eosin, and examined for the presence/absence of post-ovulatory follicles (POFs). POFs were aged according to the criteria developed by Hunter and Goldberg (1980) and Hunter and Macewicz (1985). The spawning fraction of each sample was estimated as the mean proportion of females with hydrated oocytes plus day-0 POFs (*d*0) (assumed to be spawning or

have spawned on the night of capture), day-1 POFs (*d*1) (assumed to have spawned the previous night) and day-2 POFs (*d*2) (assumed to have spawned two nights prior). The mean spawning fraction of the population was then calculated from the average of sample means weighted by proportional sample size.

$$S = \overline{\left[\overline{S_i} * \frac{n_i}{N} \right]}$$

where, n_i is the number of fish in each sample, N is the total number of fish collected in all samples and $\bar{S}_i$ is the mean spawning fraction of each sample calculated from equation:

$$\overline{S_i} = \frac{\left[(d0 + d1 + d2POFs) / 3 \right]}{n_i}$$

where *d0*, *d1* and *d2* POFs are the number of mature females with POFs in each sample and n_i is the total number of females within a sample.

Batch fecundity

Batch fecundity was estimated from females with ovaries that contained hydrated oocytes using the methods of Hunter et al. (1985). Both ovaries were weighed and the number of hydrated oocytes in three ovarian sub-sections were counted and weighed. The total batch fecundity for each female was calculated by multiplying the mean number of oocytes per gram of ovary segment by the total weight of the ovaries.

The relationship between female weight (ovaries removed) and batch fecundity was determined by linear regression. This relationship was used to estimate the batch fecundity of mature females (without hydrated ovaries) collected in every sample. A batch fecundity relationship was calculated for the pooled data from all years (1998–2018) as well as individual years, and two batch fecundities were determined for every mature female collected.

Using the two fecundity estimates (i.e. all-years or individual years), the number of eggs produced per gram of total weight (*F/W*) was calculated for each female, where each *F* was divided by the total weight of the fish (*W*). The mean *F/W* per year was determined for both estimates of *F*, and an overall F/W value was calculated by taking the mean over the entire dataset (1998–2018) of the *F/W* estimate that incorporated the all-years *F* relationship.

Estimates of uncertainty

The reliability of model fits, standard deviations (SDs) and coefficients of variation (CVs) for P_0 were estimated using bootstrap resampling methods with 10,000 iterations. Coefficients of variation and SDs for *R, S, F, W and F/W,* were calculated from the all-years adult data. A ratio estimator was used to calculate the coefficients of variation (CVs) for *S*, *R*, and *F/W* (see Rice 1995). The variance around the spawning biomass estimate was calculated by the summing the squared CVs for each parameter and multiplying by the square of the estimate of spawning biomass. All analyses were done in the R programming environment (R Core Team, 2019).

4.2.3 Spawning Biomass

Spawning biomass was calculated with Equation 1, using the all-years estimate of P_0 obtained from the log-linear model, spawning area (*A*) estimated per year and estimates of *S*, *R* and *F*/*W* obtained from adult samples collected between 1998 and 2018.

The reliability of model fits, 95% confidence intervals (CIs) and coefficients of variation (CVs) for P_0 were estimated using bootstrap resampling methods with 10,000 iterations. Coefficients of variation and CIs for *R, S, F, W and F/W,* were calculated from the all-years adult data. A ratio estimator was used calculate the coefficients of variation (CVs) for *S*, *R*, and *F/W* (see Rice 1995). The variance around the spawning biomass estimate was calculated by the summing the squared CVs for each parameter and multiplying by the square of the estimate of spawning biomass. Uncertainty estimates presented for all parameters are 95% CIs. Data analyses were done in the R programming environment (R Core Team, 2019).

4.3 Results

4.3.1 Total Daily Egg Production

Total area sampled

The total area sampled during the ichthyoplankton surveys varied from 48,379 in 1998 to 133,058 km^2 in 2003 (Figure 4–4). Changes in the area surveyed reflect the changes in the objectives of the sampling program over time. During 1995-97, the primary goal was to identify the main spawning grounds and develop an appropriate survey design. The sampling design and area sampled continued to be refined between 1998 and 2004, primarily to ensure that the spawning area was being covered (Figures 4–3, 4–5). The total survey area was stable at about 119,000 km^2 between 2006 and 2013. Total survey area increased in 2014 to 125,249 km^2, after the adaptive sampling protocol was implemented in response to the incomplete coverage of the spawning area in 2013 (Figure 4-5). Adaptive sampling remains a key element of the current survey design and is the main reason the total survey area varies slightly from year to year.

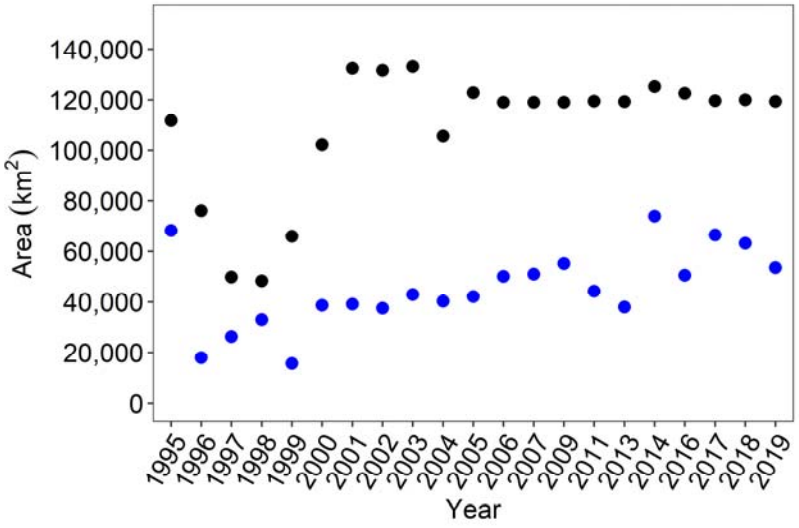

Figure 4-4. Total area sampled (km^2) (black) and corresponding spawning area (*A,* km^2) (blue) for DEPM surveys between 1998 and 2019.

Spawning area (A)

Estimates of spawning area varied among years and reflected both the size of the survey area and the spawning biomass. The spawning area declined substantially following the two mass mortality events, from 68,260 km^2 in 1995 to 17,990 km^2 in 1996 and from 32,980 km^2 in 1998 to 15,637 km^2 in 1999 (Figure 4-4). Between 2000 and 2005, the spawning area remained between 37,000 and 42,200 km^2, before increasing to >50,000 km^2 from 2006 to 2009. In 2011 and 2013, the spawning area was below 45,000 km^2, but the 2013 survey did not cover the entire spawning area as the stock had moved offshore. Spawning area peaked at 73,981 km^2 in 2014, and remained above 50,000 km^2 from 2015 to 2019 (Figure 4-4). The spawning area in 2019 was 53,600 km^2.

Egg distribution and abundance

The distribution and abundance of Sardine eggs has varied considerably among years. Areas where large numbers of eggs are sometimes found include shelf waters of the eastern Great Australian Bight, between Coffin Bay and the Head of Bight, southern Spencer Gulf, and the western end of Investigator Strait (Figure 4–5). Mass mortality events in 1995 and 1998 reduced both the total abundance of eggs and their spatial distribution off South Australia (Ward et al. 2001a). The presence of eggs into offshore waters in 2013 was a major change from the historical patterns. The recent increases in egg abundances to the south and east of Kangaroo Island are also important changes that need to be accounted for in future surveys.

Mean daily egg production (P_0)

Reanalysis of data obtained from 1998 to 2019 demonstrated the variability in estimates of mean daily egg production (P_0) among years (Figure 4–6). Annual estimates of P_0, based on the log-linear model, ranged from 39.0 egg·m^{-2}·day^{-1} in 2013 to 145.3 egg·m^{-2}·day^{-1} in 2004. The estimate of P_0 from data combined across obtained from all years combined was 81.4 egg·m^{-2}·day^{-1} (95% CI = 72.8–91.0) (Figure 4–6). The 95%CI of the overall estimate of P_0 was generally less than 50% of the estimates of 95%CIs for individual years (Figure 4–6). Annual P_0 was not correlated with A (linear relationship: $P_0 = 0.008A + 48.7$; $R^2 = 0.07$; $p = 0.33$) (Figure 4–7).

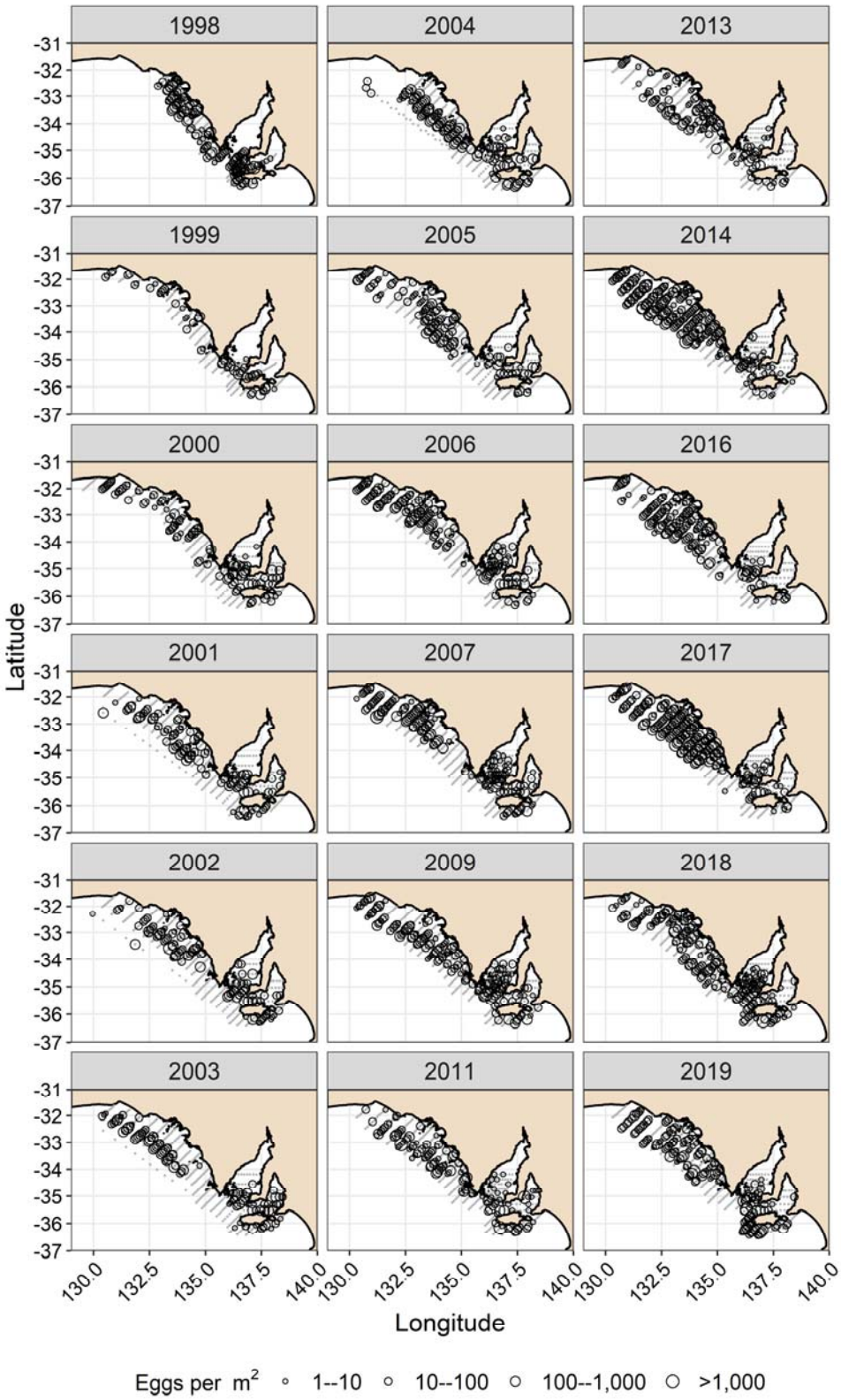

Figure 4-5. Distribution and abundance of Sardine eggs collected during surveys between 1998 and 2019.

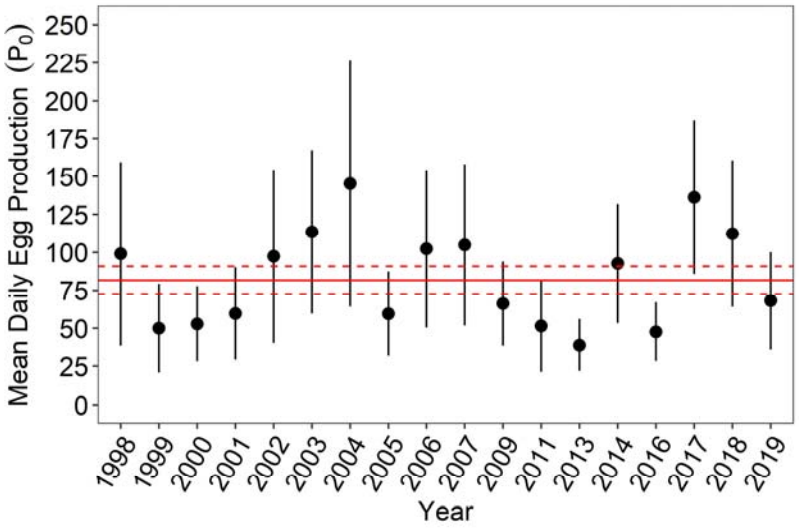

Figure 4-6. Mean daily egg production (P_0, egg.day^{-1}.m^{-2}) of Sardine per year (1998-2019) estimated using the log-linear model. The estimate of P_0 calculated using data from all years is overlaid in red. 95% confidence intervals are shown for each estimate.

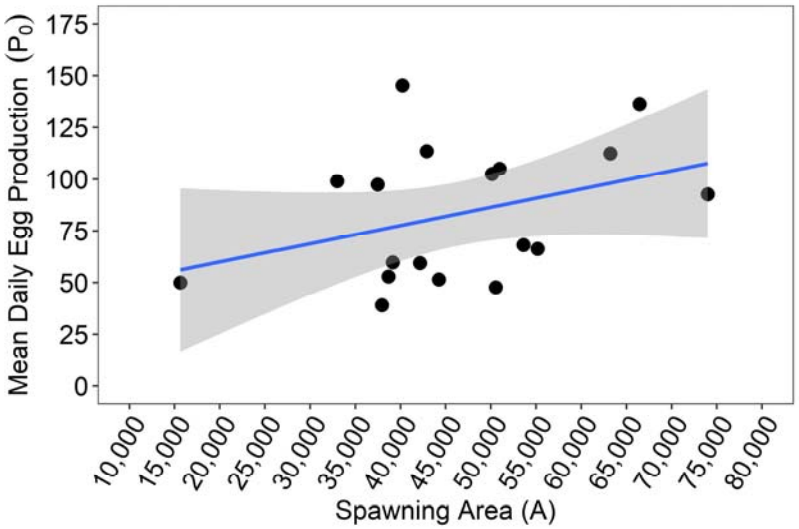

Figure 4-7. Relationship between annual estimates of mean daily egg production (P_0, egg.day^{-1}.m^{-2}) and spawning area (A) for Sardine collected from 1998 to 2019. Blue: Linear relationship: $P_0 = 0.008A + 48.7$ ($R^2 = 0.07$, $p = 0.33$); shading: 95% CI.

4.3.2 Mean Daily Fecundity

Adult Parameters

Reanalysis of data obtained from 1998 to 2019 demonstrated a high level of inter-annual variability in estimates of adult parameters.

Sex ratio (R)

Annual estimates of *R* ranged between 0.36 in 2009 and 0.70 in 2018 (Figure 4–8). The estimate of *R* from data combined across all years was 0.55 (95% CI = 0.52–0.58) (Figure 4–8). The high level of inter-annual variability reflects the challenges of obtaining representative samples of adult Sardine. The 95%CI of the overall estimate of *R* was generally less than 50% of the estimates of 95% CIs for individual years (Figure 4–8).

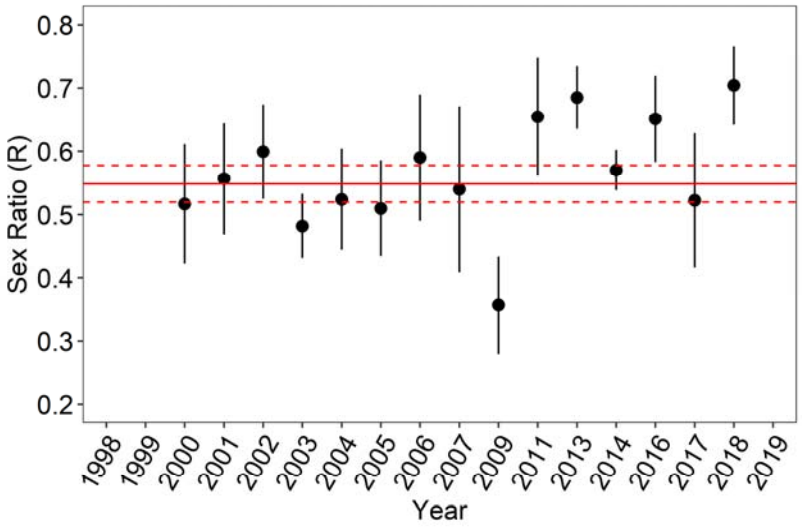

Figure 4-8. Sex ratio (*R*) of Sardine per year (1998-2018). The estimate of *R* calculated using data from all years is overlaid in red. 95% confidence intervals are shown for each estimate.

Spawning fraction (S)

Annual estimates of *S* ranged between 0.044 in 2011 and 0.179 in 2001 (Figure 4–9). The estimate of *S* from data combined across all years was 0.111 (95% CI = 0.100–0.123) (Figure 4–9). The large inter-annual variability in estimates of *S* reflects the challenges of obtaining representative samples of adult Sardine. The 95%CI of the overall estimate of *S* was generally less than 50% of the estimates of CIs for individual years (Figure 4–9).

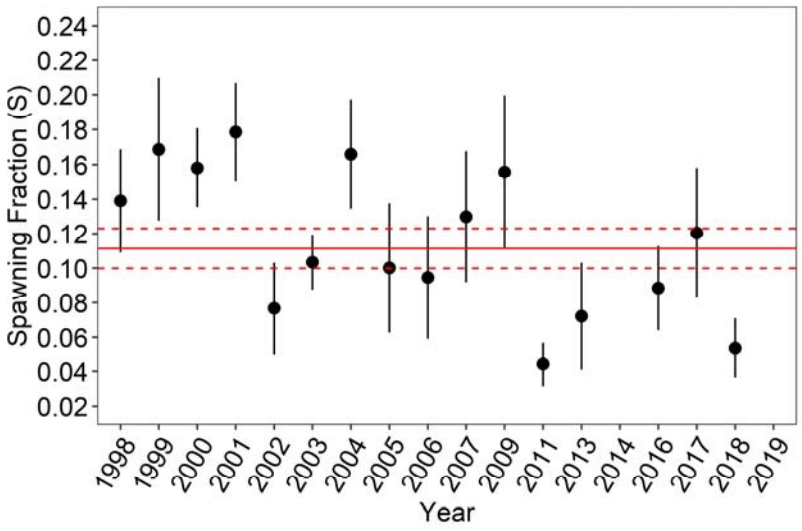

Figure 4-9. Spawning fraction (*S*) of Sardine per year (1998-2018). The estimate of *S* calculated using data from all years is overlaid in red. 95% confidence intervals are shown for each estimate.

Annual spawning fraction (*S*) was significantly correlated with sex ratio (*R*) (linear relationship: $S = -0.327R + 0.294$; $R^2 = 0.50$; $p < 0.01$) (Figure 4–10). Estimates of spawning fraction are higher when the sex ratio is skewed towards males (i.e. sex ratio is lower). This finding supports the idea that the inter-annual variation in both parameters (e.g. Figures 4.8 and 4.9) may be more reflective of the difficulties of obtaining representative samples of adult sardine rather than actual variability.

Mean female weight (W)

Annual estimates of *W* ranged from 45.0 g in 1998 to 78.7 g in 2004 (Figure 4–11). The estimate of *W* from data combined across all years was 58.0 g (95% CI = 22.2–93.8) (Figure 4–11). The mean gonad-free female weight for all samples was 55.5 g. The large confidence intervals around the all-years estimate of *W* reflects the large variation among years in the mean size of females obtained in samples.

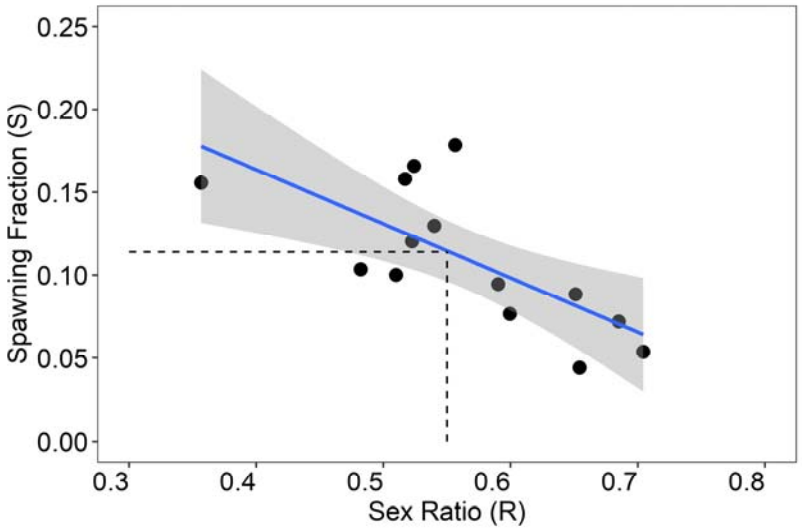

Figure 4-10. Relationship between annual estimates of spawning fraction (*S*) and sex ratio (*R*) for Sardine collected from 1998 to 2018. Blue: Linear relationship: $S = -0.327R + 0.294$ ($R^2 = 0.50$, $p < 0.01$); shading: 95% CI; dashed: all-years values for *S* (0.111) and *R* (0.55).

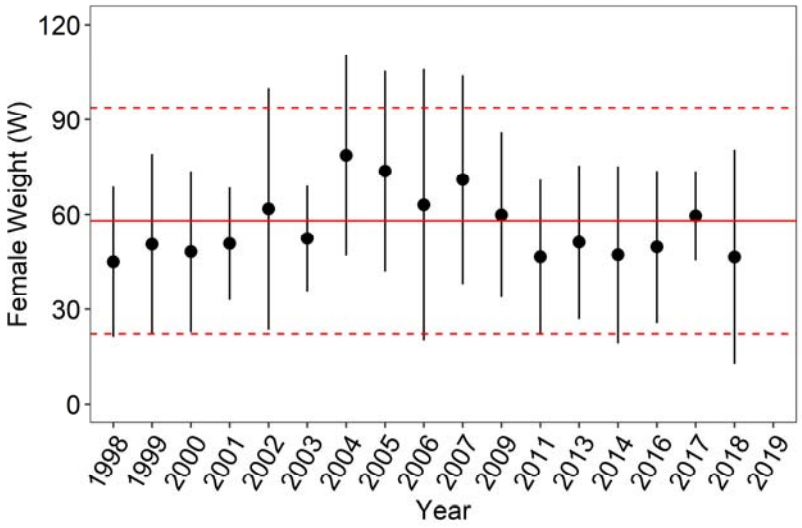

Figure 4-11. Female weight (*W*, g) of Sardine per year (1998-2018). The estimate of *W* calculated using data from all years is overlaid in red. 95% confidence intervals are shown for each estimate.

Batch fecundity (F)

The relationships between gonad-free weight and batch fecundity based on females with hydrated oocytes varied among years (Figure 4–12a). The individual year fecundity relationships produced annual estimates of *F* ranging from 10,714 oocytes in 2003 to 22,406 oocytes in 2017 (Figure 4–

13a). Inter-annual differences in *F* were driven mainly by variations in gonad-free female weight among years.

The batch fecundity relationship for all females with hydrated oocytes collected between 1998 and 2018 was Batch Fecundity = 335 × Gonad Free Female Weight – 797 (R^2 = 0.53, Figure 4–12b). Using this relationship to calculate *F* per year produced estimates of *F* that ranged from 13,722 oocytes in 1998 to 24,259 oocytes in 2004 (Figure 4–13b). Inter-annual differences in *F* were again driven mainly by variations in gonad-free female weight among years.

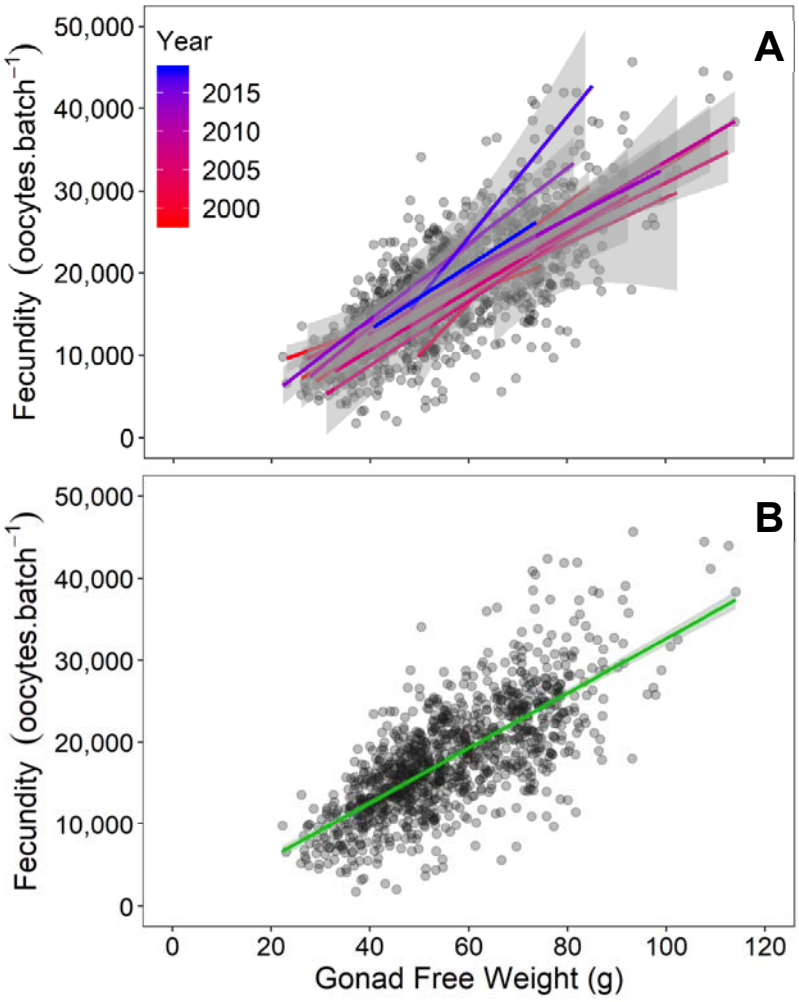

Figure 4-12. Relationships between gonad-free weight and batch fecundity for female Sardine with hydrated oocytes collected from 1998 to 2018. **A**: individual years and **B**: all years combined. All-years relationship (green) in **B**: *F* = 335*Gonad Free Weight - 797, (R^2 = 0.53). Shading around regression slopes in **A** and **B** are 95% CI.

The overall estimate of *F* was 17,776 oocytes·batch^{-1} (95% CI = 6,408–29,144). This estimate was calculated with the overall batch fecundity relationship from Figure 4–12b applied to the gonad-free weight of all mature females collected between 1998 and 2018 (Figure 4–13). The large confidence intervals around the overall estimate of *F* reflect the large variations in gonad-free female weight (and *W*) among years.

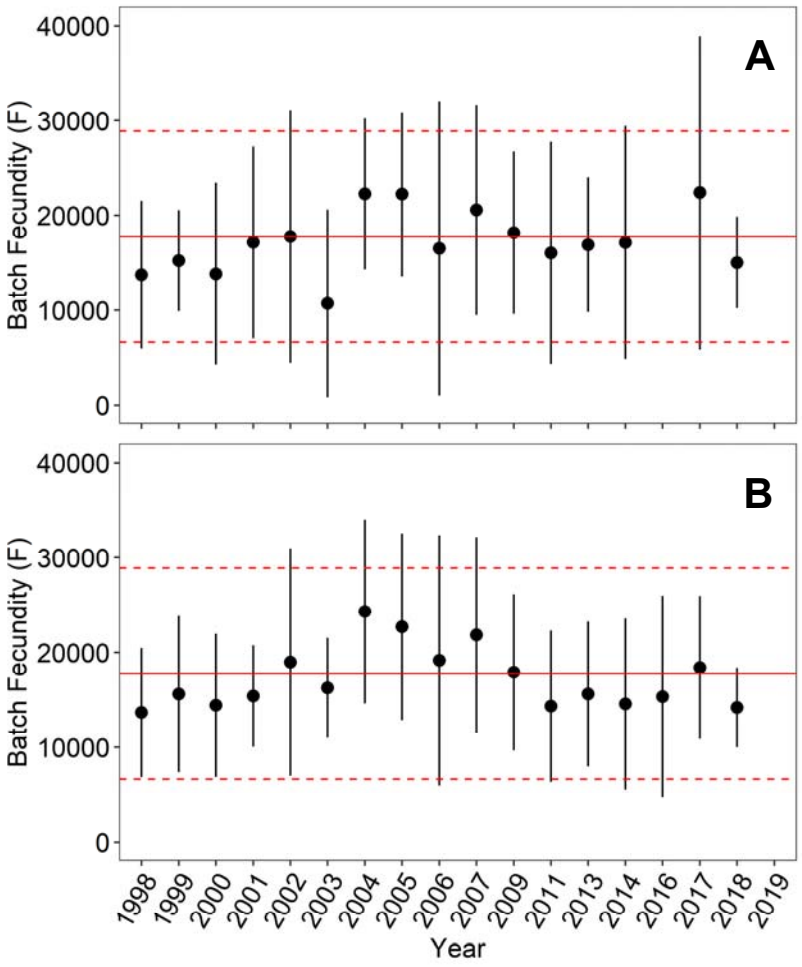

Figure 4-13. Batch fecundity (*F*, oocytes.batch^{-1}) of Sardine per year (1998-2019) estimated using batch fecundity relationships from individual years (**A**) and the relationship from all years combined (**B**). The overall estimate of *F*, calculated using data from all years combined, is overlaid in red. 95% confidence intervals are shown for each estimate.

Relative Fecundity (Eggs per gram of mature female weight (F/W))

Relative fecundity (eggs per gram of female body i.e. *F*/*W*) was almost constant among years (Figure 4–14). The large variances associated with the individual estimates of *F* and *W* were greatly reduced by combining these values into the single new parameter of relative fecundity (i.e. *F/W*) by accounting for covariance (Figure 4–14). *F* and *W* are highly correlated ($R^2 = 0.95$, $p < 0.001$).

Based on the fecundity relationships for individual years, *F/W* varied from 204.5 egg.g^{-1} in 2003 to 376.2 egg.g^{-1} in 2017 (Figure 4–14a). The overall batch fecundity relationship produced yearly values of *F/W* that were almost constant across years (range: 297.2–311.6 egg.g^{-1}; Figure 4–14b). Using the overall batch fecundity relationship and combining all data from 1998 to 2018 gave an overall estimate of *F/W* of 306.4 eggs.g^{-1} (95% CI = 258.5–354.3) (Figure 4–14).

Relative fecundity (i.e. eggs per gram of female weight (*F/W*)) is almost constant across the range of weight (*W*) of mature females obtained in samples (Figure 4–15). Fecundity increases 306 eggs for every gram of increase in total female weight.

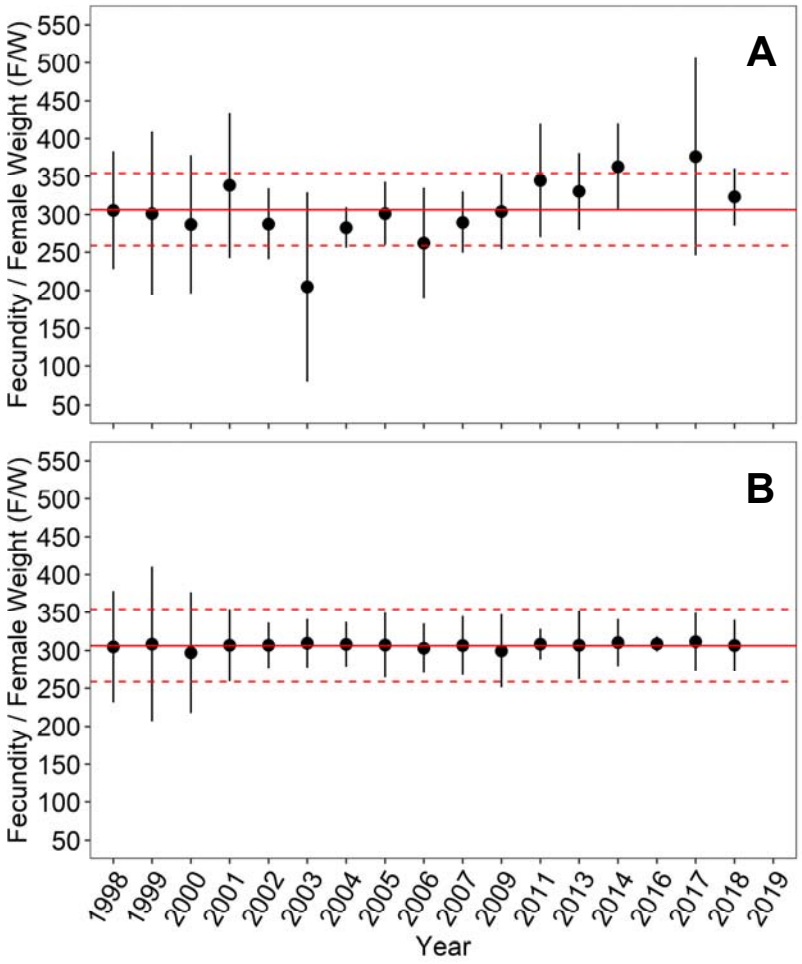

Figure 4-14. Egg per gram of female weight (*F/W*) of Sardine per year (1998-2018) estimated using batch fecundity relationships from individual years (**A**) and the relationship from all years combined (**B**). The overall estimate of *F/W* is overlaid in red. 95% confidence intervals are shown for each estimate.

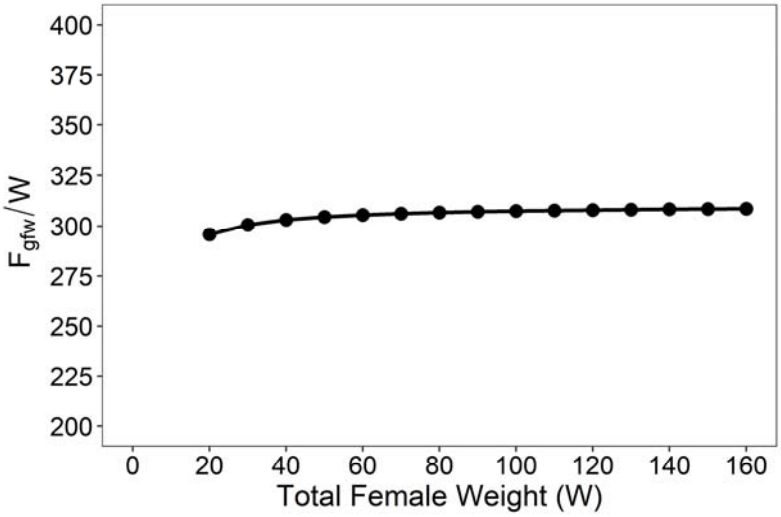

Figure 4-15. Correlation between eggs per gram of female weight (*F/W*) and female weight (*W*) of Sardine collected between 1998 and 2018.

4.3.3 Spawning Biomass

Estimates of spawning biomass obtained when the approach to applying the DEPM to Sardine off South Australia was being developed are likely have been improved by the re-analysis of historical data undertaken in this report. In particular, the estimates of adult parameters obtained from data collected from 1998 to 2018 helped to resolve uncertainties in estimates of mean daily fecundity for 1995-97 that were driven by the limited number of adult samples obtained during this initial period. Similarly, the preliminary estimates of P_0 obtained from the limited plankton sampling undertaken in the early years of this time series are likely to be improved by applying refined analytical methods used in this report.

The revised estimate of spawning biomass (95% CI) for 1995 was 297,599 (230,778–364,419) t (Figure 4–16). Spawning biomass fell to 78,432 t in 1996 t and 68,175 t in 1999 following the two mass mortality events (Figure 4–16), before recovered from 168,539 t in 2000 to 240,569 t in 2009. The relatively low estimate of spawning biomass in 2013 largely reflects the incomplete coverage of the spawning area in that year. Since the adaptive approach to sampling was adopted in 2014, estimates of spawning biomass have been above 220,000 t. In 2019, the spawning biomass was estimated to be 233,684 (181,214–286,153) t (Figure 4–16).

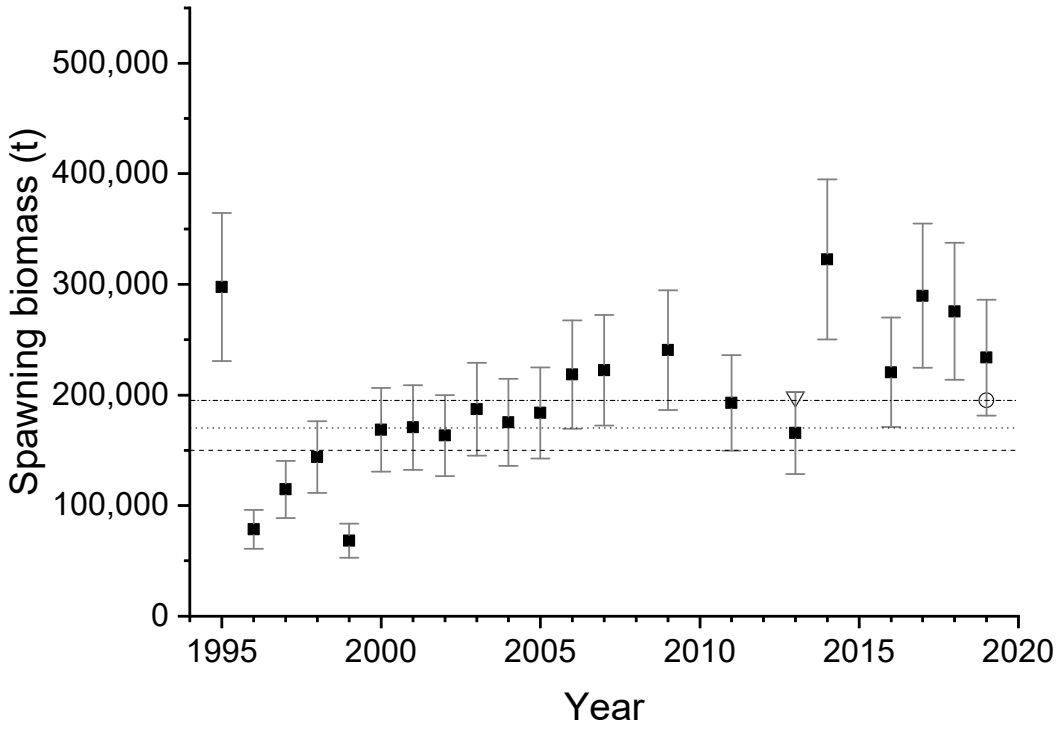

Figure 4-16. Estimates of spawning biomass (95% CI) obtained for Sardine off South Australia from 1995 to 2019 using the Daily Egg Production Method (DEPM). Adult parameters were estimated from data obtained during 1998-2018. Spawning area (*A*) was estimated annually. The log-linear model was used to estimate mean daily egg production (P_0) from data collected between 1998 and 2019 and data from 2019 only (68.1 eggs·day^{-1}·m^{-2}). The open triangle for 2013 (when the survey did not cover the entire spawning area) is the estimate of spawning biomass obtained using the mean *A* from 2002 to 2011 (45,406 km^2). The horizontal lines indicate the 150,000 t (dash), 170,000 t (dotted) and 190,000 t (dash/dot) reference points in the harvest strategy for the SASF (PIRSA 2014).

4.4 Discussion

The DEPM has been integral to the rapid and sustainable development of the SASF. The information about the size of spawning stock of Sardine in waters off South Australia provided by the DEPM has underpinned the growth of the fishery. Estimates of spawning biomass obtained during the first few years during which the method was applied off South Australia were uncertain, due to limited understanding of key parameters, especially mean daily egg production (P_0) and spawning fraction (S) (e.g. Ward et al. 2001a, 2011). Improved knowledge obtained over the last two decades provided a valuable opportunity to re-evaluate how the size of the population has fluctuated over time and develop recommendations about how the method should be applied to ensure that future estimates of spawning biomass are as accurate and precise as possible.

The revised estimate of spawning biomass for 1995 of 297,599 t (95% CI = 230,778–364,419), provides a useful proxy for unfished spawning biomass (see Chapter 5). Similarly, the estimates of spawning biomass of 78,432 t in 1996 t and 68,175 t in 1999 provide useful insights into the likely impacts of the two mass mortality events on the adult population. The increase in the spawning biomass from 168,539 t in 2000 to 240,569 t in 2009 shows how quickly the population recovered from the two mortality events. The low estimate of spawning biomass in 2013 largely reflects the failure of that year's survey to cover the entire spawning area. Since the adaptive approach to sampling was adopted in 2014, estimates of spawning biomass have been consistently above 220,000 t. The estimate of spawning biomass of Sardine off South Australia in 2019 was 233,684 (181,214–286,153) t.

Previous studies have shown that Sardine abundance is strongly correlated with spawning area (Mangel and Smith 1990, Gaughan et al. 2004). The analyses conducted in this report and elsewhere (Ward et al. 2017, SARDI unpublished a, b) confirm that spawning area is a good proxy for the abundance of adult Sardine off South Australia. Using historical data to estimate all DEPM parameters except spawning area means that fluctuations in estimates of spawning biomass are driven entirely by changes in the measure of spawning area. As a result, future surveys must cover as much of the spawning area as possible and should continue to involve the adaptive approach to sampling that has been in place from 2014 onwards.

The estimate of spawning area in 2019 of 53,600 km^2 was the fifth highest on record. Spawning area has been consistently above 50,000 km^2 since peaking at 73,981 km^2 in 2014. The large spawning area observed in this study provides strong evidence that Sardines were widespread and abundant off South Australia in 2019.

Recent studies (e.g. Ward et al. 2018, SARDI unpublished b) have shown that for Sardine off South Australia inter-annual variability in estimates of P_0 is low compared to statistical uncertainty (imprecision). In the present study, we addressed this issue by estimating P_0 from data obtained from all years between 1998 and 2019. The estimate of P_0 obtained using this approach was more precise (SD = 4.6) than the estimate obtained using data from 2019 only (SD = 16.3). Using historical data to estimate of P_0 will prevent large inter-annual fluctuations in estimates of spawning biomass driven by variations in the annual estimates of this parameter caused by statistical uncertainty. In future applications of the DEPM to Sardine off South Australia, P_0 should be estimated using data obtained in all years since 1998.

Evidence complied in this report and elsewhere (e.g. SARDI unpublished b) suggest that the large variations among years observed in the estimates of the adult parameters of Sardine off South Australia are more likely to reflect the limitations of the adult sampling program, rather than actual differences among years in the reproductive patterns of the population. Re-analysis of adult samples collected off South Australia since 1998 suggest that both individual parameters and mean daily fecundity are relatively stable among years, especially when inter-annual variability is evaluated within the context of potential sources of statistical uncertainty (i.e. precision and bias).

Inter-annual variability in the estimates of sex ratio (*R*) exemplifies the problems associated with annual estimation of individual adult parameters. One of the sexes often dominates adult samples taken in a given year, with values of *R* for individual years ranging between 0.36 in 2009 and 0.70 in 2018. Large variations in R occurred between consecutive surveys. Annual estimates of *R* near the upper and lower ends of the observed range are unlikely to reflect the sex ratio in the broader population. The mean value of 0.55 obtained by combining all available data is likely to be a better approximation of the sex ratio of the population in any one year than the estimate obtained from that year's data. A value of sex ratio by weight of greater than 0.5 (i.e. 0.55) is appropriate because on average adult females sampled during the spawning season are slightly heavier at any given size than males. The marginally higher proportion of females (51.1%) than males (49.8%) obtained in samples collected between 1998 and 2018 also helps to explain why *R* was greater than 0.5. Uncertainty in the estimate of spawning biomass is reduced by using the mean value of *R* from the entire dataset rather than the estimate obtained in any single year.

Other studies have shown that *S* is correlated with *R* (e.g. Ward et al. 2016; SARDI unpublished b). Samples obtained in years when estimates of *R* were low (e.g. 0.35) typically produced estimates of *S* that were high (e.g. 0.18). This correlation exists because a large proportion of the

females present in samples dominated by males were actively spawning, and vice-versa (Ganias et al. 2009). This dominance of males and females in samples has previously been interpreted as an artefact of differential sampling of spawning and non-spawning schools, respectively (Ganias et al. 2009). The mean value of *S* (0.11) obtained using all available data from South Australia is similar to the global mean spawning fraction for Sardine of 0.12 (Ganias et al. 2009). Like *R*, the all-years value of *S* is likely to be a better approximation of spawning fraction in any one year than the estimate obtained only using data collected in that year.

The data collected since 1998 used in the sensitivity analysis shows that estimates of *F* and *W* are highly variable among years. This variability may be explained, at least in part, by the sampling limitations discussed for *R* and *S*. However, the adult population includes fish of a wide range of sizes and the number of eggs produced by individual fish of similar sizes is also variable, so the variance of both parameters is high. Despite these sampling limitations and high levels of variability in *F* and *W* among years, the estimates of relative fecundity (*F*/*W*) obtained in individual years are remarkably similar (i.e. range 300–311 eggs.g^{-1}). This low variability among years in relative fecundity means that this combined parameter has minimal influence on estimates of spawning biomass. For this reason, there is limited benefit in estimating F and W annually. Relative fecundity (F/W) rather than F and W estimated separately should be used to calculate spawning biomass as this approach improves precision.

For reasons outlined above, in the foreseeable future, adult parameters used to calculate the spawning biomass of Sardine off South Australia should be estimated from data obtained in adult surveys conducted between 1998 and 2018.

5. Stock Assessment model

5.1 Introduction

This chapter describes the application of a new integrated stock assessment model ('SardEst') developed specifically for the SASF. This model supersedes the Stock Synthesis model (the "SS model") used in the previous two assessments (Ward et al. 2015, 2017), but is also based on a single stock, single fleet and single area. This model fits to commercial catch data (Chapter 2), fishery-dependent age-composition data (Chapter 3) and fishery-independent estimates of spawning biomass obtained using the DEPM (Chapter 4). Biological parameters (e.g. growth, maturity and weight-at-age) are estimated from fishery-dependent and fishery-independent data (Chapter 3).

The SS model performed well in the 2017 assessment, providing better fits to spawning biomass and age compositions than had been achieved in previous assessments (Ward et al. 2010; 2012). However, as Stock Synthesis is a generalised package for building stock assessment models, there were aspects of the model that were not well suited to the SASF, and required a more tailored model. One of these issues was the estimation of annual recruitment. Stock Synthesis can only estimate recruitment at age zero and must use a stock recruitment relationship (Methot 2000). However, the SS model demonstrated that the relationship between stock size and recruitment was weak (Ward et al. 2017). Additionally, recruitment in the SASF occurs at age one rather than age zero due to fishery selectivity (Chapter 3). Therefore, model recruitment was defined to occur at age one, i.e. the age at which recruits appear in the catch. The most important improvement in the new model is the better representation of the two mass mortality events, which was done by explicitly estimating additional natural mortality rates in those two years.

The SardEst model is an improved integrated assessment model compared to both the recent SS model (Ward et al. 2015, 2017) and the previous age-structured model developed in AD Model Builder (Ward et al. 2005). SardEst was built using the same population dynamics as the SS model, and has effectively the same population structure (the only major change is that SardEst is sex independent). This allowed the strengths of the SS model (good fits to spawning biomass and age-compositions) to be maintained, while providing improvements that could not be incorporated into the SS model. The SardEst model represents an evolution of the previous SASF stock assessment models rather than a reinvention.

There are two principle improvements incorporated into the SardEst model: 1) recruitment is estimated at age one, as deviations to an average value ($\bar{R}$) that are fit as random effects, and, 2) the mass mortality events of 1995 and 1998 are now explicitly estimated using increased natural mortality (*M*) in those years. SardEst is built in Template Model Builder (TMB), which is a contemporary auto differentiation program that allows stock assessment models to incorporate random effects (Kristensen et al 2016). This approach provides better estimates of recruitment deviations that are now explicitly recognised as random processes that vary annually about $\bar{R}$ (Thorson et al 2014). Improved estimates of recruitment are important as they ensure the model provides better estimates annual fishing mortality (*F*) and natural mortality in 1995 and 1998, when the mass mortality events occurred (Ward et al 2001).

In this report, the new SardEst model is presented and its continuing development is discussed. A full technical description of SardEst is presented in Appendix B. Comparisons to the previous SS model (using current data) are provided in Appendix C.

5.2 Methods

5.2.1 Base-case model

Model structure

The 2019 SardEst model is age-structured and sex-independent and assumes a single area fleet and stock for the SASF. The model includes data from the commencement of the fishery to present (1991 to 2019 by calendar year). As catch data are only available until 2018, the 2019 catch value in the model is set at the 2019 quota (42,750 t), which is typically caught. Age-composition data were available from 1995–2018 with the exception of 2007. Therefore, predicted catch-at-age in 2007 and 2019 are not fitted to data. Spawning biomass estimates are available from 1995–2019 but are not available in 2008, 2010, 2012 and 2015 when surveys were not done. Therefore, spawning biomass is not fitted to data in those years. As SardEst is a single sex model, spawning biomass includes both males and females. The model time step remains one year.

SardEst uses the 'Hybrid *F* method' to determine fishing mortality (*F*) which is also implemented by Stock Synthesis (Methot 2000). It is called hybrid because it combines the best features of the standard Pope-approximation catch-conditioned models and effort-conditioned Baranov models. It assumes exponential survival within each time step of Baranov, but rather than setting *F* proportional to fishing effort, it computes the Baranov *F* that is needed to remove the exact reported catch across each model time step. The survival of Sardines in each age class is then

adjusted with these estimates of *F* and fitted to fishery age composition data and DEPM estimates of spawning biomass. The advantage of this approach is that it reduces the number of parameters estimated by the model (no catchability is defined), while giving exact reported catch removals (Methot 2000).

Biological and fishery parameters

The biological parameters (i.e. growth and maturity) used in the models were based on information presented in previous chapters. Previous analyses have found no significant temporal changes to these parameters during the history of the fishery, or that there has been insufficient sampling to detect inter-annual variations (Ward et al. 2010, 2012, 2015, 2017). Each parameter was fixed at historical values and held constant in the stock assessment model.

Growth was assumed to follow the von Bertalanffy growth function with sex-independent parameters (Table 5-1). Sex specific weight-length relationships were derived from both commercial and fishery-independent samples. An allometric relationship of the form $W = A * FL^B$ was applied, where *W* is weight in kg, *FL* is caudal fork length in mm and *A* and *B* are the scaling and power coefficients respectively.

Maturity-at-age was determined for females using a logistic regression fit with a binomial error structure and a logit-link function where the logistic function takes the form:

$$P(a) = \left(1 + e^{-\ln(19)\left(\frac{a-a_{50}}{a_{95}-a_{50}}\right)}\right)^{-1}$$

Where *P(a)* is the proportion mature-at-age *a,* a_{50} is the age at 50% mature and a_{95} is the age at 95% mature. Female a_{50} and a_{95} were estimated as 2.63 years and 4.1 years, respectively (Table 5-1; Figure 5-1).

The base-case assessment model assumes that fishing occurs across a single stock and single area, and that selectivity for the commercial fishing fleet is a time-invariant, dome-shaped function of age. This was implemented by estimating the parameters of a ‘double-normal’ function (Methot 2000). This results in a selectivity curve with a descending right-side limb that mimics the expected reduced availability of older fish to the main components of the fishery, where younger (and smaller) fish dominate (Figure 5-1). The selectivity of the DEPM survey was determined as the mature portion of the population based on the maturity at-age-estimates.

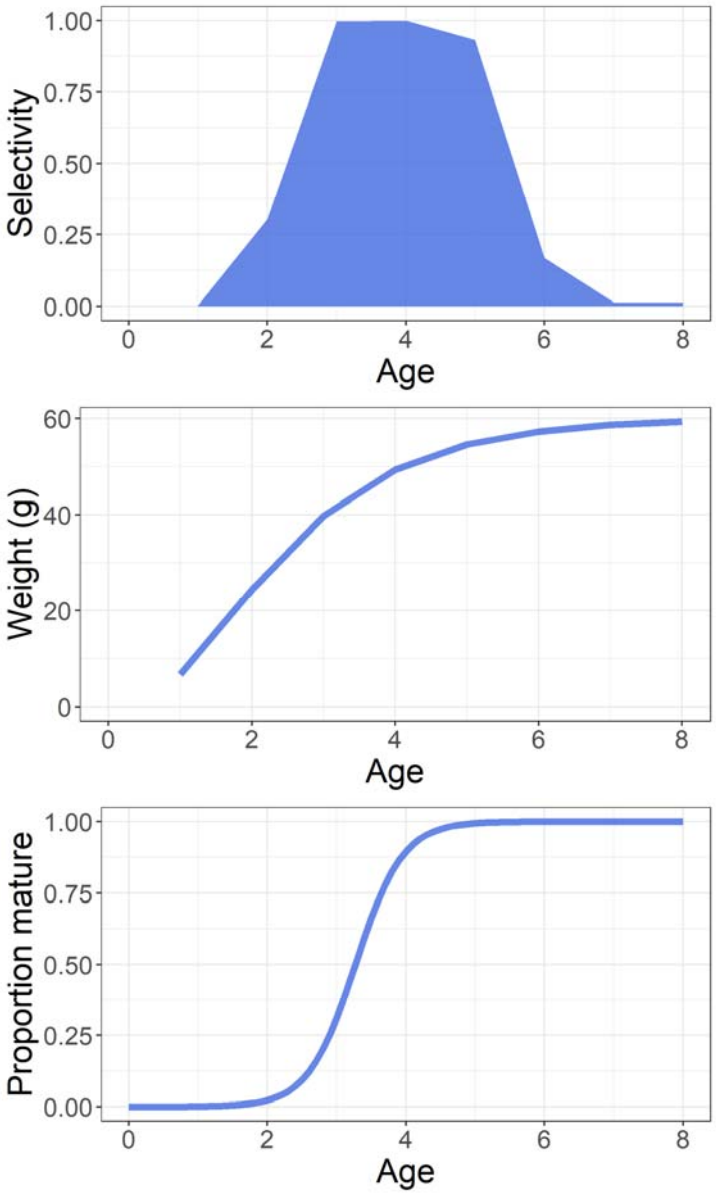

Figure 5-1. Age-based selectivity (expected proportion available to fishing by age), weight (g) and proportion of mature females used as inputs to SardEst and SS models.

Natural mortality and mass mortality events

Natural mortality (*M*) was assumed constant for all ages and across all years (*M* = 0.7) with the exception of 1995 and 1998. In those years, two mass mortality events each killed an estimated 70% of the adult population (Ward et al. 2001). Here, the SardEst model estimated the increased natural mortality for the adult population based on declines in spawning biomass determined

through DEPM surveys. Mass mortality was assumed to only effect only the mature fish. This was performed by estimating the maximum level of additional mortality (M_t^{max}) in year *t* (where *t* = 1995 or 1998) and multiplying this value by the proportion mature at each age class. For example, natural mortality-at-age *a* in 1995 (M_{1995}^{max}) was estimated as:

$$M_{1995,a} = M + M_{1995}^{max} * P(a)$$

Where *P(a)* is the proportion mature-at-age *a*. Total mortality-at-age ($Z_{t,\,a}$) is then the sum of total natural mortality-at-age and fishing mortality-at-age *a* ($F_{t,\,a}$) determined via the hybrid method:

$$Z_{1995,a} = M_{1995,a} + F_{1995,a}$$

Model parameters and likelihood weighting

The SardEst model fits to two data sources as likelihood components: 1) Annual age-compositions (1995–2006 and 2008–2018), and, 2) DEPM spawning biomass estimates (1995–2008, 2009, 2011, 2013, 2015, 2016–2019). Additionally, annual total catches are used to condition estimates of *F* during the Hybrid *F* tuning method (Methot 2000). The likelihood components include the fits to age compositions and DEPM estimates, as well as the log-recruitment deviates, which are fitted as random effects. The estimated parameters of SardEst are:

1. $\bar{R}$ – mean number of recruits in log space.
2. $\tilde{R}_t$ – recruitment deviations for year *t* in log space
3. σ_R – the standard deviation of the recruitment deviates in log space
4. M_t^{max} – the maximum level of additional mortality in year *t* (where *t* = 1995 or 1998).

During model estimation, TMB first maximises the likelihood for the random effects (recruitment deviates) for a proposed set of fixed effects. Following this, TMB calculates the hessian matrix for these random effects and uses this to compute the joint likelihood of both random and fixed effects (Thorson et al 2015). Due to random effects being estimated prior to the fixed effects, it was apparent that the model was initially maximising the joint likelihood at lower estimates of σ_R. Therefore, without any data weighting being applied, σ_R approached zero and caused shrinkage towards $\bar{R}$. This was overcome by increasing the weighting on the spawning biomass likelihood component by a factor of two in order to produce base case model outputs that more closely

matched DEPM estimates of spawning biomass (Chapter 4). This was performed, as spawning biomass is the primary data source informing SardEst.

5.2.2 Input data

Data from multiple sources were integrated for the purposes of the assessment, including age-composition data, spawning stock biomass estimates from DEPM surveys (Chapter 4), and catch data from the commercial fishery. Table 5–1 shows the data used in the model by type, year, and data source.

Table 5-1. Model specifications for the base-case assessment model, developed using SardEst

Specification	Base-case Model
Time-step	Yearly
Model years	1992–2019
Catch (t)	1992–2018
Spawning biomass (t, yearly, from DEPM)	1995–2007; 2009; 2011; 2013–14, 2016–19
CPUE index	Not included
Model age classes	Ages 1–8+
Age composition data	Ages 1–8, 1995–2018 (excluding 2007)
Natural mortality (M)	
1992–94; 96,97; 1999+	M = 0.70
1995, 1998	Estimated as additional mortality in each year over mature age classes
Growth parameters	Fixed, time-invariant von-Bertalanffy
K	0.71
L_∞	177.8
L_0	3.45
Length-weight relationship (both sexes)	Fixed power function (approx. cubic)
A (Scalar parameter)	$5.03*10^{-6}$
B (Power parameter)	3.26
Maturity (females only)	Fixed logistic function of age
A_{50}	2.63 years
A_{95}	4.10 years
Stock-recruitment	Estimated Average recruitment ($\bar{R}$)
Recruitment deviations	Estimated as random effects
Recruitment variance, σ_R	Estimated
Selectivity	
Commercial Fishery	Fixed, domed-shaped function of age

Commercial catch data

Commercial catch data were available for all years between 1992 and 2018. Data based on catch disposal records (CDRs) were used, as they are considered most accurate. Full details on the collection and analyses of commercial catch data are presented in Chapter 2. As no catch data

was available for 2019, an assumption was made that the 2019 catch would match the quota (42,750 t); as has been the case for the last 10 years.

Fishery-independent spawning biomass estimates

Spawning biomass estimates obtained from annual DEPM surveys between 1995 and 2007, and 2009, 2011, 2013, 2014, 2016 and 2017 were used as a measure of absolute abundance in the model. The methodology for estimating daily egg production was updated in Chapter 4 of this assessment so that consistent methodology was applied across the time series of surveys. These refined estimates of spawning biomass and their coefficients of variation were included in the SardEst model.

Age data

Age composition data from commercial catches were available for all years between 1995 and 2018, except for 2007. Ages were determined from an estimated otolith-weight-age relationship and applied to fish in commercial catch samples for which an otolith weight was available. Details on the collection of age-composition data and determination of age from otolith weights are presented in Chapter 3.

5.2.3 Sensitivity analyses and model diagnostics

The sensitivity of the base-case assessment model to changes in key parameters was tested in relation to important model outputs, such as the estimated time series of spawning biomass. These included natural mortality (*M*) and age-at-recruitment. This was achieved by re-fitting the model across a greater range of values for these parameters and examining the change in the joint and marginal likelihoods. These analyses indicate the values for these fixed quantities that best suit the base-case model.

5.3 Results

5.3.1 Model fits to data

The model fitted well to the DEPM estimates during the mass mortality years (1995 and 1998) which had been overestimated in previous models (Ward et al 2017). During the 2000's, model estimates of spawning biomass fitted closely to DEPM estimates. In recent years (2013–2019), estimated biomass smoothed out DEPM estimates that were low and high in 2013 and 2014, respectively (Figure 5-3). In these years, SardEst determined that these DEPM estimates of

spawning biomass were not supported by age-compositions, determined levels of *F* nor estimated recruitment and were likely influenced by limitations in the DEPM surveys. SardEst smoothed out the estimates of spawning biomass in those years. The standard errors of the SardEst estimates of spawning biomass were lower than the DEPM estimates, demonstrating good compatibility between data sources (i.e. catch, DEPM estimates and age compositions).

SardEst provided good fits to age composition data in most years of the fishery (Figure 5-4). Poorer fits occurred in the years following the mass mortality events of 1995 and 1998. However, fits these years were also problematic in the 2017 SS model (Ward et al 2017; Figure C–2). Overall, the fits to age composition data were satisfactory and years where fits are less accurate are likely influenced by likelihood weighting adjustments for the DEPM data.

5.3.2 Parameter estimates

The two fixed effects recruitment parameters ($\log(\bar{R})$ and $log(\sigma_R)$) were estimated with high levels of precision (Table 5-2) while estimates of M_{1995}^{max} and M_{1998}^{max} were less precise. This was anticipated given that estimating natural mortality is a difficult undertaking in integrated stock assessment models (Sippel et al 2017). The annual recruitment deviates (random effect parameters in log space) were estimated between 0.73 and 1.70.

Table 5-2. Fixed effects parameters with standard errors estimated by SardEst.

Parameter	Estimate	Standard Error
$\log(\bar{R})$	16.28	0.07
$log(\sigma_R)$	-1.18	0.27
M_{1995}^{max}	2.94	0.76
M_{1998}^{max}	3.37	1.09

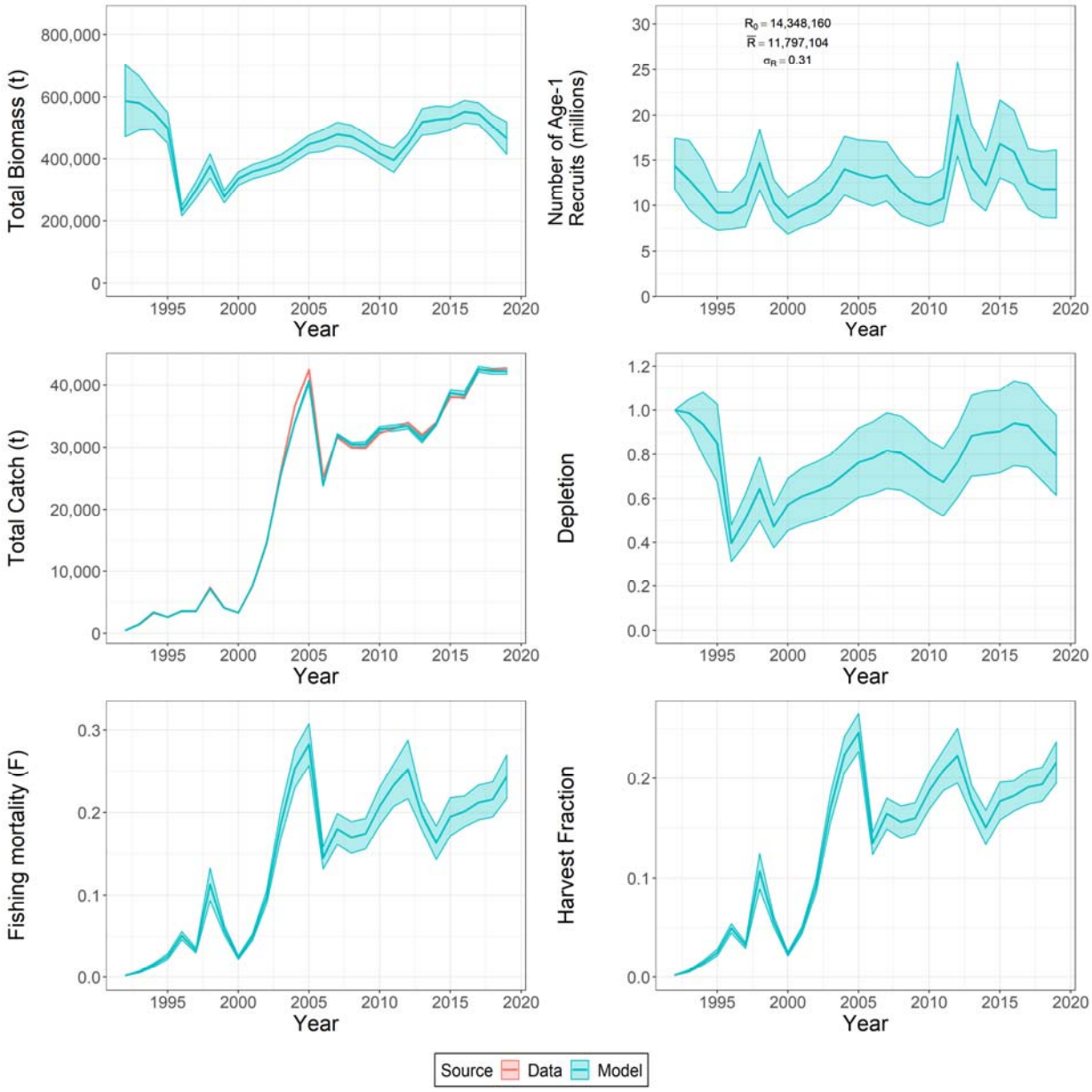

Figure 5-2. Estimates and standard error of time series derived quantities from SardEst. These include (left to right and top to bottom) 1) Total biomass (total weight of all age 1+ fish), 2) Annual recruitment (number of age 1 fish), 3) Annual total catch, 4) Level of depletion (Total biomass in 1992 [B_0] divided by annual total biomass), 5) Full, annual, instantaneous, fishing mortality (F) and 6) Harvest fraction (H). Blue lines denote model estimated values and blue shading represents the standard error around each estimate. Observed annual catches are represented by the red line.

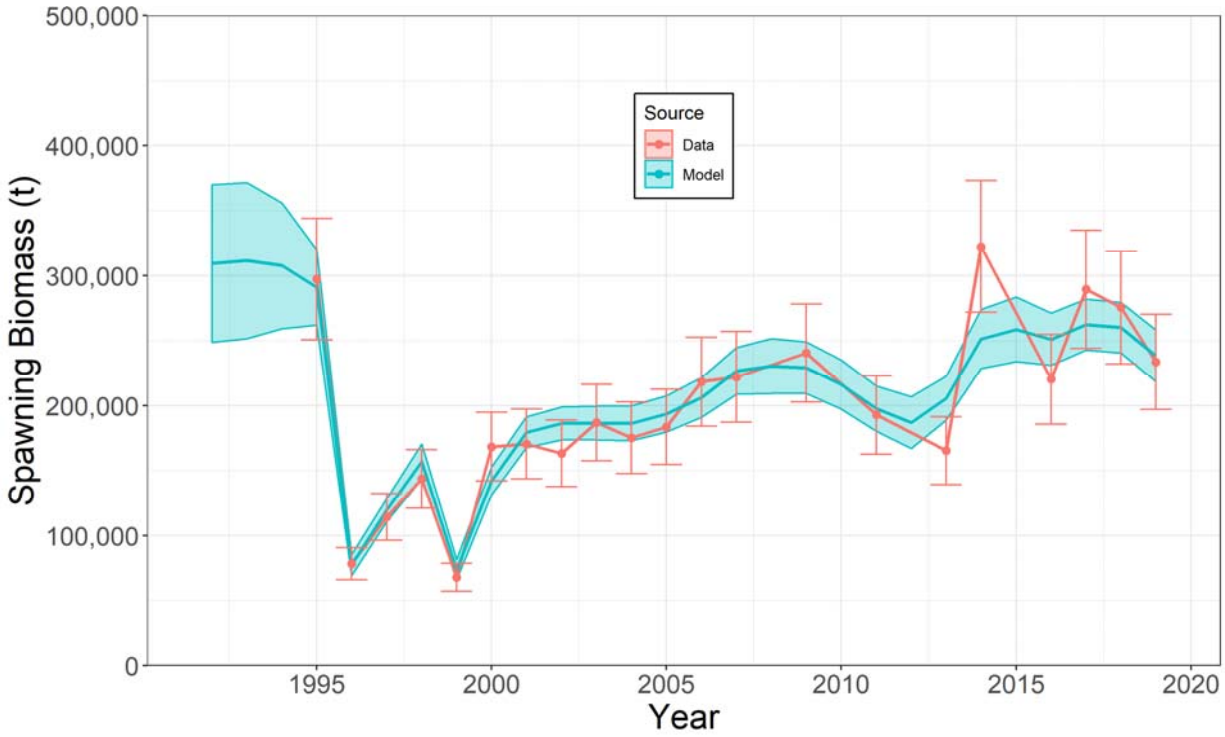

Figure 5-3. Estimated spawning biomass (total weight of mature fish) from the SardEst model. Blue line and shading represents the annual model estimates and respective standard error. Red points and lines show annual estimates of spawning biomass from DEPM surveys. Red Error bars are the standard error of these survey estimates. Note that surveys did not occur in 2008, 2010, 2012 and 2015.

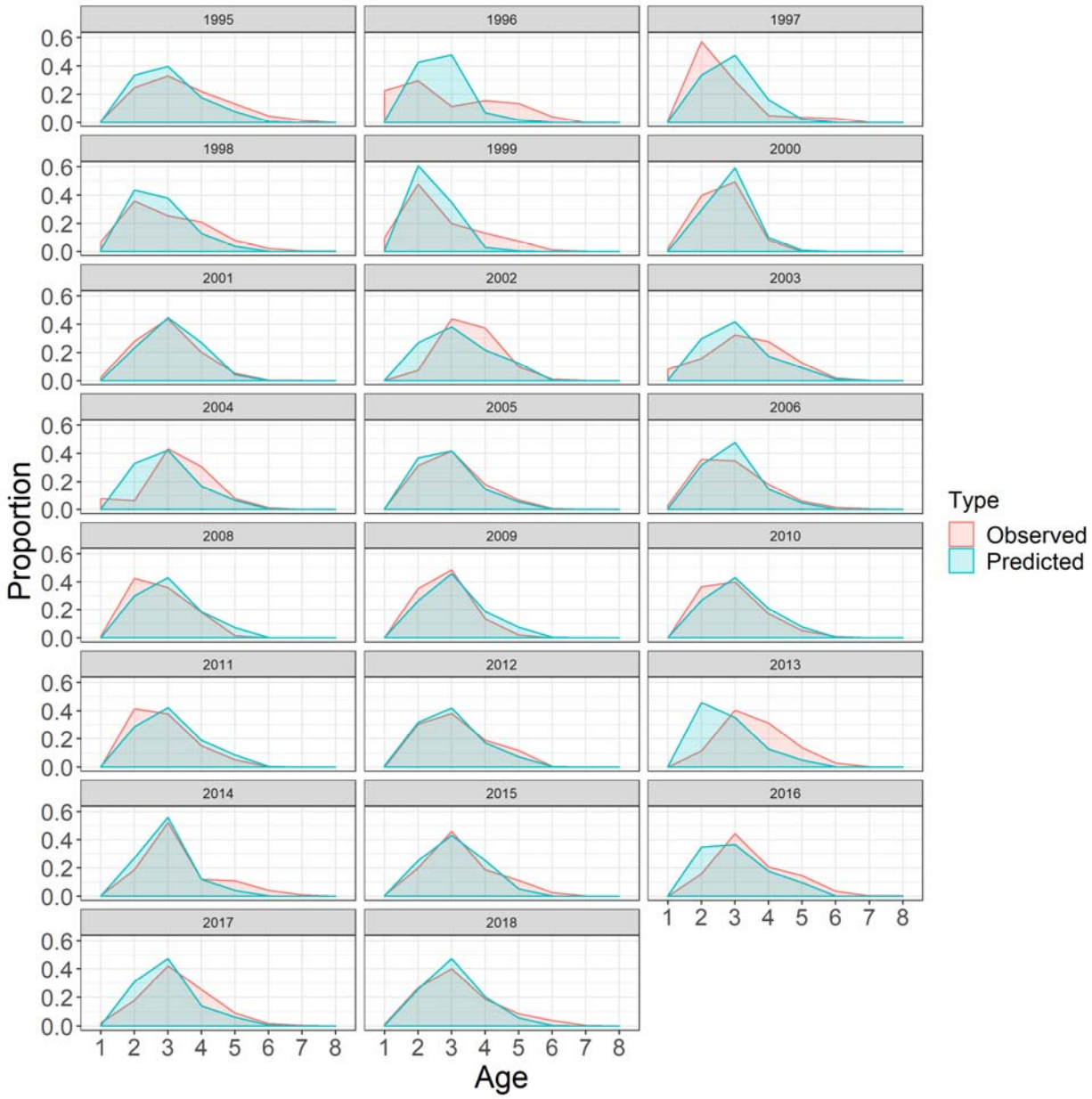

Figure 5-4. Comparison of annual observed (red shading) and model estimated (blue shading) age compositions. Note that no age compositions are available in 2007 and 2019.

5.3.3 Biomass and relative depletion

The SardEst model estimated unfished equilibrium total biomass (B_0) as 588,000 t (± 115,000 t). The lowest level of total biomass in the history of the fishery was 233,000 t (± 17,000 t) in 1996; the year following the first mass mortality event. This represents lowest level of depletion at 40% (± 8%). Since 1999, the fishery has recovered and consistently remained above 45% depletion. The mean level of depletion over the history of the fishery has been 72 % (± 16 %) and in 2019, the estimated depletion was 76% (± 16 %). This corresponds to a total biomass of 447,000 t (± 93,000 t).

Model estimated spawning biomass in 2019 was 239,000 t (± 20,000 t), which is well above the target reference point of 150,000 t set in the management plan (PIRSA 2014). The spawning biomass has only breached this target reference point twice in the history of the fishery (Figure 5-4), which occurred following both mass mortality events. Only once in the history of the fishery has the limit reference point of 75,000 t been breached. This occurred in 1999 when spawning biomass was 73,000 t (± 8,000 t).

5.3.4 Mass mortality events of 1995 and 1998

Earlier estimates of mortality rates in the mass mortality events of 1995 and 1998 were around 70% adult mortality (Ward et al 2001). In the previous SS model, natural mortality was therefore increased in these years for ages 3 and above using fixed values of 1.47yr^{-1} (~70% annual mortality). However, the SardEst model determined that ages 5 and older had an M of 3.64 yr^{-1} in 1995 and 4.07 yr^{-1} in 1998. This was 95% and 97% annual mortality respectively for fish aged 5 and older. Mass mortality was assumed to be less for Sardines aged 4 and under (Figure 5-5), for which the maximum level of additional mortality (M_t^{max}) was assumed to be reduced by the independent estimates of proportion-mature-at-age.

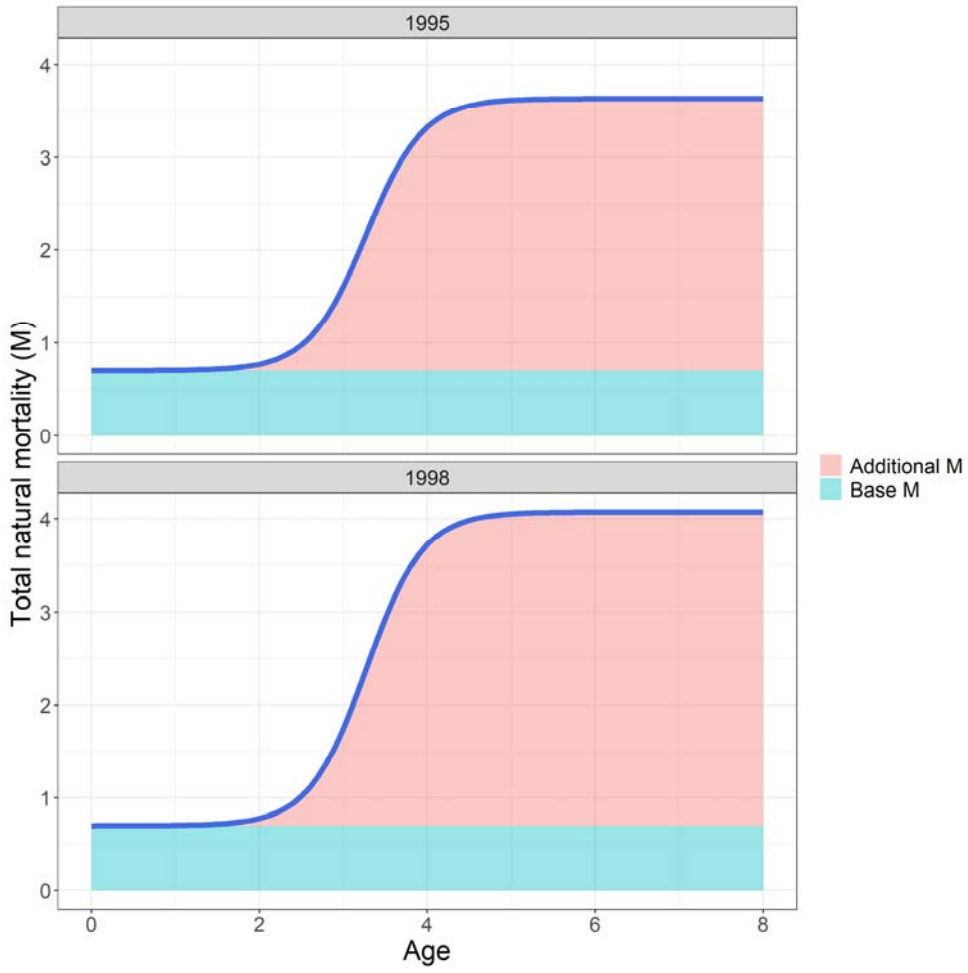

Figure 5-5. Natural mortality-at-age (M_a) during the 1995 and 1998 mass mortality events. The blue line indicates the total level of M for each age class. The blue shading shows the fixed level of M applied to all ages and years in the model (M = 0.7). The red shading shows the additional M_a estimated by the SardEst model in 1995 and 1998.

These estimates of mortality allowed SardEst to provide significantly closer fits the DEPM spawning biomass estimates in 1996 and 1998, than other stock assessment models (Ward et al. 2005, Ward et al 2017).

5.3.5 Recruitment

Model estimated unfished equilibrium recruitment (R_0) was 14.3-million age-one fish (± 2.8-million). The model-estimated mean recruitment ($\bar{R}$) was 11.8-million which differed from R_0 by approximately 18%. Recruitment consistently remained above 10 million recruits (Figure 5-2) with a maximum of 20 million recruits in 2012. The model estimated 2012 to be the year of maximum

recruitment as 2014 had a high biomass (Figure 5-3) and was composed mostly of age three fish (Figure 5-4).

Estimates of recruitment in the previous SS model were problematic; e.g. poor recruitment was estimated in the years preceding the mass mortality events (Ward et al 2017). This occurred as natural mortality was fixed at 1.47, which the SardEst model found to be an underestimate for the mortality events (Figure 5-5). SardEst was able to model the additional mortality that occurred in these years, yielding much more realistic time series of recruitment.

5.3.6 Exploitation rates

The Hybrid *F* method provided nearly exact agreement with the yearly catch totals in weight, therefore yielding more accurate estimates of annual fishing mortality (*F*) (assuming the biomass estimates are correct, which in turn depend on the assumed value of natural mortality). The highest level of *F* (0.283 yr^{-1}, ± 0.025) occurred in 2005 when total catch was highest (Figure 5-2). Another high level of *F* (0.252 yr^{-1}, ± 0.036) occurred in 2012, although this increase in *F* was due to a decline in model-estimated biomass rather than an increase in catch (Figure 5-3). Over the last 10 years, *F* has remained between 0.16 and 0.25 yr^{-1} (with the exception of 2012). The level of *F* in 2019 was 0.243 yr^{-1} (± 0.027) which equates to an exploitation rate of 21% (± 2%).

5.3.7 Model Diagnostics

Two key inputs are fixed quantities in the SardEst model: natural mortality (*M*) which is time and age invariant (mass mortality years excepted) and the age-at-recruitment. Sensitivity analyses were performed where different values of these quantities were provided to the model so that changes to the likelihood components and estimates of spawning biomass could be examined (Figure 5-6). This analysis demonstrated that the fixed value of *M* had little influence on the model. Estimates of spawning biomass varied little between values of 0.6 and 0.8yr^{-1} and the likelihoods were not overly influenced by a range of values from 0.4 to 1.2yr^{-1} (Figure 5-6). The likelihood sensitivities demonstrate that a value of 0.7 yr^{-1} was most appropriate as this gave the lowest negative log-likelihood for the joint likelihood (Figure 5-6). Therefore, 0.7 yr^{-1} was the fixed value of *M* used in the base case model (Table 5-1).

Age-at-recruitment had a greater effect on model spawning biomass than *M* (Figure 5-6). However, an age-at-recruitment from zero to two years had little effect on the spawning biomass estimates, which the exception of years 1992–1994, where there are no spawning biomass estimates to inform the model (Figure 5-6). The rest of the spawning biomass time series only

differed when age-at-recruitment was three (Figure 5-6). However, this is an unrealistic age-at-recruitment as age one and two fish are regularly present in age samples (Figure 5-3; Chapter 3). Therefore, this difference can be disregarded. The likelihood profiles demonstrate that an age-at-recruitment of one was the most appropriate for fitting to age-composition data (Figure 5-6). Consequently, this gave the lowest negative log-likelihood for the joint likelihood.

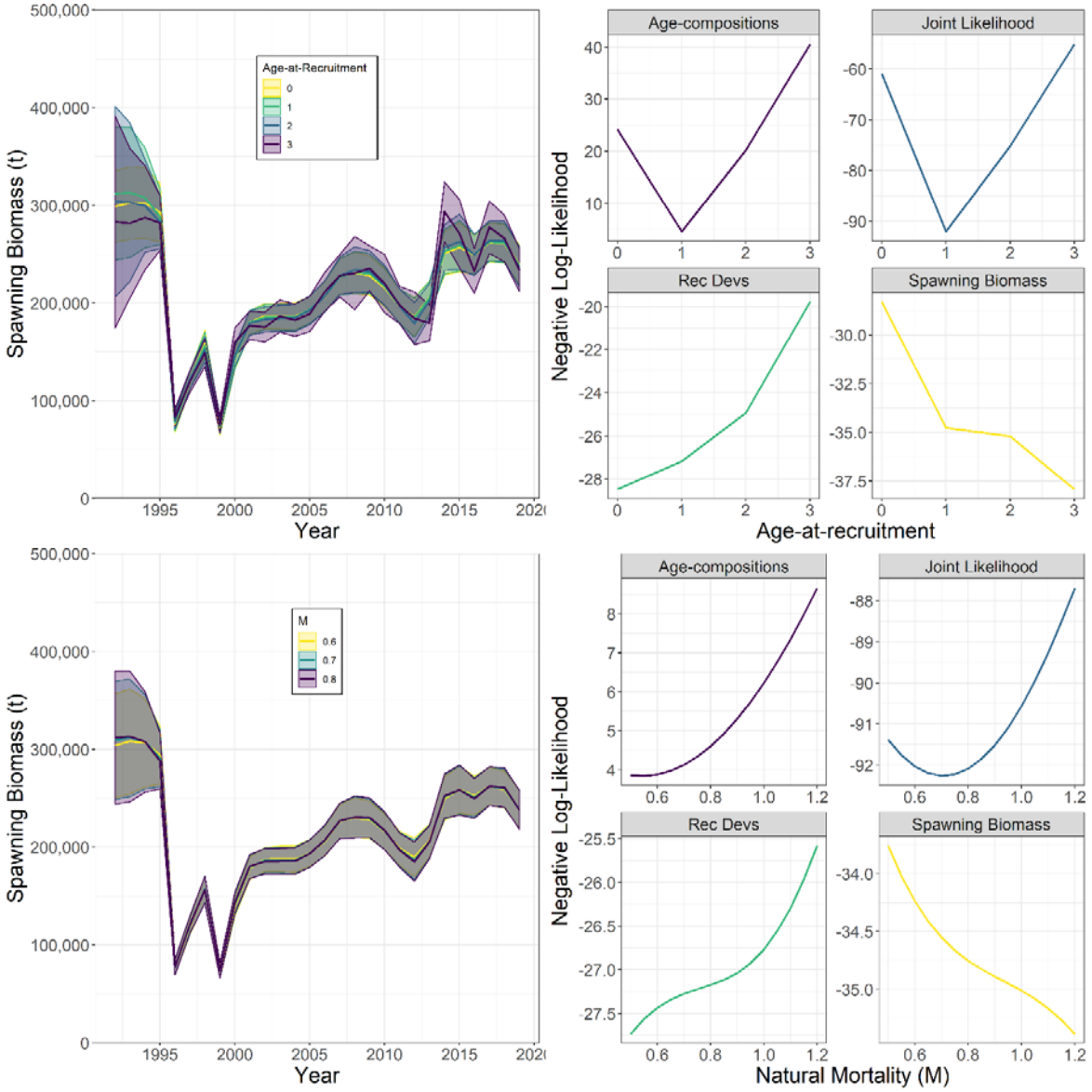

Figure 5-6. Model sensitivities to fixed values of natural mortality (*M*) and age-at-recruitment. Left hand panels show different model estimates of spawning biomass using different values of each quantity in the base-case model. Lines are the model estimates and shaded areas are the standard errors. Right hand plots show the profiles of the joint likelihood and likelihood components over a range of values for each quantity when applied to the base case model. The

lowest negative log-likelihoods demonstrate the most appropriate value for each likelihood component. The lowest joint likelihood value determined the most appropriate value for the model.

5.4 Discussion

The new 'SardEst' model was built specifically for the SASF and addresses some limitations of the previous model that was implemented in Stock Synthesis. These improvements include better estimates of recruitment, estimation of additional mortality rates during the 1995 and 1998 mass mortality events, and reduced standard errors around key outputs (such as spawning biomass). As SardEst was built for the SASF, it has been tailored to the specific needs and dynamics of this fishery.

The most important developments in SardEst were related to recruitment and mortality. Recruitment is now estimated for age-one fish without requiring a stock recruitment relationship. This allows the model to make better use of information on age compositions. Recruitment is also estimated as random effects about a mean recruitment value, which decreases the variability around their estimates (Thorson et al 2014). This is important, as all stock assessment models have to reconcile changes in biomass through changes in either mortality or recruitment. If biomass increases, a model could interpret this as a pulse in recruitment or a decline in mortality. When explicitly attempting to determine the effects of catches on a population, these aspects become increasingly significant. By better handling of recruitment, SardEst can more effectively model mortality, providing greater confidence in its estimates of exploitation rate and levels of catch. The improved fits to spawning biomass in 1996 and 1999 demonstrate this point. Previously, the SS model could not reconcile these declines in biomass to mortality as only small catches occurred in the preceding years. As natural mortality was fixed in those years, the catches were insufficient to cause the decline in biomass from the mass mortality events. Therefore, the SS model estimated recruitment failures two years prior to the mortality events. SardEst did not have this issue as it estimated natural mortality in the mass mortality years. In addition, recruitment is less prone to variation because it is fitted with random effects, meaning that pulses or failures in recruitment will only occur when the model can find no other explanation in the data.

The explicit estimation of M_{1995}^{max} during the mass mortality events of 1995 and 1998 (Ward et al 2001) is a novel aspect of SardEst. Estimating *M* in integrated stock assessment models has long been discussed, but has rarely been achieved with confidence (Brodziak et al 2011). Simulation studies have shown that estimating *M* is theoretically possible when a model is correctly specified (Lee et al 2011, Sippel et al 2017). However, it has also been highlighted that all stock assessment models have some degree of mis-specification and therefore estimating *M* is rarely achievable (Francis 2012). Here, SardEst only attempted to estimate *M* for mature individuals that succumbed to mass mortality events caused by a herpes virus in two years of the time series

(Ward et al 2001). Sufficient information was available for the model to estimate *M* in 1995 and 1998 and produce closer fits to the DEPM estimates of spawning biomass in those years. In many cases, attempts to estimate time variant *M* can be problematic as it can influence results across the entire time series (Johnson et al 2015). Therefore, estimating *M* in stock assessment models remains controversial (Francis 2012, Johnson et al 2015). Here, the process for estimating *M* in 1995 and 1998 is not contentious as the remainder of the time series is mostly unaffected. The estimation of *M* during the mass mortality events improved model accuracy only in the necessary years, with little bias incorporated into the rest of the time series. We acknowledge however that the estimate of overall natural mortality, $M = 0.7$, is not easily differentiated given these data from other possible levels of *M*, confirming the difficulty of estimating *M* in this analysis, as found by Francis and others. Lower estimates of *M* would imply higher levels of fishery exploitation.

The model-estimated biomass in 2019 was 239,000 t (± 20,000 t) which is well above the target reference point of 150,000 t (PIRSA 2014). The model estimated exploitation rate for spawning biomass is 18%, which is below the maximum rate of 22.5% outlined for Tier 2 identified in the management plan (PIRSA 2014).

SardEst is a new model and there is scope for further development. Firstly, SardEst does not currently provide projections. Development of a projection component would be beneficial and could possibly be expanded to include management strategy evaluation (MSE). Secondly, SardEst is currently a single sex model that uses the maturity data for females only. Therefore, there may be potential benefits in developing a two-sex model. Thirdly, SardEst is a single area model that does not consider the two zones of the fishery. This has not been problematic thus far for the SASF. However, should increases in catch proportions occur outside the Gulfs Zone, developing a two-zone model may be beneficial.

6. DISCUSSION

6.1 Stock status and uncertainty

Under the criteria outlined in the harvest strategy for the SASF (PIRSA 2014), the Southern Stock of Australian Sardine in 2019 is classified as **Sustainable**. The estimate of spawning biomass obtained using the DEPM in 2019 was 233,684 (181,214–286,153) t, which is above the target reference point of 150,000 t and above the upper reference point of 190,000 t (PIRSA 2014). The model estimate of spawning biomass for 2019 of 239,000 (± 93,000) t was also above the target reference point. The exploitation rate for spawning biomass was approximately 18%, which is below the maximum rate at Tier 2 of 22.5% identified in the Management Plan. These findings are consistent with other recent assessments of the status of the southern stock of Sardine which classified the stock as sustainable (e.g. Ward et al. 2017; Stewardson et al. 2018).

The strongest single piece of empirical evidence indicating that the Southern Stock of Sardine should be classified as sustainable is that the spawning area recorded during the 2019 survey was 53,600 km^2, which is fifth largest on record. It is widely recognised that spawning area is strongly correlated with the size of the spawning stock of Sardine (e.g. Mangel and Smith 1990, Gaughan et al. 2004). Under the refined approach used to apply the DEPM in this report, inter-annual variations in estimates of spawning biomass are driven primarily by fluctuations in the spawning area (Chapter 4).

The population modelling undertaken in this report also addresses some of the previous uncertainties in the historical estimates of spawning biomass. For example, because natural mortality during the mass mortality events of 1995 and 1998 is now estimated explicitly, SardEst fits to the DEPM estimates of spawning biomass in those years much better than previous models. SardEst also smoothed out the low and high estimates of spawning biomass obtained in 2013 and 2014, respectively, because they were not supported by other data sources (e.g. age-compositions, estimates of *F* or recruitment). It is likely that the fluctuations observed in these years reflected (at least in part) limitations of the DEPM surveys rather than fluctuations in actual abundance. For example, the low estimate of spawning biomass in 2013 is likely to have resulted from incomplete coverage of the survey area during that year (Chapter 5). Importantly, the low standard errors of the SardEst estimates of spawning biomass compared to those from the DEPM, demonstrate a high level of compatibility among data sources (i.e. catch, DEPM estimates and age compositions) that has not been achieved using previous models.

6.2 Management implications

The re-analysis of historical data for Sardine off South Australia conducted in this report provided revised estimates of spawning biomass from 1995 to 2019. This revision addressed significant uncertainties in estimates of key parameters obtained early in the time-series, especially P_0 and S. It also increased the precision of estimates of spawning biomass obtained over the entire time period. These improvements have increased our understanding of the fluctuations in the spawning biomass of Sardine off South Australia over the last 25 years. Application of the revised approach to applying the DEPM described in this report will help to ensure that future estimates of spawning biomass are accurate and precise as possible.

Estimates of spawning biomass and outputs from the population model suggests that the harvest strategy for the SASF (PIRSA 2014) is appropriate for a relatively new fishery for a low trophic level species, or forage fish, such as Sardine, in Australian waters (Smith et al. 2015). Ecological modelling undertaken by Smith et al. (2015) suggested that target and limit reference points for spawning biomass of B_{50} and $B_{20,}$ respectively, are likely to be ecologically sustainable for several species of small pelagic fishes in Australian, including Sardine. Smith et al. (2015) also indicated that exploitation rates for Sardine of below 33% are likely to ensure that stocks remain above these target (B_{50}) and limit (B_{20}) reference points over a 50 year time period.

The maximum exploitation rate in the current harvest strategy of 25% at Tier 1 was established at this precautionary level to reflect the level of information available for the fishery when the harvest strategy was established in 2014. The target reference point for the SASF of 150,000 t is appropriate because it is approximately equal to 50% of the unfished spawning biomass (i.e. 298,000 t in 1995). The limit reference of point of 75,000 t is also conservative because it is higher than the 20% of the unfished spawning biomass (i.e. ~60,000 t) recommended for Australian small pelagic fisheries by Smith et al. (2015).

6.3 Future directions

Future applications of the DEPM to Sardine off South Australia should adopt the revised approach taken in this report. Because future estimates of spawning biomass will be driven primarily by the estimate of spawning area it will be critical that future surveys utilize the adaptive sampling implemented after 2013 and cover other areas off South Australia where Sardine are likely to spawn, including waters east of Kangaroo Island. Consideration should also be given to further developing SardEst as a two-sex, two-zone population model with capability to undertake projections and conduct management strategy evaluations.

7. REFERENCES

Alheit, J. 1993. Use of the daily egg production method for estimating biomass of clupeoid fishes: A review and evaluation. Bulletin of Marine Science **53**:750–767.

Barnes, J. T., A. D. Maccall, L. D. Jacobson, and P. Wolf. 1992. Recent Population Trends and Abundance Estimates for the Pacific Sardine (*Sardinops sagax*). California Cooperative Oceanic Fisheries Investigations Reports **33**:60–75.

Blackburn, M. 1950. Studies on the age, growth, and life history of the sardine *Sardinops neopilchardus* (Steindachner), in Southern and Western Australia. Australian Journal of Marine and Freshwater Research **1**:221–258.

Brodziak, J. K. T., J. N. Ianelli, K. Lorenzen, and R. D. Methot. 2011. Estimating natural mortality in stock assessment applications August 11-13, 2009, Alaska Fisheries Science Center, Seattle, WA.

Bulman, C. M., Condie, S. A., Neira, F. J., Goldsworthy, S. D., and Fulton, E. A. (2011). The trophodynamics of small pelagic fishes in the southern Australian ecosystem and the implications for ecosystem modelling of southern temperate fisheries. Final Report for FRDC Project 2008/023.

Butler, J. L., M. L. Granados, J. T. Barnes, M. Yaremko, and B. J. Macewicz. 1996. Age composition, growth, and maturation of the Pacific sardine (*Sardinops sagax*) during 1994. California Cooperative Oceanic Fisheries Investigations Reports **37**:152–159.

Checkley, D.M. Jr, R.G. Asch and R.R. Rykaczewski. 2017. Climate, anchovy and sardine. Annual Reviews in Marine Science. **9:** 469-493.

Cochrane, K. L. 1999. Review of the Western Australian sardine fishery 12-16 April 1999. Report to Fisheries Western Australia.

Cury, P., Bakun, A., Crawford, R. J. M., Jarre, A., Quin˜ones, R. A., Shannon, L. J., and Verheye, H. M. 2000. Small pelagics in upwelling systems: patterns of interaction and structural changes in ‘‘wasp-waist’’ ecosystems. – ICES Journal of Marine Science, **57**: 603–618.

Cury PM, Boyd IL, Bonhommeau S, Anker-Nilssen T and others (2011) Global seabird response to forage fish de - pletion—one-third for the birds. Science **334**: 1703−1706

Daly, K. 2007. The diet and guild structure of the small pelagic fish community in the eastern Great Australian Bight, South Australia. Honours Thesis. Adelaide University and SARDI Aquatic Sciences.

De Oliveira, J. A. A., D. S. Butterworth, B. A. Roel, K. L. Cochrane, and J. P. Brown. 1998. The application of a management procedure to regulate the directed and bycatch fishery of South African sardine *Sardinops sagax*. South African Journal of Marine Science **19**:449–469.

Dimmlich, W. F., W. G. Breed, M. Geddes, and T. M. Ward. 2004. Relative importance of gulf and shelf waters for spawning and recruitment of Australian anchovy, *Engraulis australis*, in South Australia. Fisheries Oceanography **13**:310–323.

Dimmlich, W. F., and Ward, T.M. 2006. Ontogenetic shifts in the distribution and reproductive patterns of Australian anchovy (Engraulis australis) by otolith microstructure analysis. Marine and Freshwater Research **57**:373–381

Dimmlich, W. F., T. M. Ward, and Breed, W.G. 2009. Spawning dynamics and biomass estimates of an anchovy Engraulis australis population in contrasting gulf and shelf environments. Journal of Fish Biology **75**:1560–1576.

Espinoza, P., A. Bertrand, C. van der Lingen, S. Garrido, and B. Rojas de Mendiola. 2009. Diet of Sardine (Sardinops sagax) in the northern Humboldt Current system and comparison with the diets of clupeoids in this and other eastern boundary upwelling systems. Progress in Oceanography **83**:242–250.

Fletcher, W., and R. Tregonning. 1992. Distribution and timing of spawning by the Australian pilchard (<I>Sardinops sagax neopilchardus</I>) off Albany, Western Australia. Marine and Freshwater Research **43**:1437–1449.

Fletcher, W. J., R. J. Tregonning, and G. J. Sant. 1994. Interseasonal variation in the transport of pilchard eggs and larvae off southern Western Australia. Marine Ecology Progress Series **111**:209–224.

Fletcher, W. J. 1995. Application of the otolith weight-age relationship for the pilchard, *Sardinops sagax neopilchardus*. . Canadian Journal of Fisheries and Aquatic Science. **52**:657–664.

Fletcher, W. J., and S. J. Blight. 1996. Validity of using translucent zones of otoliths to age the pilchard *Sardinops sagax neopilchardus* from Albany, western Australia. Marine and Freshwater Research **47**:617–624.

Fletcher, W. J., N. C. H. Lo, E. A. Hayes, R. J. Tregonning, and S. J. Blight. 1996. Use of the daily egg production method to estimate the stock size of western Australian sardines (*Sardinops sagax*). Marine and Freshwater Research **47**:819–825.

Francis, R. I. C. C. 2012. The reliability of estimates of natural mortality from stock assessment models. Fisheries Research 119-120:133-134.

Gaughan, D. J., W. J. Fletcher, and J. P. McKinlay. 2002. Functionally distinct adult assemblages within a single breeding stock of the sardine, *Sardinops sagax*: management units within a management unit. Fisheries Research **59**:217–231.

Gaughan, D. J., T. I. Leary, R. W. Mitchell, and I. W. Wright. 2004. A sudden collapse in distribution of Pacific sardine (*Sardinops sagax*) off southwestern Australia enables an objective re-assessment of biomass estimates. Fishery Bulletin **102**:617–633.

Goldsworthy, S.D., Page, B., Rogers, P.J., Bulman, C., Wiebkin, A., McLeay, L.J., Einoder, L., Baylis, A.M.M., Braley, M., Caines, R., Daly, K., Huveneers, C., Peters, K., Lowther, A.D. and Ward, T.M. (2013) Trophodynamics of the eastern Great Australia Bight ecosystem: ecological change associated with the growth of Australia's largest fishery. Ecological Monitoring 255: 38– 57

Grant, W. S., and R. W. Leslie. 1996. Late Pleistocene dispersal of IIndian-Pacific Sardine populations of the genus *Sardinops*. Marine Biology **126**:133–142.

Grant, W. S., A. M. Clark, and B. W. Bowen. 1998. Why restriction fragment length polymorphism analysis of mitochondrial DNA failed to resolve sardine (*Sardinops*) biogeography: insights from mitochondrial DNA cytochrome b sequences. Canadian Journal of Fisheries and Aquatic Sciences **55**:2539–2547.

Hayashi, A., Y. Yamashita, K. Kawaguchi, and T. Ishii. 1989. Rearing method and daily otolith ring of Japanese Sardine larvae. NIPPON SUISAN GAKKAISHI **55**:997–1000.

Hilborne, R., Amoroso, R.O., Bogazzi, E., Jensen, O.P., Parma, A.M., Szuwalski, C., Walters, C.J., 2017. When does fishing forage species affect their predators? Fisheries Research. **191:** 211–221.

Hill, K. T., N. C. H. Lo, B. J. Macewicz, and R. Felix-Uraga. 2005. Assessment of the Pacific Sardine (*Sardinops sagax*). National Oceanic and Atmospheric Administration Fisheries. South West Fisheries Science Center, La Jola California.

Hunter, J. R., and S. R. Goldberg. 1980. Spawning incidence and batch fecundity in northern anchovy, Engraulis mordax. FIsheries Bulletin **77**:641–652.

Hunter, J. R., N. C. H. Lo, and J. H. L. Roderick. 1985. Batch Fecundity in Multiple Spawning Fishes. Pages 67–79 *in* R. Lasker, (eds). An egg production method for estimating spawning biomass of pelagic fish: Application to the northern anchovy, Engraulis mordax., NOAA Tech. Rep. NMFS.

Hunter, J. R., and B. J. Macewicz. 1985. Measurement of spawning frequency in multiple spawning fishes. Pages 79–94 *in* R. Lasker, (eds). An egg production method for estimating spawning biomass of pelagic fish: Application to the northern anchovy, Engraulis mordax., NOAA Tech. Rep. NMFS.

Hunter, J. R., and N. C. H. Lo. 1997. The daily egg production method of biomass estimation: Some problems and potential improvements. . Ozeanografika **2**.

Izzo, C., B. M. Gillanders, and T. M. Ward. 2012. Movement patterns and stock structure of sardine (*Sardinops sagax*) off South Australia and the East Coast: implications for future stock assessment and management. South Australian Research and Development Institute (Aquatic Sciences), Adelaide.

Izzo, C., T. M. Ward, A. R. Ivey, I. M. Suthers, J. Stewart, S. C. Sexton, and B. M. Gillanders. 2017. Integrated approach to determining stock structure: implications for fisheries management of sardine, *Sardinops sagax*, in Australian waters. Reviews in Fish Biology and Fisheries **27**:267–284.

Jones, J. B., A. D. Hyatt, P. M. Hine, R. J. Whittington, D. A. Griffin, and N. J. Bax. 1997. Australasian pilchard mortalities. World Journal of Microbiology & Biotechnology **13**:383–392.

Kailola, P.J., Williams, M.J., Stewart, P.C., Reichelt, R.E., McNee, A., Grieve, C., 1993. Australian Fisheries Resources. Bureau of Resource Sciences and Fisheries Research Development Corporation, Canberra, Australia.

Kerstan, M. 2000. Estimation of precise ages from the marginal increment widths of differently growing sardine (*Sardinops sagax*) otoliths. Fisheries Research **46**:207–225.

Kristensen, K., A. Nielsen, C. W. Berg, H. Skaug, and B. M. Bell. 2016. TMB: Automatic Differentiation and Laplace Approximation. **70**:21.

Lasker, R. 1985. An egg production method for estimating spawning biomass of pelagic fish: application to northern anchovy, *Engraulis mordax*. NOAA. Tech. Rep. NMFS **36**:1–99.

Lee, H.-H., M. N. Maunder, K. R. Piner, and R. D. Methot. 2011. Estimating natural mortality within a fisheries stock assessment model: An evaluation using simulation analysis based on twelve stock assessments. Fisheries Research **109**:89-94.

Louw, G. G., C. D. Van der Lingen, and M. J. Gibbons. 1998. Differential feeding by sardine *Sardinops sagax* and anchovy *Engraulis capensis* recruits in mixed shoals. South African Journal of Marine Science **19**:227–232.

Mangel, M., and Smith, P.E. (1990) Presence-absence sampling for fisheries management. Canadian Journal of Fisheries and Aquatic Sciences **47**: 1875–1887.

Methot, R. D. 2000. Technical description of the stock synthesis assessment program. NOAA Technical Memorandum. Seattle, Washington.

McGarvey, R., and M. A. Kinloch. 2001. An analysis of the sensitivity of stock biomass estimates derived from the daily egg production method (DEPM) to uncertainty in egg mortality rates. Fisheries Research **49**:303–307.

Neira, F. J., A. G. Miskiewicz, and T. Trnski. 1998. Larvae of temperate Australian fishes: Laboratory guide for larval fish identification. University of Western Australia Press: Western Australia.

Parker, K. 1980. A direct method for estimating northern anchovy, Engraulis mordax, spawning biomass. . FIsheries Bulletin **78**:541–544.

Parrish, R. H., R. Serra, and W. S. Grant. 1989. The Monotypic Sardines, Sardina and Sardinops—Their Taxonomy, Distribution, Stock Structure, and Zoogeography. Canadian Journal of Fisheries and Aquatic Sciences **46**:2019–2036.

Picquelle, S., and G. Stauffer. 1985. Parameter estimation for an egg production method of anchovy biomass assessment. Pages 7–17 *in* R. Lasker, (eds). An egg production method for estimating spawning biomass of pelagic fish: application to northern anchovy, Engraulis mordax. NOAA Tech. Rep. NMFS.

Pikitch, E., Boersma, P.D., Boyd, I.L., Conover, D.O., Cury, P., Essington, T., Heppell, S.S., Houde, E.D., Mangel, M., Pauly, D., Plagányi, É., Sainsbury, K., and Steneck, R.S. 2012. Little Fish, Big Impact: Managing a Crucial Link in Ocean Food Webs. Lenfest Ocean Program. Washington, DC. 108 pp.

PIRSA. 2007. Addendum to the management plan for the South Australian pilchard fishery. South Australian fisheries management series, Paper No. 47.

PIRSA. 2014. Management plan for the South Australian commercial marine scalefish fishery. Part B–Management arrangements for the taking of Sardines. Paper number 68.

Quinonez-Velazquez, C., M. O. Nevarez-Martinez, and M. G. Gluyas-Millan. 2000. Growth and hatching dates of juvenile pacific sardine *Sardinops caeruleus* in the Gulf of California. Fisheries Research **48**:99–106.

Rogers, P. J., M. Geddes, and T. M. Ward. 2003. Blue sprat Spratelloides robustus (Clupeidae: Dussumieriinae): A temperate clupeoid with a tropical life history strategy? Marine Biology **142**.

Rogers, P. J., and T. M. Ward. 2007. Application of a 'case-building approach' to investigate the age distributions and growth dynamics of Australian sardine (Sardinops sagax) off South Australia. Marine and Freshwater Research **58**:461–474.

Schwartzlose, R. A., J. Alheit, A. Bakun, T. R. Baumgartner, R. Cloete, R. J. M. Crawford, W. J. Fletcher, Y. Green-Ruiz, E. Hagen, T. Kawasaki, D. Lluch-Belda, S. E. Lluch-Cota, A. D. MacCall, Y. Matsuura, M. O. Nevárez-Martínez, R. H. Parrish, C. Roy, R. Serra, K. V. Shust, M. N. Ward and J. Z. Zuzunaga. 1999. Worldwide large-scale fluctuations of sardine and anchovy populations, South African Journal of Marine Science, **21**:1, 289-347

Sexton, S. C., T. M. Ward, J. Stewart, K. M. Swadling, and C. Huveneers. 2019. Spawning patterns provide further evidence for multiple stocks of sardine (Sardinops sagax) off eastern Australia. Fisheries Oceanography **28**: 18-32.

Sippel, T., H. H. Lee, K. Piner, and S. L. H. Teo. 2017. Searching for M: Is there more information about natural mortality in stock assessments than we realize? Fisheries Research **192**:135-140.

Smith, A., T. M. Ward, F. Hurtado, N. Klaer, E. Fulton, and A. Punt. 2015. Review and update of harvest strategy settings for the Commonwealth Small Pelagic Fishery—Single species and ecosystem considerations. Hobart. Final Report of FRDC Project No. 2013/028.

Smith, A. D. M., C. J. Brown, C. M. Bulman, E. A. Fulton, P. Johnson, I. C. Kaplan, H. Lozano-Montes, S. Mackinson, M. Marzloff, L. J. Shannon, Y.J. Shin, and J. Tam. 2011. Impacts of Fishing Low–Trophic Level Species on Marine Ecosystems. Science **333**:1147–1150.

Smith, P. E., and S. L. Richardson. 1977. Standard techniques for pelagic fish egg and larva surveys. FAO Fisheries Technical Paper **175**:100p.

Somarakis, S., I. Palomera, A. Garcia, L. Quintanilla, C. Kousikopoulos, A. Uriarte, and L. Motos. 2004. Daily egg production of Anchovy in European waters. ICES Journal of Marine Science. **61**.

Stratoudakis, Y., M. Bernal, K. Ganias, and A. Uriate. 2006. The daily egg production method: recent advances, current applications and future challenges. Fish and Fisheries 7:35–57.

Stewardson, C., Andrews, J., Ashby, C., Haddon, M., Hartmann, K., Hone, H., Horvat, P., Mayfield, S., Roelofs, A., Sainsbury, K., Saunders, T., Stewart, J., Nicol, S. and Brent Wise (eds) 2018, Status of Australian fish stocks reports 2016, Fisheries Research and Development Corporation, Canberra.

Thomas, R. M. 1984. A method of age determination for the South West African pilchard Sardinops ocellata. South African Journal of Marine Science 2.

Thorson, J. T., A. C. Hicks, and R. D. Methot. 2014. Random effect estimation of time-varying factors in Stock Synthesis. ICES Journal of Marine Science **72**:178-185.

Thorson, J. T., J. N. Ianelli, S. B. Munch, K. Ono, and P. D. Spencer. 2015. Spatial delay-difference models for estimating spatiotemporal variation in juvenile production and population abundance. Canadian Journal of Fisheries and Aquatic Sciences **72**:1897-1915.

Tourre, Y. M., Lluch-Cota, S. E., and White, W. B. 2007. Global multidecadal ocean climate and small-pelagic fish population. Environmental Research Letters, 2: 9pp.

Turner, R. 2016. deldir: Delaunay Triangulation and Dirichlet (Voronoi) Tessellation. R package version 0.1–12. https://CRAN.R-project.org/package=deldir

van der Lingen, C. D. 1994. Effect of Particle-Size and Concentration on the Feeding-Behavior of Adult Pilchard *Sardinops sagax*. Marine Ecology Progress Series **109**:1–13.

van Der Lingen, C. D. 2002. Diet of Sardine Sardinops sagax in the southern Benguela upwelling ecosystem. South African Journal of Marine Science **24**:301–316.

Ward, T., A. Ivey, and J. Carroll. 2016. Spawning biomass of Sardine, *Sardinops sagax*, in waters off South Australia.

Ward, T. M., F. Hoedt, L. McLeay, W. F. Dimmlich, G. Jackson, P. J. Rogers, and K. Jones. 2001a. Have recent mass mortalities of the sardine *Sardinops sagax* facilitated an expansion in the distribution and abundance of the anchovy *Engraulis australis* in South Australia? Marine Ecology Progress Series **220**:241–251.

Ward, T. M., F. Hoedt, L. McLeay, W. F. Dimmlich, M. Kinloch, G. Jackson, R. McGarvey, P. J. Rogers, and K. Jones. 2001b. Effects of the 1995 and 1998 mass mortality events on the spawning biomass of *Sardinops sagax* in South Australian waters. ICES Journal of Marine Science **58**:830–841.

Ward, T. M., and J. Staunton-Smith. 2002. Comparison of the spawning patterns and fisheries biology of the sardine, *Sardinops sagax*, in temperate South Australia and sub-tropical southern Queensland. Fisheries Research **56**:37–49.

Ward, T. M., P. J. Rogers, P. Stephenson, D. K. Schmarr, N. Strong, and L. J. McLeay. 2005. Implementation of an Age Structured Stock Assessment Model for Sardine (*Sardinops sagax*) in South Australia. Final report to Fisheries Research and Development Corporation.

Ward, T. M., L. J. McLeay, W. F. Dimmlich, P. J. Rogers, S. McClatchie, R. Matthews, J. Kampf, and P. D. Van Ruth. 2006. Pelagic ecology of a northern boundary current system: effects of upwelling on the production and distribution of sardine (*Sardinops sagax*), anchovy (*Engraulis australis*) and southern bluefin tuna (*Thunnus maccoyii*) in the Great Australian Bight. Fisheries Oceanography **15**:191–207.

Ward, T. M., P. Burch, and A. R. Ivey. 2010. South Australian Sardine (*Sardinops sagax*) Fishery: Stock Assessment Report 2010: Report to PIRSA Fisheries. SARDI Aquatic Sciences (Adelaide).

Ward, T. M., P. Burch, L. J. McLeay, and A. R. Ivey. 2011. Use of the Daily Egg Production Method for stock assessment of sardine, *Sardinops sagax*; lessons learned over a decade of application off southern Australia Reviews in Fisheries Science **19**:1–20.

Ward, T. M., P. Burch, and A. R. Ivey. 2012. South Australian Sardine (Sardinops sagax) Fishery: Stock Assessment Report 2012. South Australian Research and Development Institute (Aquatic Sciences), Adelaide.

Ward, T. M., A. R. Ivey, and P. Burch. 2013. Spawning biomass of sardine, *Sardinops sagax*, in waters off South Australia in 2013. Report to PIRSA Fisheries and Aquaculture. South Australian Research and Development Institute (Aquatic Sciences), Adelaide. SARDI Publication No. F2007/000566–5. SARDI Research Report Series No. 740.41 pp.

Ward, T. M., A. R. Ivey, and J. D. Carroll. 2014. Spawning biomass of sardine, *Sardinops sagax*, in waters off South Australia in 2014. Report to PIRSA Fisheries and Aquaculture. South Australian Research and Development Institute (Aquatic Sciences), Adelaide. SARDI Publication No. F2007/000566–6. SARDI Research Report Series No. 807. 33 pp.

Ward, T., A. Whitten, and A. Ivey. 2015. South Australian Sardine (*Sardinops sagax*) Fishery: Stock Assessment Report 2015.

Ward, T. M., Carroll, J., Grammer, G. L., James, C., McGarvey, R., Smart, J. and Ivey, A. R. 2018. Improving the precision of estimates of egg production and spawning biomass obtained using the Daily Egg Production Method. South Australian Research and Development Institute (Aquatic Sciences), Adelaide. FRDC Project No. 2014/026.

Ward, T.M, J. J. Smart, and A. Ivey. 2017. South Australian Sardine (Sardinops sagax) Fishery: Stock Assessment Report 2017.

Ward, T.M., Ivey, A.R. and Grammer, G.L. 2019. Spawning biomass of Sardine, Sardinops sagax, in waters off South Australia in 2019. Report to PIRSA Fisheries and Aquaculture. South Australian Research and Development Institute (Aquatic Sciences), Adelaide. SARDI Publication No. F2007/000566-9. SARDI Research Report Series No. 996. 31pp.

Ward, T.M., McGarvey, R., Ivey, A., and Grammer, G.L. Unpublished. Validating a new sampling technique for estimating egg production. South Australian Research and Development institute (SARDI). Adelaide. FRDC Project No 2017-027

White, K. V., and W. J. Fletcher. 1998. Identifying the developmental stages for eggs of the Australian pilchard, Sardinops sagax. Fisheries Western Australia. Fisheries Research Report No.103.

Whittington, I. D., M. Crockford, D. Jordan, and B. Jones. 2008. Herpesvirus that caused epizootic mortality in 1995 and 1998 in pilchard, *Sardinops sagax* (Steindachner), in Australia is now endemic. Journal of Fish Diseases **31**:97–105.

APPENDIX A: COMPARISON OF ESTIMATES OF MEAN DAILY EGG PRODUCTION (P_0)

Reanalysis of all egg production data from 1998 to 2019 with standard methods showed estimates of egg production (P_0, egg·m^{-2}·day^{-1}) varied between models and across years (Figure A–1). The log-linear model produced estimates of P_0 that varied least among years (min: 39.0 egg·m^{-2}·day^{-1} in 2013, max: 145.3 egg·m^{-2}·day^{-1} in 2004). The GLMM with a negative binomial error structure (GLMM NB) also produced plausible estimates of P_0 across years (min: 53.2 egg·m^{-2}·day^{-1} in 2001, max: 170.0 egg·m^{-2}·day^{-1} in 2014) (Figure 4-6). The NLS and GLMs tended to either over- or under-fit in most years and produce improbable estimates of P_0 (e.g. 2004, 2013, 2014) (Figure A–1).

Estimates of egg production produced by fitting the five models to data combined across all years ranged between 81.4 and 171.0 egg·m^{-2}·day^{-1} (Table A–1, Figure A–2).

The estimate of mean daily egg production for all-years combined using the log-linear model was 81.4 egg·m^{-2}·day^{-1} (95% CI = 72.8–91.0, Table A–1, Figure A–2). The alternative egg production models produced estimates of between 97.0 and 171.0 egg·m^{-2}·day^{-1} (Table A–1, Figure A–2).

The all-years estimate of P_0 is considered more robust than the individual year estimate of P_0, because sampling error within a year is much greater than inter-annual variability of egg density (Ward et al. 2018, SARDI unpublished a, b).

Table A-1. Mean daily egg production (P_0) and instantaneous daily mortality (Z) estimated using the log-linear model and four alternate models, based on all data collected from 1998 to 2019.

Model fit	P_0 (eggs·day^{-1}·m^{-2}) (95% CI)	Z
Linear version of exponential model, corrected	81.4 (72.8–91.0)	0.51
GLM Negative Binomial	169.9 (117.2–248.9)	1.10
Exponential model, NLS	146.7 (95.4–315.0)	0.88
GLM Quasi	171.0 (118.3–249.1)	1.10
GLMM, Negative Binomial, log link	97.0 (80.5–119.6)	0.35

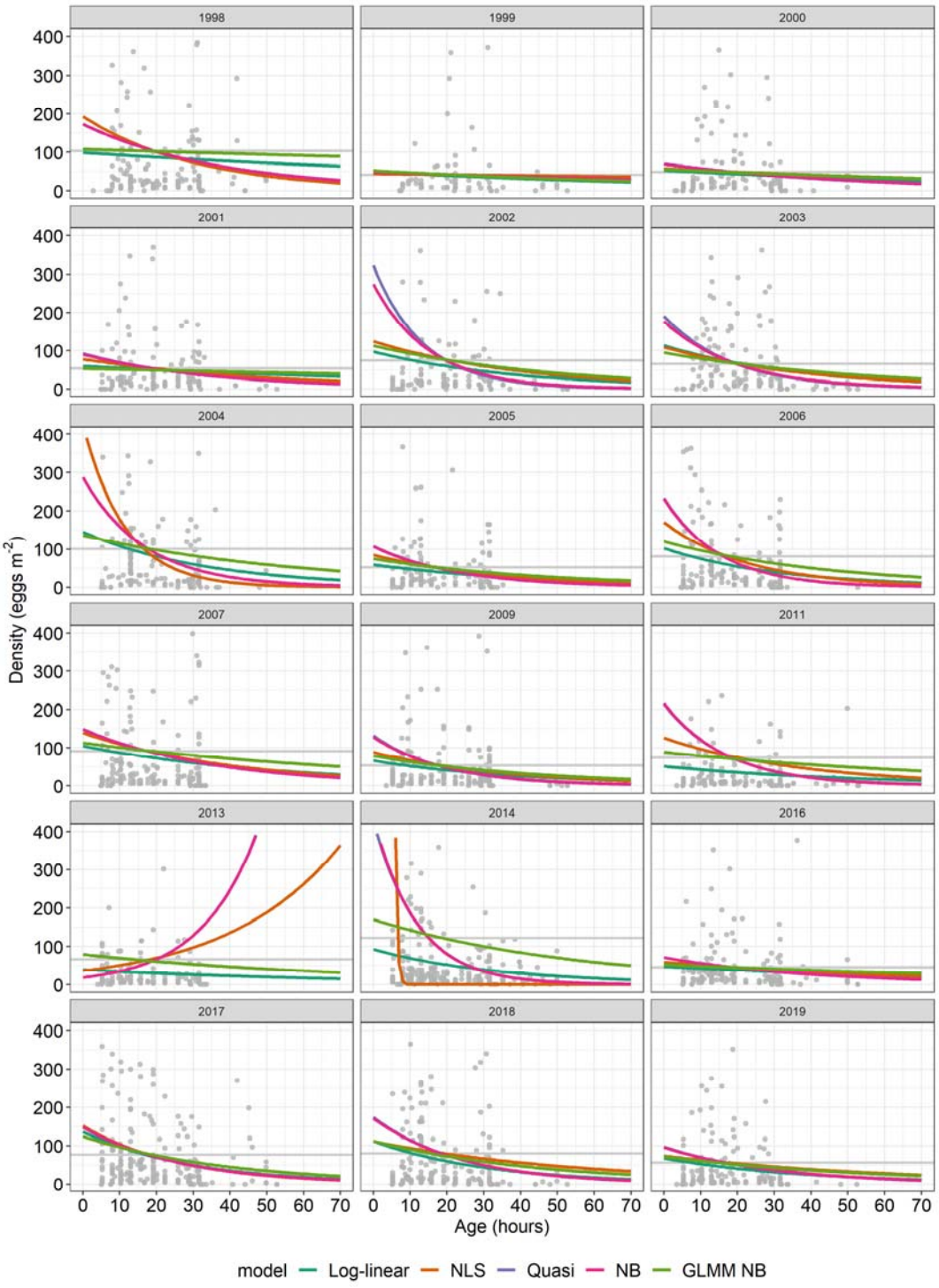

Figure A-1. Egg production models (coloured lines) for Sardine fitted to cohort egg densities (eggs.m^{-2}) and egg age (hours) per year from 1998 to 2019. Grey horizontal line: mean egg density. NLS: non-linear least squares; Quasi and NB: general linear models with either quasi or negative binomial error structures; GLMM NB: general linear mixed model with negative binomial error structure.

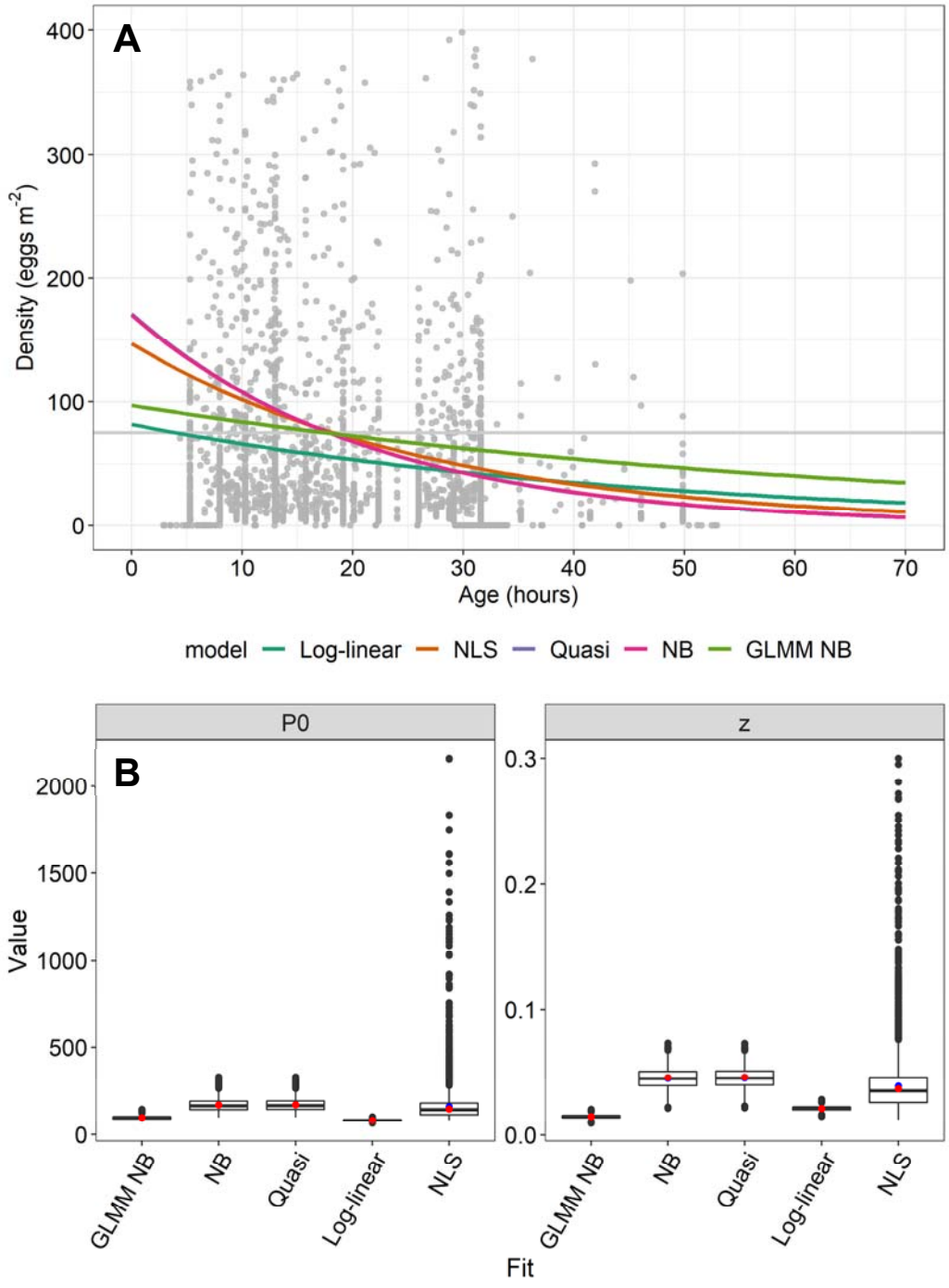

Figure A-2. **A**: Egg production models (coloured lines) for Sardine fitted to cohort egg densities (eggs.m^{-2}) and egg age (hours) for all years combined (1998 to 2019). Grey horizontal line: overall mean egg density. **B**: Bootstrapped values for mean daily egg production (P_0, egg·day^{-1}·m^{-2}) and instantaneous daily mortality (z, day^{-1}) for data presented in plot A. Red dot: model point estimate; blue dot: bootstrapped mean. NLS: non-linear least squares; Quasi and NB: general linear models with either quasi or negative binomial error structures; GLMM NB: general linear mixed model with negative binomial error structure.

APPENDIX B: MODEL SPECIFICATIONS

This section describes the components of the SardEst model fitted in TMB. The likelihood function fits to three components: 1) Estimates of spawning biomass from DEPM surveys, 2) Age-compositions and 3) deviations around mean annual recruitment ($\bar{R}$).

The model is age-structured with recruitment occurring at age one. The age index (*a*) therefore extends from 1 to 8+ with the final age-class forming a plus group (a_{max}).

Biological Parameters

$$P_a = 1 * (1 + e^{-\log(19) * (a - a_{50}) / (a_{95} - a_{50})})^{-1}$$

where P_a is the proportion mature at age *a*, a_{50} is the age where 50% of the population is mature and a_{95} is the age where 95% of the population is mature

$$W_a = A * (l_a)^B$$

where *A* and *B* are the scalar and power parameters of the length-weight relationship for both sexes, respectively.

Growth, as (caudal fork) length l_a versus age, was assumed to follow a von Bertalanffy curve l_a was calculated as:

$$l_a = l_\infty - (l_\infty - l_0) * e^{(-k * a)}$$

where l_∞ is the asymptotic length, l_0 is the length at age zero, and *k* is the growth coefficient.

Selectivity

The selectivity-at-age was determined as a 'double normal' function, which describes dome-shaped selectivity. There are three components to the function: an ascending limb, a descending limb and a plateau, which are connected by steep logistic 'joiners' that provide differentiability.

Selectivity-at-age *a* is calculated as

$$S_a = asc_a \left(1 - j_{1,a}\right) + j_{1,a} \left(\left(1 - j_{2,a}\right) + j_{2,a} dsc_a\right)$$

where the joiner functions are:

$$j_{1,a} = 1/\left(1+e^{\left(-20\frac{a-\beta_1}{1+(a-\beta_1)}\right)}\right)$$

$$j_{2,a} = 1/\left(1+e^{\left(-20\frac{a-peak_2}{1+(a-peak_2)}\right)}\right)$$

and the ascending and descending limbs are:

$$\text{asc}_a = \left(1+e^{-\beta_5}\right)^{-1} + \left(1-\left(1+e^{-\beta_5}\right)^{-1}\right)\frac{e^{\left(\frac{-(a-\beta_1)^2}{e^{\beta_3}}\right)^2} - t1_{\min}}{1-t1_{\min}}$$

$$dsc_a = 1+\left(\left(1+e^{-\beta_6}\right)^{-1}-1\right)\frac{e^{\left(\frac{-(a-peak_{2,})^2}{e^{\beta_4}}\right)}}{t2_{\min}-1}.$$

β_1 is the age where selectivity = 1.0 begins, β_2 is age where selectivity = 1.0 ends, β_3 determines the slope of the ascending limb (this is the width of the top, $peak_2$ is the endpoint), β_4 determines the slope of the descending limb, β_5 is the selectivity at age-at-recruitment and β_6 is the selectivity at a_{max}. $t1_{min}$ and $t2_{min}$ are defined as:

$$t1_{\min} = e^{\left(-\frac{(a_{\min}-\beta_1)^2}{e^{\beta_3}}\right)}$$

$$t2_{\min} = e^{\left(-\frac{(a_{\max}-peak_2)^2}{e^{\beta_3}}\right)}.$$

$peak_2$ is the endpoint where selectivity = 1.0, while

$$peak_2 = \beta_1 + 1 + \left(\frac{0.99a_{\max} - \beta_1 - 1}{1+e^{-\beta_2}}\right).$$

Recruitment

Annual recruitment is fit using a lognormal distributed recruitment deviates around a mean number of recruits:

$$R_t = \bar{R} * \exp\left(\log(\tilde{R}_t)\right)$$

where $\tilde{R}_t$ are fitted as random effects with σ_R as the standard deviation among recruitment deviations.

$$\log(\tilde{R}_t) = N(0; \sigma_R^2)$$

Population dynamics

Starting numbers-at-age

Because exploitation was nearly zero prior to the first year of data, initial numbers-at-age are determined from the estimated recruitment at time zero (R_0) and the fixed rate of natural mortality (M = 0.7 yr^{-1}):

$$N_{0,a} = \begin{cases} R_0 & \text{for } a = 1 \\ N_{0,a-1} * e^{-M} & \text{for } a > 1 \end{cases}.$$

Population with fishing mortality

Sardine population numbers $N_{t+1,a}$ at age a having recruited that year or undergone survival from start of year t to start of year $t+1$ are written

$$N_{t+1,a} = \begin{cases} R_{t+1} & \text{for } a = 1 \\ N_{t,a-1} * e^{-Z_{t,a-1}} & 2 \le a \le a_{\max} - 1 \\ N_{t,a-1} * e^{-Z_{t,a-1}} + N_{t,a} * e^{-Z_{t,a}} & \text{for } a = a_{\max} \end{cases}$$

where survival to the plus group occurs from both the plus group and the age below, and where $Z_{t,a}$ is the total instantaneous mortality rate at age a over year t,

$$Z_{t,a} = M_a + (F_{t,a} * S_a),$$

and where $F_{t,a}$ is the fishing mortality rate at age a over year t, determined using the hybrid fishing mortality method.

The hybrid fishing method allows the full *F* (F_t) to be tuning coefficients to match predicted catch ($\hat{C}_t$) to observed catch (C_t^{obs}), rather than full estimated parameters. Pope's approximation is used to determine the initial (first iteration) harvest rate, which is used as the initial Baranov continuous *F*. These values of *F* are then tuned over a series of iterations (approximately five) until the resulting predicted catch matches observed catch for each corresponding *F*:

$$temp_{1,t} = \frac{C_t^{obs}}{B_t + 0.1C_t^{obs}}$$

$$j_{1,t} = \left(1 + e^{\left(30\left(temp_{1,t} - 0.95\right)\right)}\right)^{-1}$$

$$F_{1,t} = \frac{-\ln\left(1 - \left(j_{1,t} temp_{1,t} + 0.95\left(1 - j_{1,t}\right)\right)\right)}{\delta}$$

where δ = 1.0 for the duration of the season , B_t is the estimated biomass in year *t, and* $j_{1,t}$ is a logistic joiner that prevents the initial values of *F* from exceeding 0.95yr^{-1}.

Catch in numbers for year *t* at age *a* is:

$$C_{t,a} = \frac{F_t}{Z'_{t,a}}\left(S_a N_{t,a}\right)\lambda_{t,a}$$

where $\lambda_{t,a}$ is survivorship in year *t* at age *a*:

$$\lambda_{t,a} = 1 - \mathrm{e}^{\left(-\delta Z_{t,a}\right)} / Z_{t,a}\,.$$

Estimated catch in weight in year *t* is estimated as:

$$\hat{C}_t = \sum_a \frac{F_{1,t,}}{Z_{t,a}}\left(W_a N_{t,a} S_{,a}\right)\lambda_{t,a}\,.$$

An adjustment is made to yearly Z_t^{adj} in each iteration based on how closely predicted catch matches observed catch:

$$Z_t^{adj} = \frac{C_t^{obs}}{\hat{C}_t + 0.0001}$$

This adjustment is then applied to all *F*'s and $Z_{t,a}$ and $\lambda_{t,a}$ are tuned.

$$Z_{t,a} = M + Z_{t,a}^{adj}\left(Z_{t,a} - M\right)$$

$$\lambda_{t,a} = \left(1 - \mathrm{e}^{\left(-\delta Z_{t,a}\right)}\right) / \left(Z_{t,a}\right).$$

This adjusted mortality rate is then used to calculate a new value for total catch and the new *F* estimate is the ratio of this value to observed catch:

$$temp_{2,t} = \sum_a \left(W_a N_{t,a} S_a\right)\lambda_{t,a}$$

$$F_{2,t} = \frac{C_t^{\mathrm{obs}}}{temp_{2,t} + 0.0001}.$$

A second joining function prevents any *F* from exceeding a maximum value F_{max}:

$$j_{2,t} = \left(1 + \exp^{30\left(F_{2,t} - 0.95 * F_{\max}\right)}\right)^{-1}.$$

The final updated F_t are calculated as:

$$F_t = j_{2,t} F_{2,t} + \left(1 - j_{2,t}\right) F_{\max}.$$

Spawning stock biomass was calculated as the proportion of the population that was mature:

$$\hat{G}_t = \sum_a W_a P_a N_{t,a}.$$

Total biomass was calculated as the total weight of the population:

$$B_t = \sum_a W_a N_{t,a}.$$

Proportional age-composition was calculated as:

$$\hat{p}_{t,a} = \hat{C}^{W}_{t,a} \sum_{a} \hat{C}^{W}_{t,a} .$$

Likelihoods

The probability of the recruitment deviates were estimated as lognormal random effects around mean recruitment ($\bar{R}$) as:

$$L_{\tilde{R}} = \sum_{t} \log(\sigma_R) + 0.5 * (\log(R_t) - \log(\bar{R}))^2 / \sigma_R^2 .$$

The proportional age-compositions were fit using a multinomial likelihood:

$$L_p = \sum_{t,a} p_{t,a} * \log(p_{t,a} / \hat{p}_{t,a})$$

where $p_{t,a}$ is the proportional age composition data in year *t* for age *a*.

Estimated spawning stock biomass was fit to the DEPM estimates as:

$$L_I = \sum_{t} 0.5 \cdot \log(\sigma_t^2) + \frac{\left[\log(I_t) - \left(\log(\hat{G}_t) - \sigma_t^2 / 2\right)\right]^2}{2\sigma_t^2}$$

where I_t is the DEPM estimate of spawning stock biomass in year t, and where the lognormal likelihood σ_t^2 parameter for each year can be written in terms of the coefficient of variation, Cv_t^2 , obtained for each yearly spawning biomass estimate from the DEPM survey analysis as $\sigma_t^2 = \log(Cv_t^2 + 1)$.

The joint likelihood function was the sum of the three likelihood components with weightings of 10 (λ_I) and 1.0 (λ_p) applied to the DEPM and age-composition data, respectively:

$$L(\theta \mid D) = L_I * \lambda_I + L_p * \lambda_p + L_{\tilde{R}} .$$

APPENDIX C: COMPARISON TO PREVIOUS SS MODEL

In this section, the SardEst model is compared to the Stock Synthesis (SS) model used in the 2017 assessment. Three updates have been made to the SS model presented here: 1) current data (1992–2019) were used, 2) natural motility (*M*) has been updated to 0.7yr^{-1} to match SardEst and 3) Stock Synthesis version 3.3 is used rather than 3.24.

1. Fits to spawning biomass

The SS model provided good fits to DEPM spawning biomass estimates, but underestimated the first available DEPM estimate (Figure C–1). The standard error around the SS model was consistently larger than SardEst with the exception of 1992–1994 when no data were available.

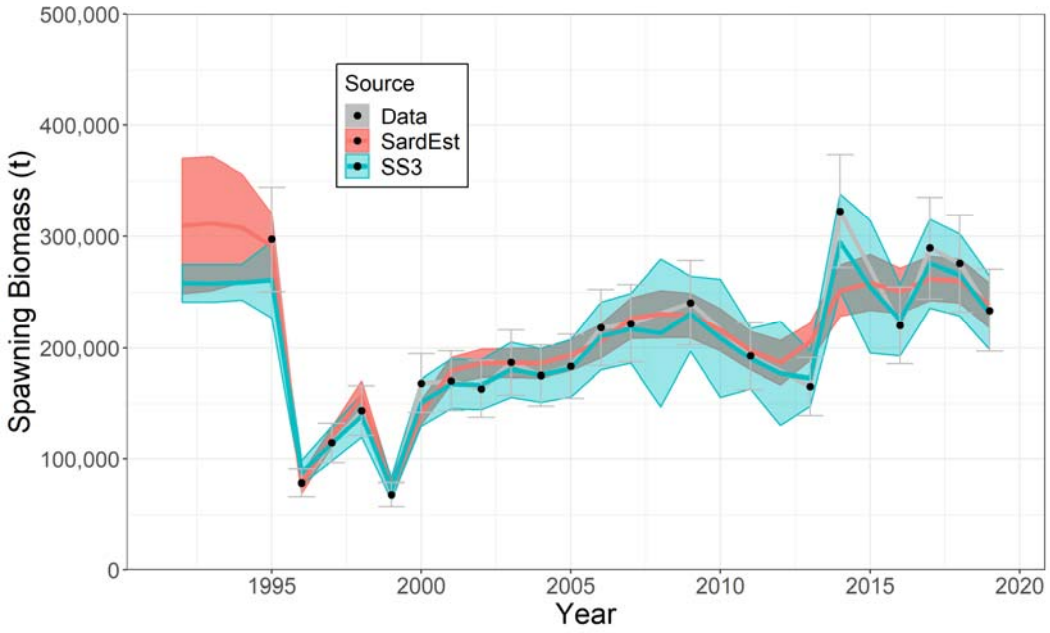

Figure C-1. Model comparisons of spawning biomass estimates between SardEst and the SS model. Red line and shaded area represent the estimates and standard error of SardEst. Blue line and shaded area represent the estimates and standard error of the SS model. Grey line, black points and grey error bars are the estimates and standard error of the DEPM surveys.

2. Fits to age compositions

Estimated proportions-at-age were similar between the two models. Both generally provided good fits to the data in most years. The poorest fits in both models were in the years following the mass mortality events (Figure C–2). Examination of fit residuals for the two models shows that in certain years, one model performed better than the other. However, overall both showed very similar

patterns for the residuals, both across ages in each year and across years. This may imply that these differences of model to data could lie in the data.

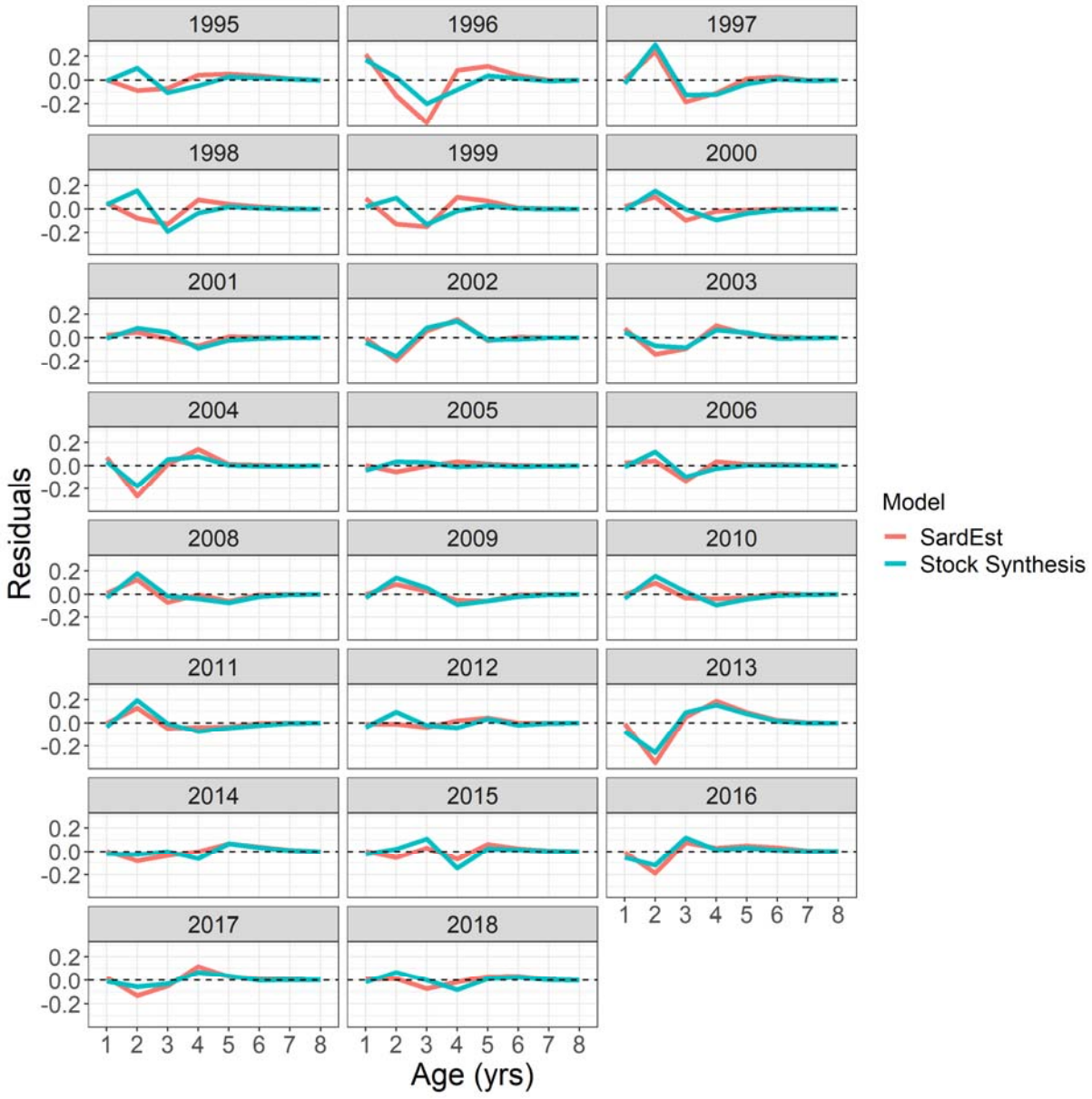

Figure C-2. Residuals between model-estimated proportions-at-age and the observed proportions-at-age. The red line shows the bias of the SardEst model and the blue line shows the bias of the SS model. The dashed line at zero represents the observed proportion at age that each model is being compared with. Age composition data are not available for 2007 or 2019.

3. Estimated recruitment

The estimation of recruitment was the biggest difference between the two stock assessment models. Stock Synthesis estimated recruitments as deviations to a stock recruitment relationship as fixed effects, whereas SardEst estimates recruitments as deviations to a mean recruitment as random effects. Additionally, Stock Synthesis can only estimate recruitment for fish at age zero, whereas SardEst estimates recruitment at age one, which is the true age-at-recruitment for the fishery. The benefits of the SardEst approach were 1) a stock recruitment relationship that did not suit the population was no longer applied, 2) age-at-recruitment occurs at the appropriate age and thus the model has more information available to estimate it and 3) fitting recruitment deviations as random effects reduced their variance (Figure C–3).

In Figure C–3 a comparison analysis has been performed for the two models. Here, SardEst has been re-fitted with an age-at-recruitment of zero to allow for a direct comparison. This analysis revealed two key findings: 1) for most of the time series, recruitment estimates were similar between models. However, the error around the SardEst estimates were significantly lower than the SS model. This is a result of fitting recruitment deviations as random rather than fixed effects. The estimated standard errors reflect the estimated random effect variance, which was lower, and reflects the penalty that random effects implicitly impose on yearly recruitment variation. 2) The SS model determined that there were two recruitment failures in 1993 and 1996. This was caused by the inability of the SS model to reconcile the declines in biomass in 1996 and 1998 due to the mass mortality events through either natural or fishing mortality. Therefore, in order to fit to these low estimates of biomass, the SS model has to assume that there was a failure in recruitment two years prior. This does not occur in the SardEst model in which those natural mortality events made explicit and their rates estimated. Therefore, SardEst can attribute those declines in biomass to mortality and does not need to assume that it was caused by recruitment failures. This demonstrates that SardEst is better handling both mortality and recruitment than the SS model.

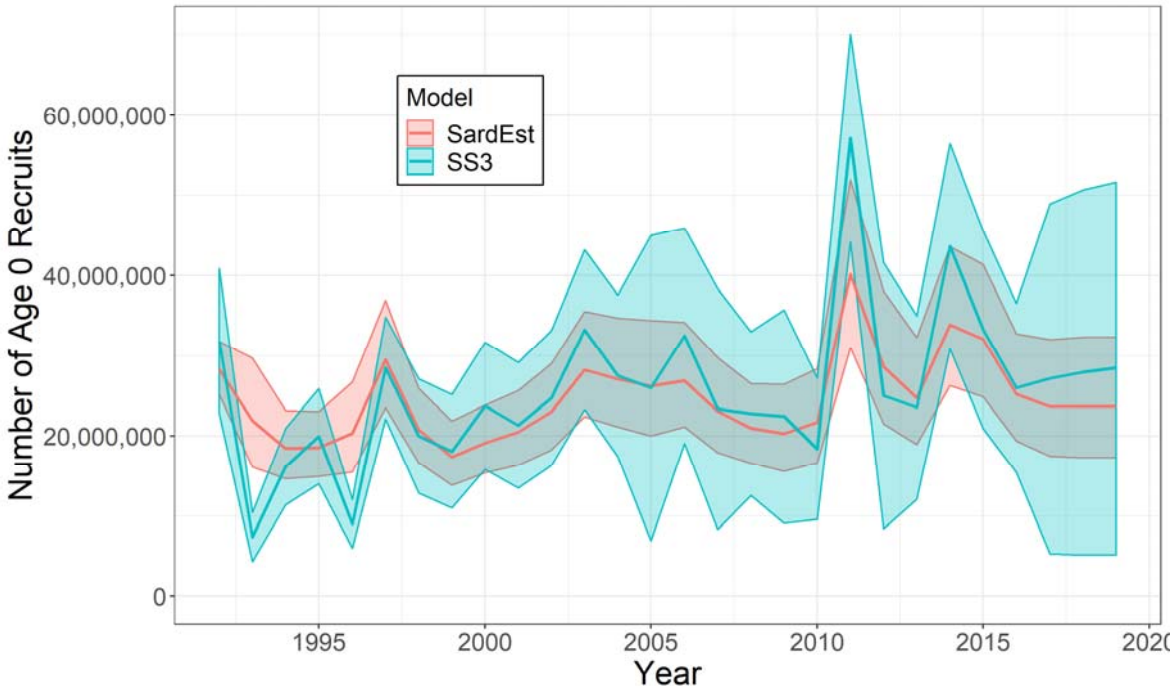

Figure C-3. Estimated recruitment (here zero age fish) for the SardEst (red) and SS model (blue). Shaded areas represent standard error of respective models. The SardEst model was re-run with age-at-recruitment set at zero rather than one to facilitate this comparison.